COLUMBIA UNIVERSITY
IN THE CITY OF NEW YORK

PHENIX

Direct Jet Reconstruction in $p+p$ and Cu + Cu Collisions at $\sqrt{s_{NN}} = 200$ GeV

Yue Shi Lai

Columbia University and Nevis Laboratories

August 2, 2011

Phases of QCD

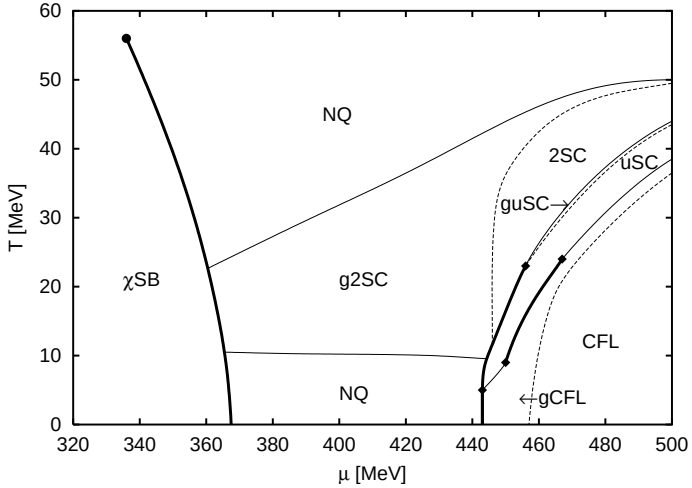

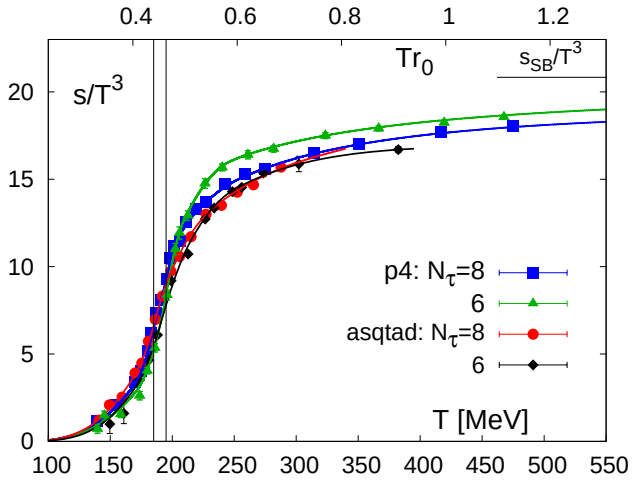

- Asymptotic freedom provides a rich structure to the QCD
- Normal matter is "locked" to low T, low μ_B
- Heavy ion collider recreates the primodial, high T, low μ_B phase

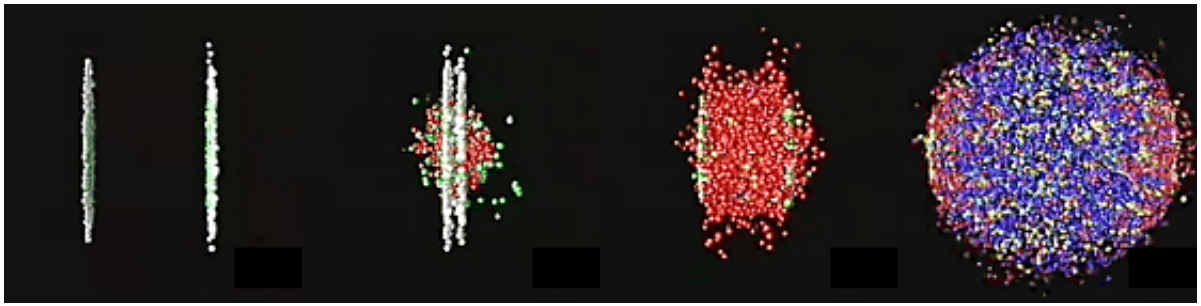

QCD Hard Scattering

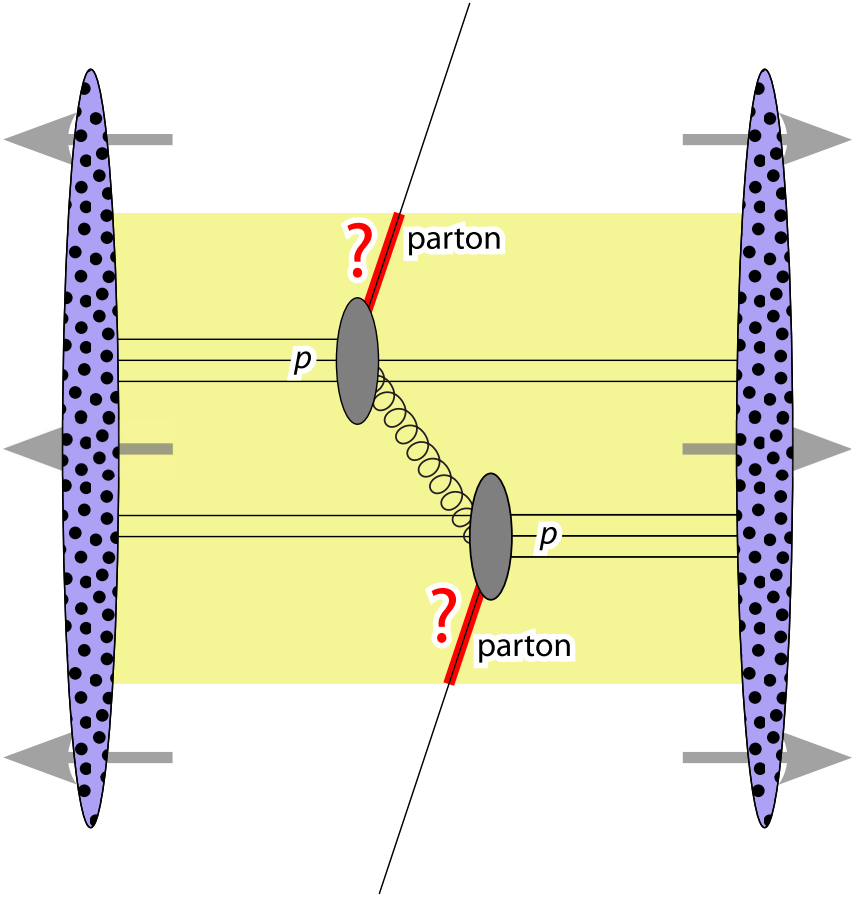

- Jets are probes for the medium

Signature of Jet Energy Loss

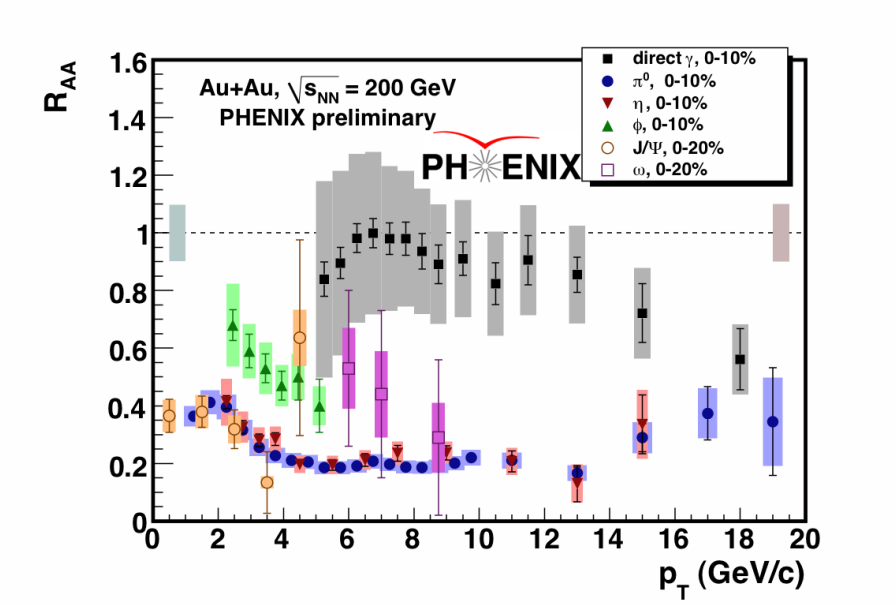

Single particle suppression

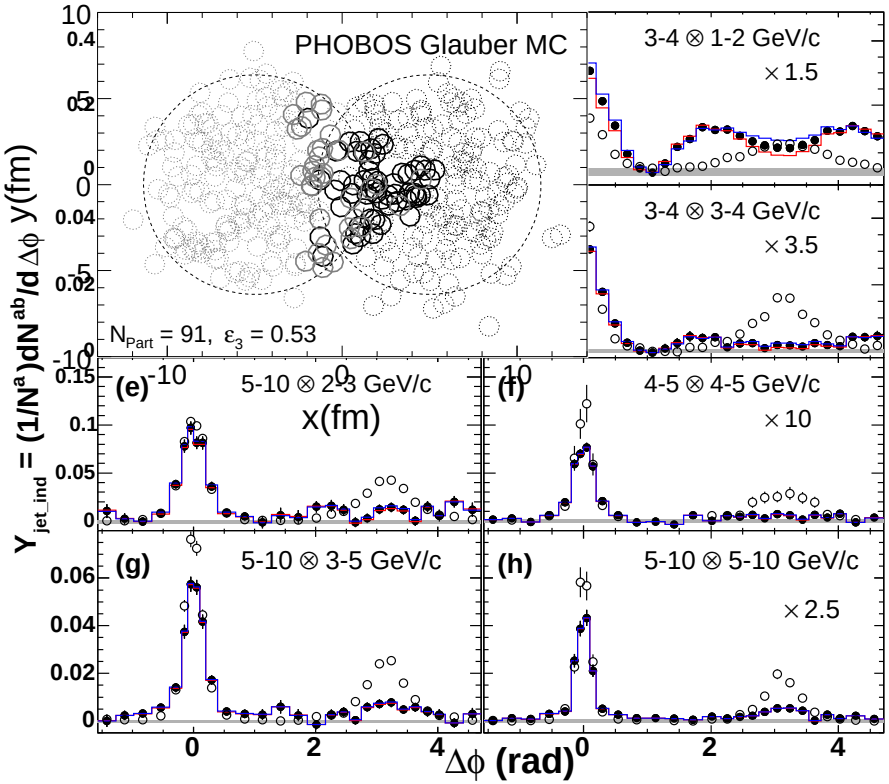

Two particle correlation

K. Reygers (PHENIX), QM2008

B. Alver, G. Roland, Phys. Rev. C 81, 054905 (2010)

PHENIX, Phys. Rev. C 78, 014901 (2008)

30 Years of Jet Measurement

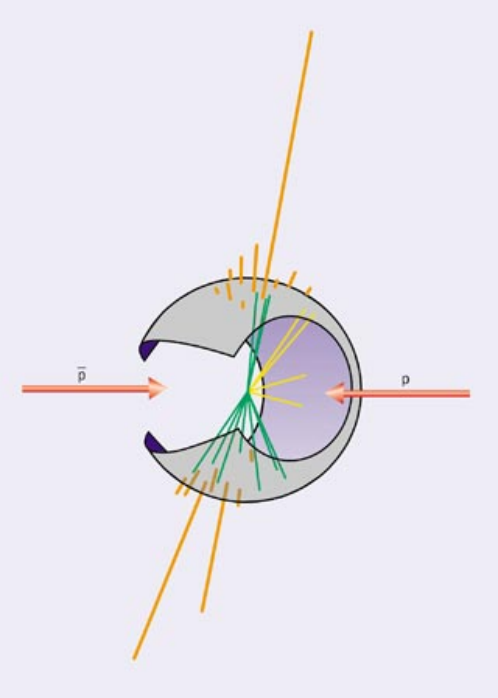

ca. 1982

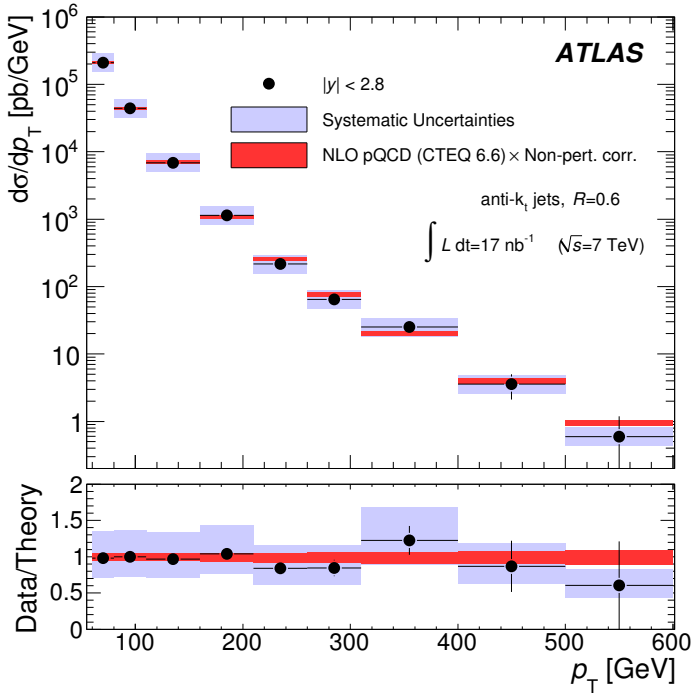

2011

- Jet transitioned from being unsure of existing to a precision probe for QCD

CERN Courier, May 1, 2003

ATLAS, Eur. Phys. J. C 71, 1512 (2011)

QCD Hard Scattering

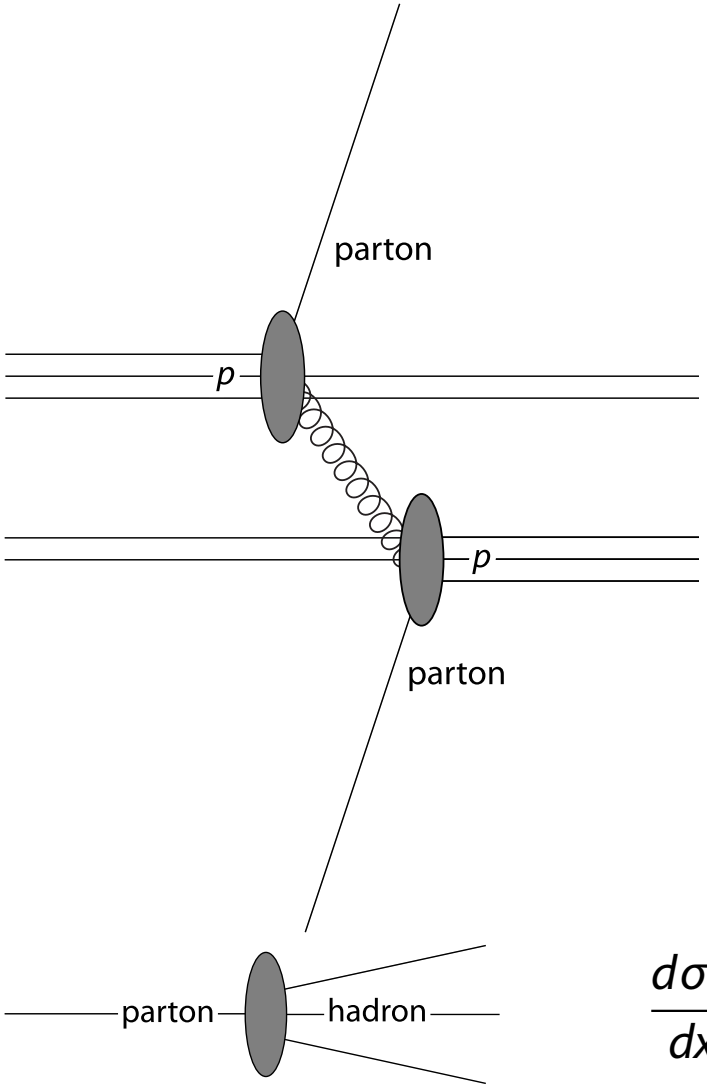

$$\frac{d^3\sigma(p+p\to \text{parton}+X)}{dy_3\,dy_4\,dp_T^2} =$$

$$\frac{1}{16\pi^2}\sum_{i,j,k,l=q,\bar{q},g}\iint dx_1\,dx_2 f_{i/p}(x_1,\mu^2)f_{j/p}(x_2,\mu^2)$$

$$\times\,\overline{\Sigma}|\mathcal{M}(ij\to kl)|^2\frac{1}{1+\delta_{kl}}$$

$$\frac{d\sigma^h}{dx} = \sigma_{\text{tot}}F^h(x,s) = \sigma_{\text{tot}}\sum_i\int_x^1\frac{dz}{z}C_iD_i^h(x/z,s)$$

Jet Reconstruction Algorithms

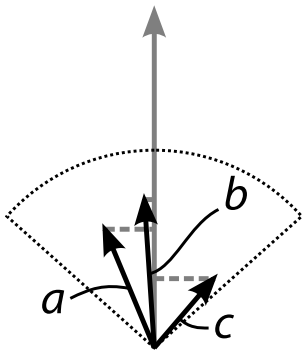

Cone

- Energy summed in a circular $(\Delta\eta, \Delta\varphi)$ region (fixed geometry), split/merge
- Traditionally seeded: not IRC safe
- Transverse energy is balanced for the stable cone axis
- Subtlety: Energy flow is maximized with respect to the Epanechnikov kernel $h(r) = \max(0, R^2 - r^2)$, not a (flat) "cone"

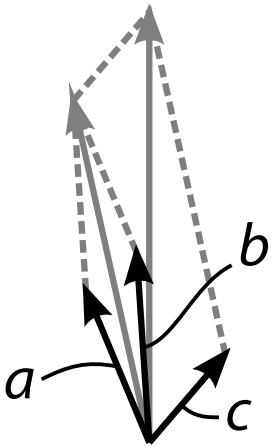

Iterative Recombination

- Dynamic geometry
- Classical $k_\perp$: QCD $k_\perp = p_T \sin\theta$ ordering
- Pure angular version: Cambridge–Aachen
- $p_T^{-1} \sin\theta$: anti-$k_\perp$, which tries to emulate cone
- But: with underlying event, cone grows and anti-$k_\perp$ shrinks

Going Further Back...

Sphericity

- Principal component analysis of event quadrupole moment

$$Q^{\alpha\beta} = \sum_{k=1}^{N} p_k^\alpha p_k^\beta \quad \text{or} \quad T^{\alpha\beta} = \frac{1}{2}\sum_{k=1}^{N}\left(3p_k^\alpha p_k^\beta - \delta^{\alpha\beta} p_k^2\right)$$

- Order $\lambda_1 \geq \lambda_2 \geq \lambda_3$, λ_3 corresponds to spread orthogonal to dijet axis

Thrust

- Spherical maximization

$$d(\hat{\mathbf{r}}) = \frac{\sum_k (\mathbf{p}_k \cdot \hat{\mathbf{r}})\, \theta(\mathbf{p}_k \cdot \hat{\mathbf{r}})}{\sum_k |\mathbf{p}_k|} \tag{1}$$

- Generalized by Berger, Kúcs, Sterman to a power a weighted energy flow variable

From Cone to Gaussian Filter

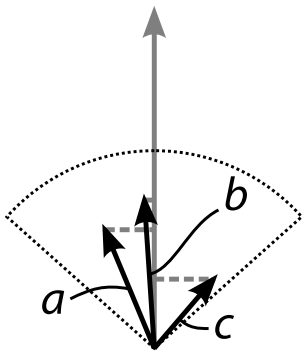

Cone

$$\iint_{\mathbb{R}\times S^1} d\eta' d\varphi' p_T(\eta', \varphi') \exp\left[-\frac{(\eta-\eta')^2+(\varphi-\varphi')^2}{2\sigma^2}\right] = \text{max!}$$

- Seedless
- Cone-like, but "automatically" infrared and collinear safe
- Shape of the filter:
  - Optimizes the signal-to-background by focusing on the core of the jet
  - Stabilizes the jet axis in the presence of background
- Naturally handles isolated particles vs. collective background

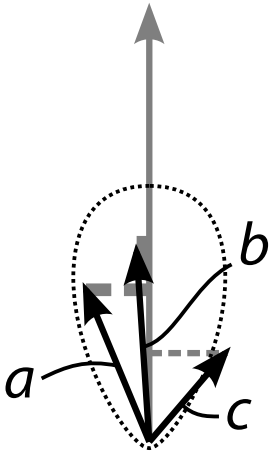

Filter

From Cone to Gaussian Filter

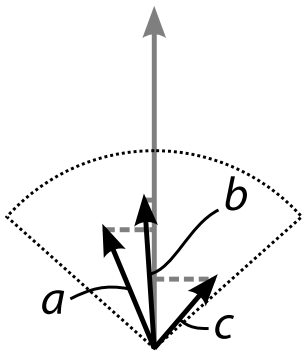

Cone

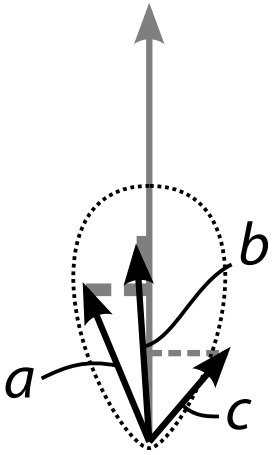

Filter

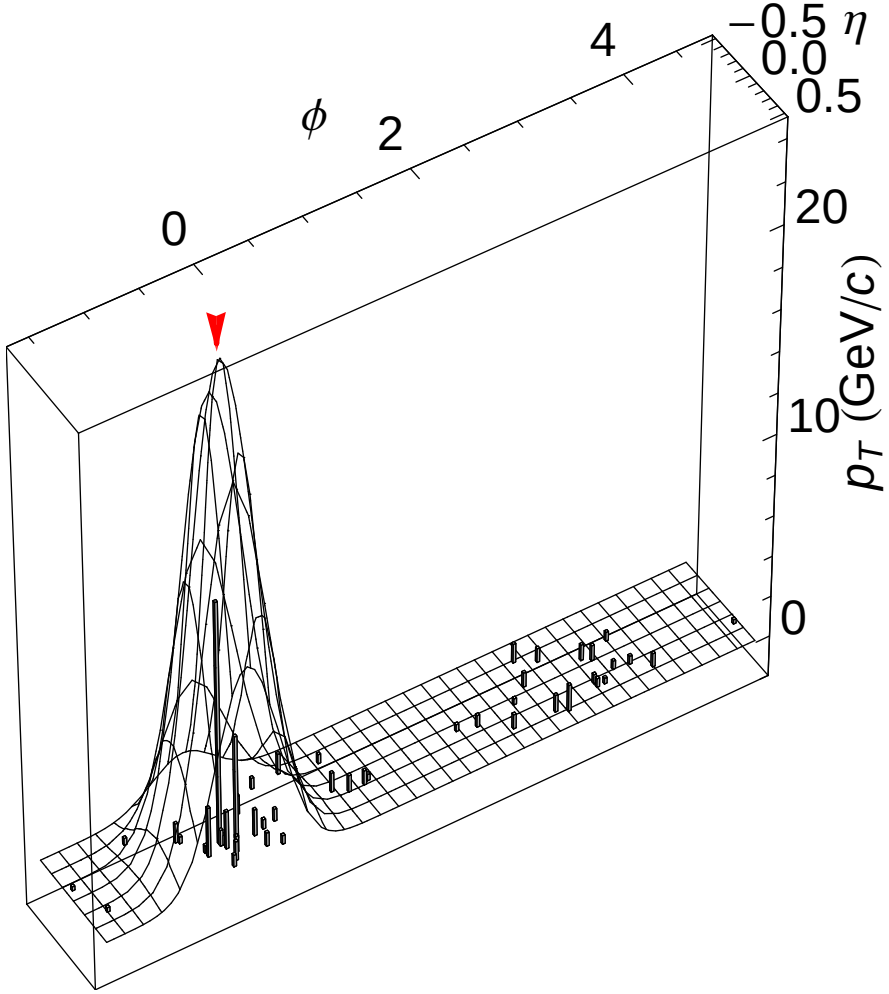

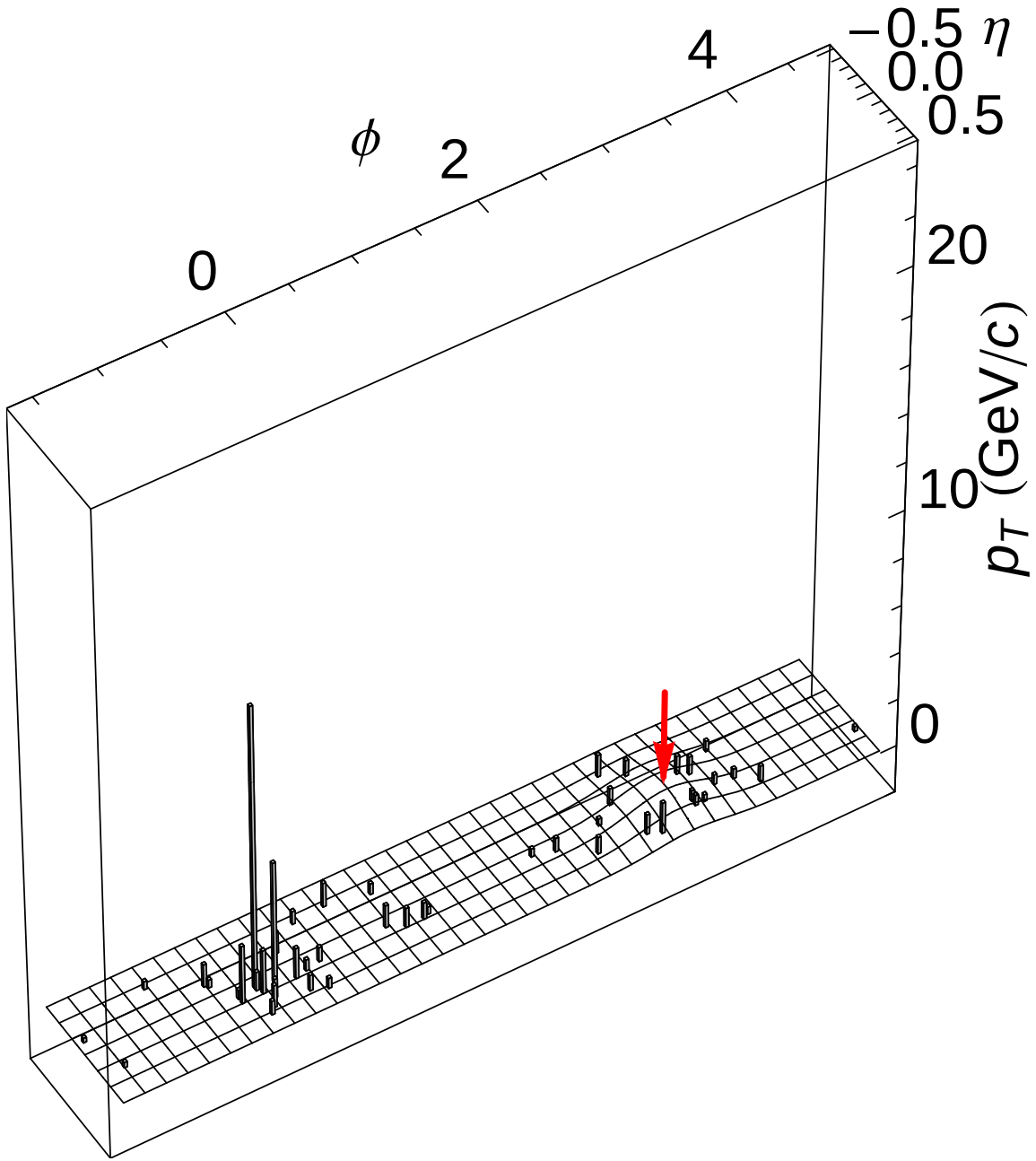
ϕ
0
2
4
η
−0.5
0.0
0.5
p_T (GeV/c)
0
10
20

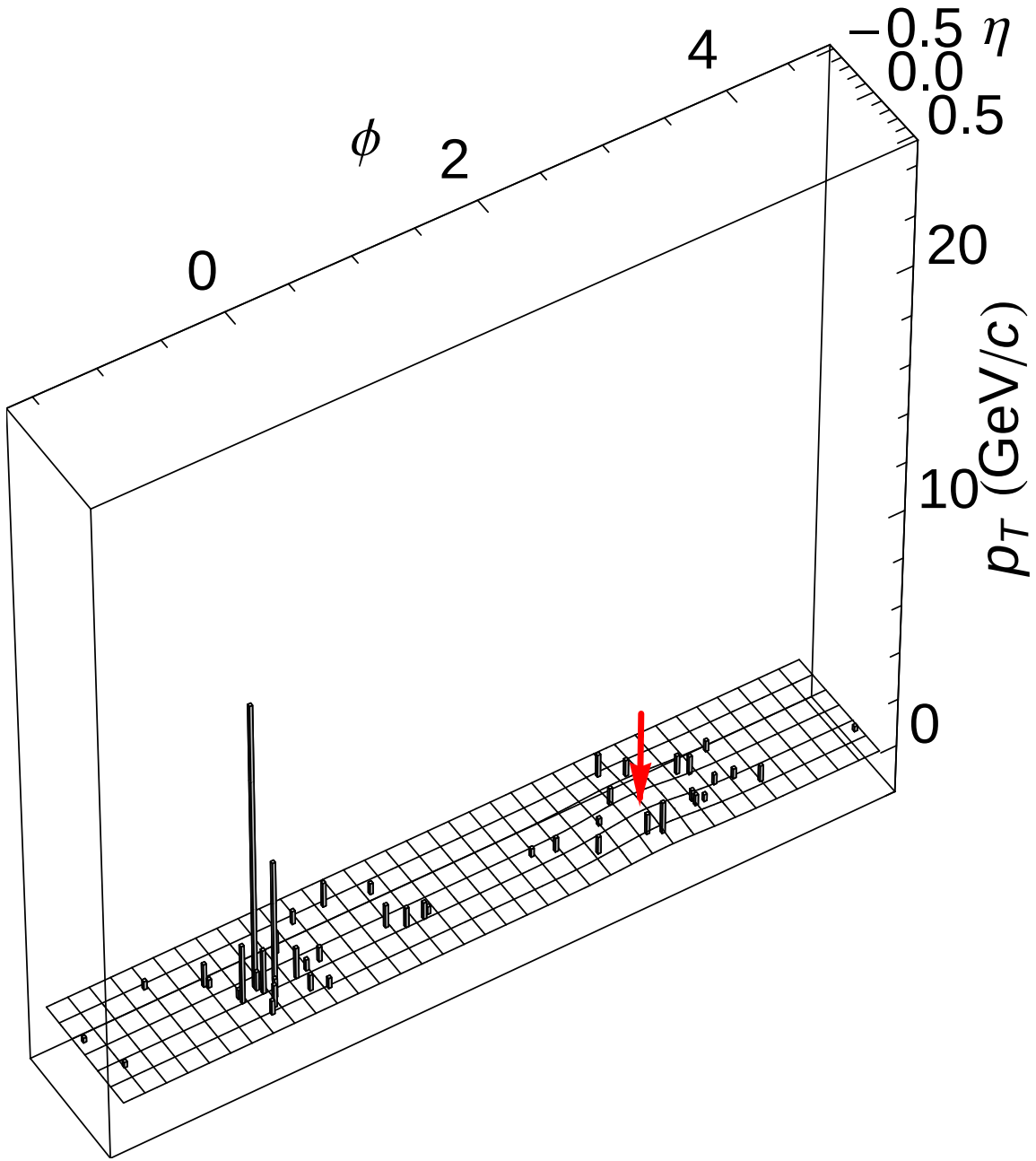
ϕ
0
2
4
η
−0.5
0.0
0.5
p_T (GeV/c)
0
10
20

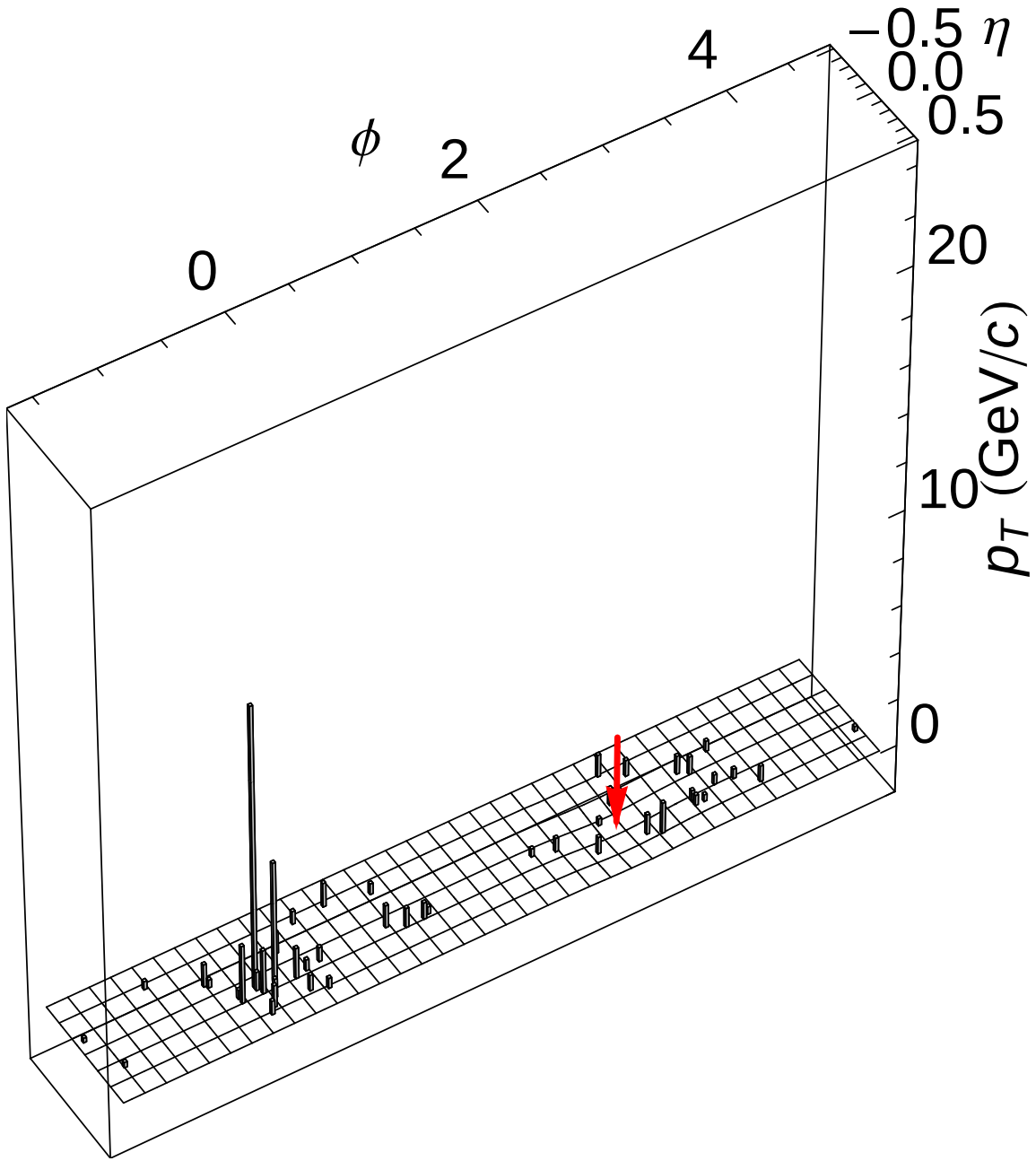
ϕ
0
2
4
η
−0.5
0.0
0.5
p_T (GeV/c)
0
10
20

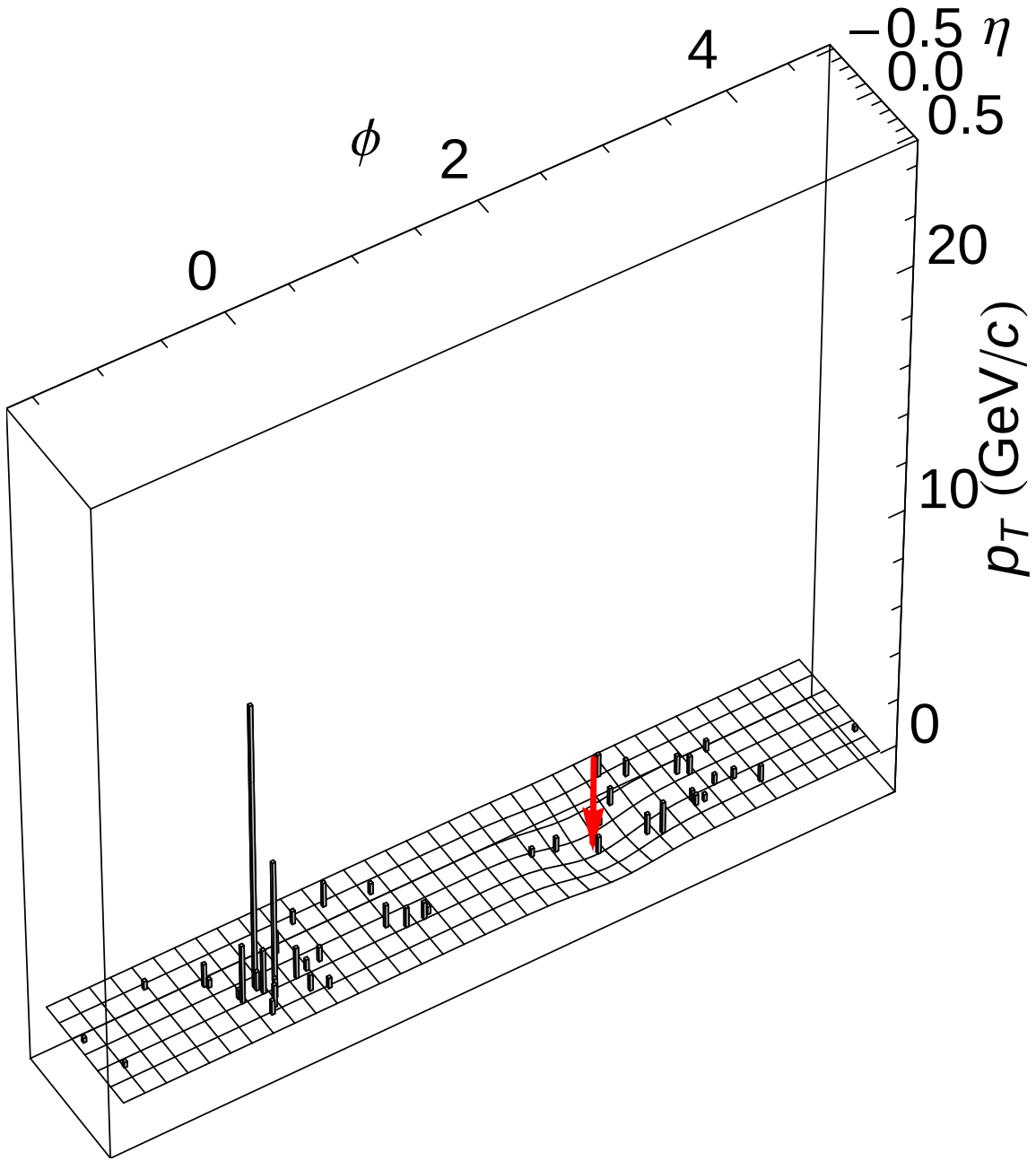
ϕ
0
2
4
η
−0.5
0.0
0.5
p_T (GeV/c)
0
10
20

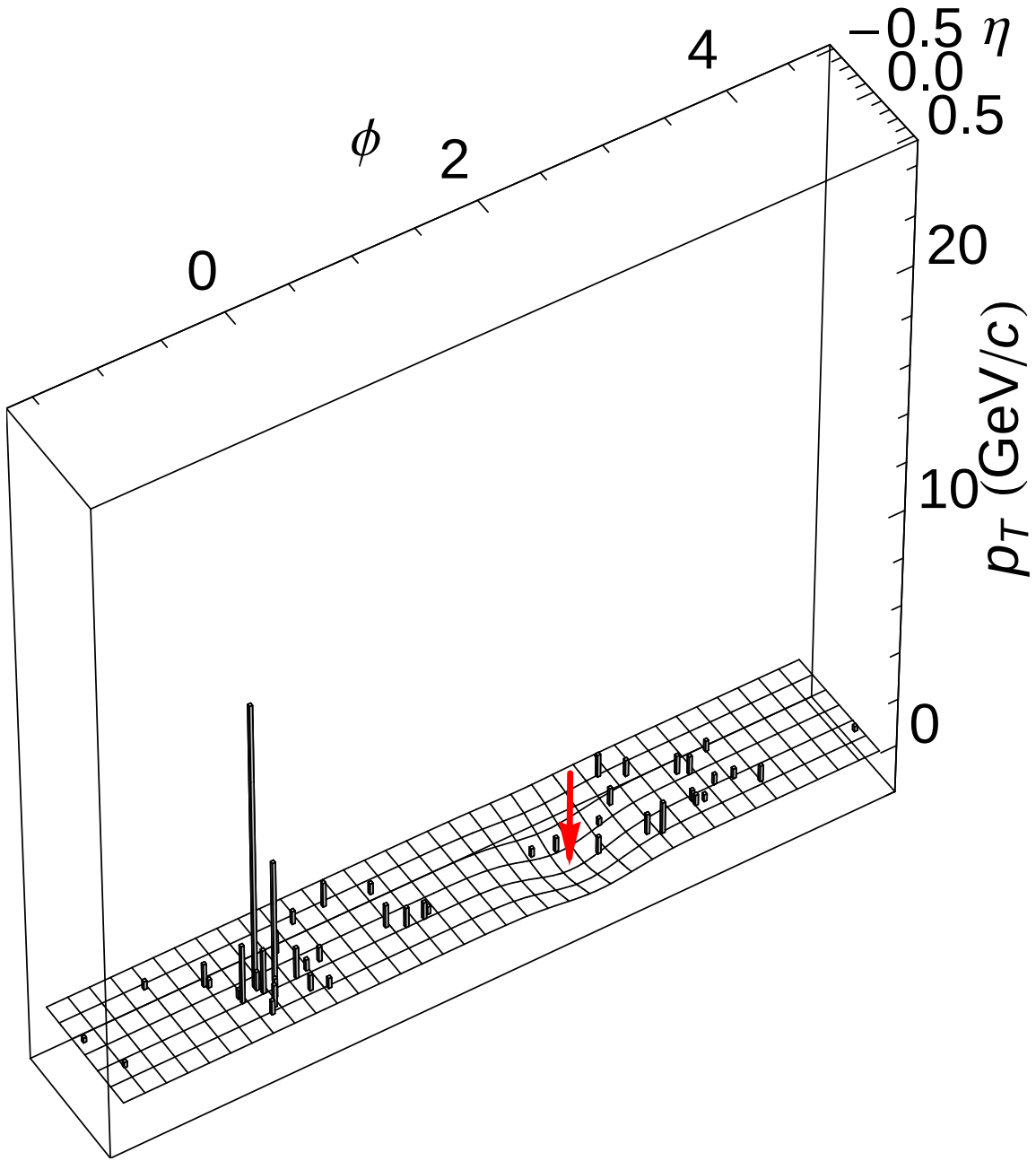
ϕ
0
2
4
η
−0.5
0.0
0.5
p_T (GeV/c)
0
10
20

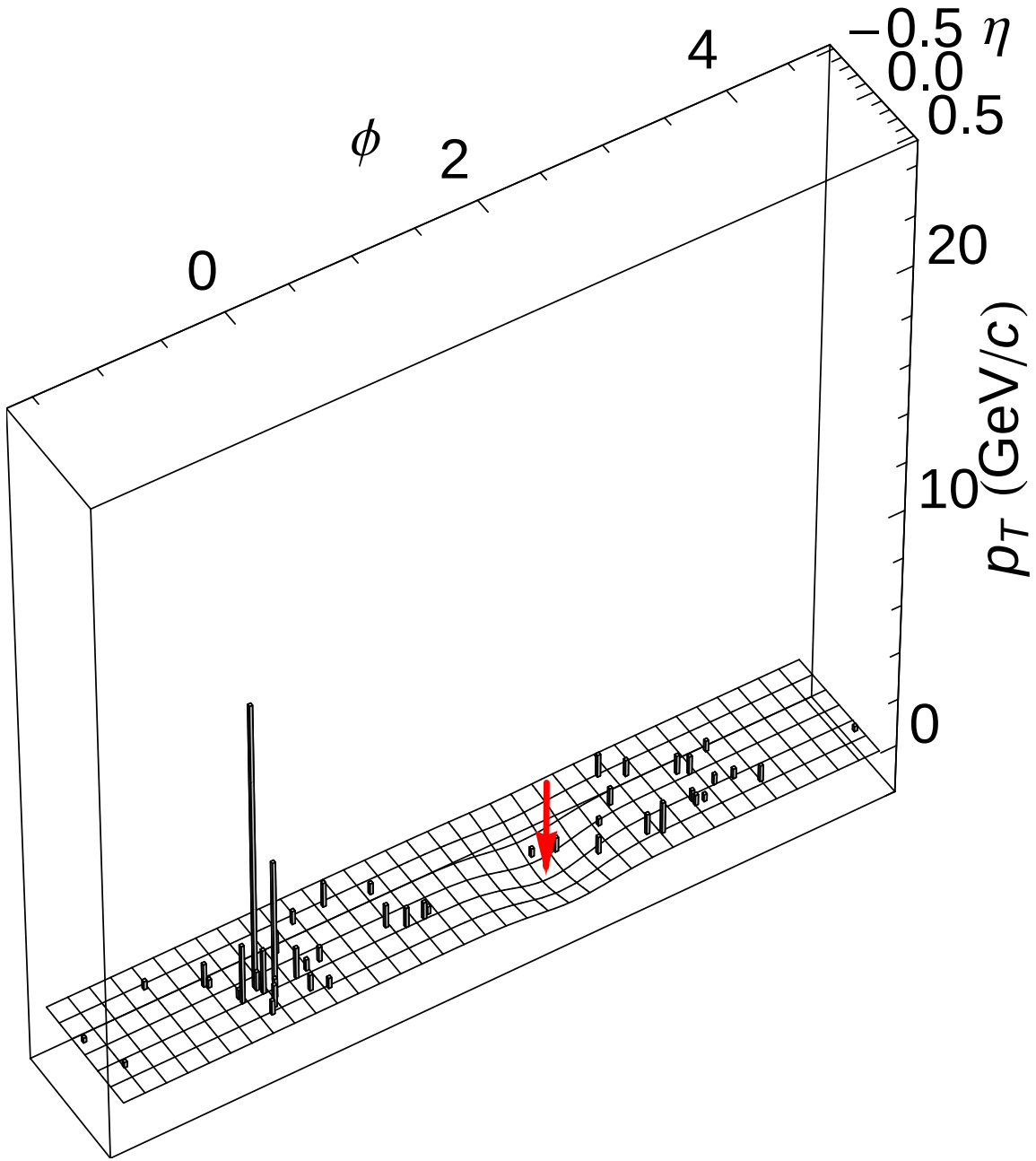
ϕ
0
2
4
η
−0.5
0.0
0.5
p_T (GeV/c)
0
10
20

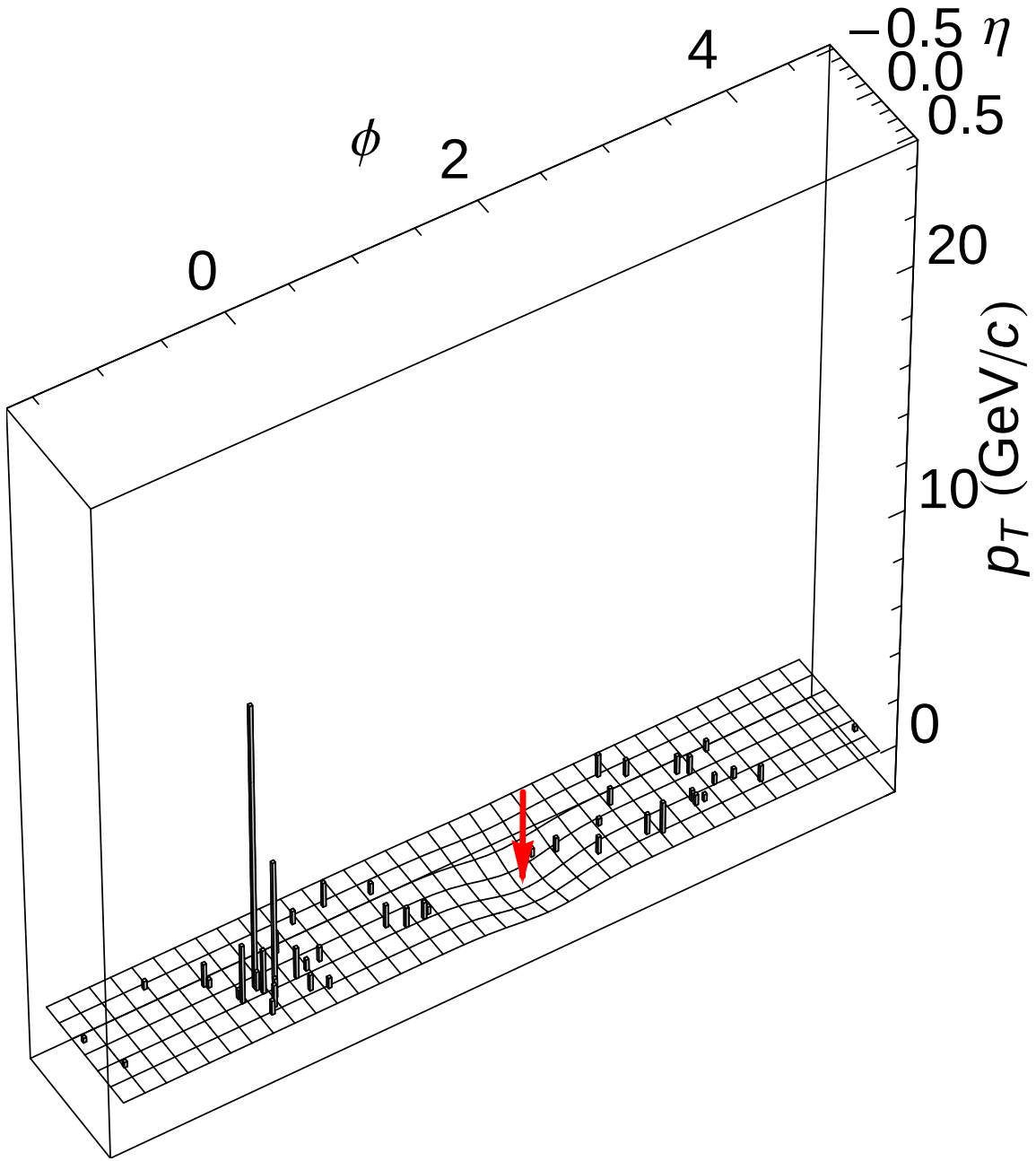
ϕ
0
2
4
η
−0.5
0.0
0.5
p_T (GeV/c)
0
10
20

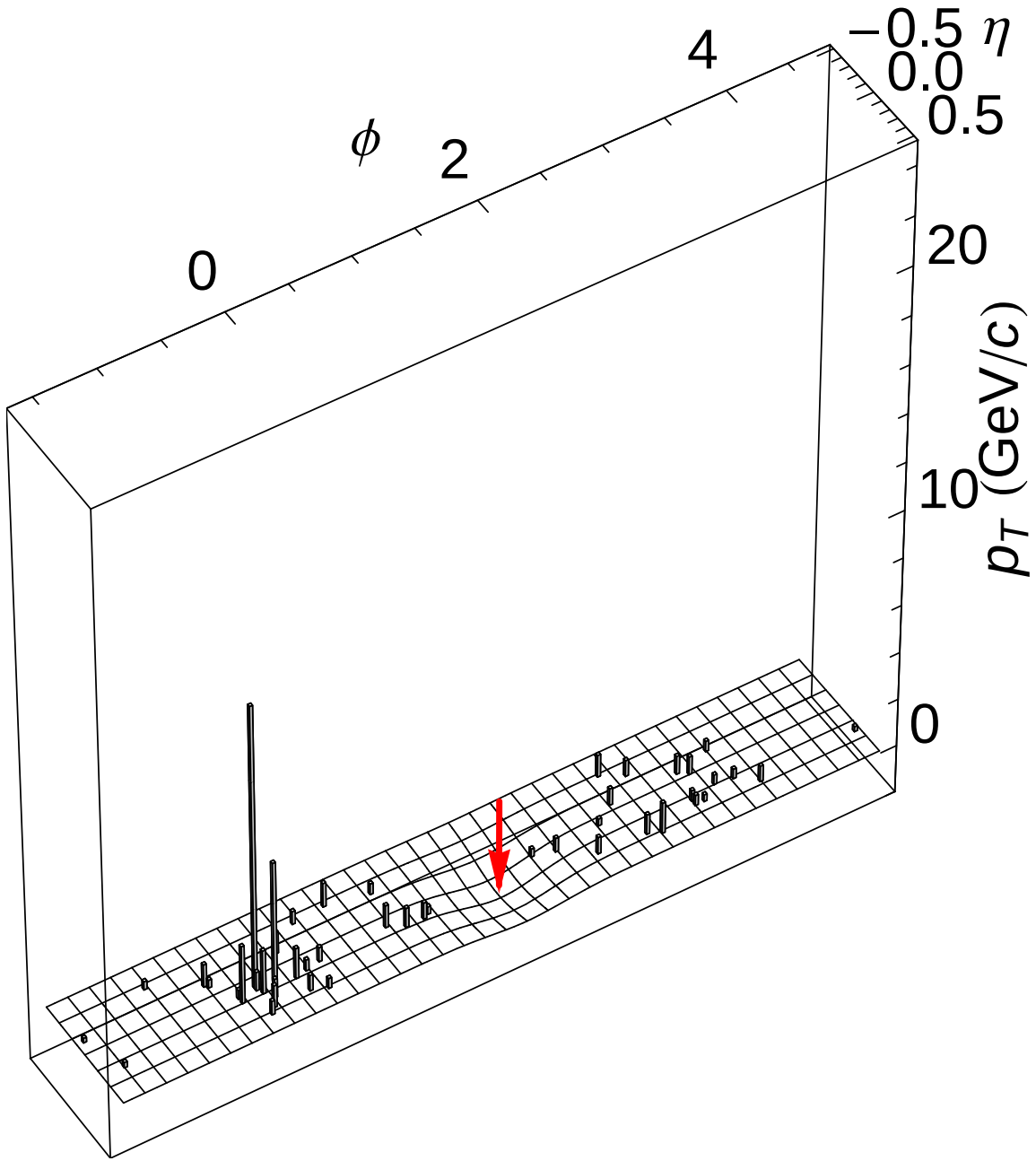
ϕ
0
2
4
η
−0.5
0.0
0.5
p_T (GeV/c)
0
10
20

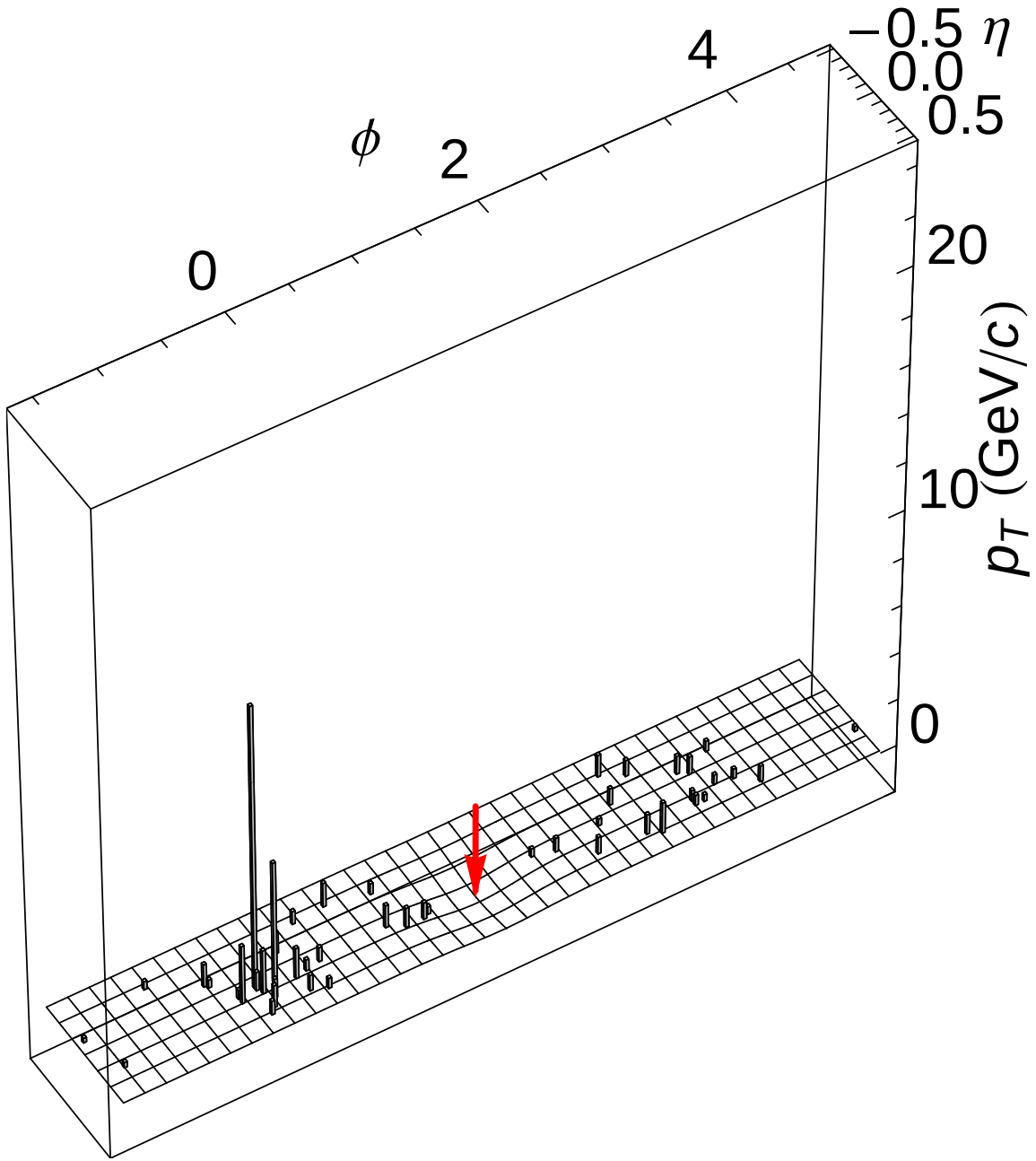
ϕ
0
2
4
η
−0.5
0.0
0.5
p_T (GeV/c)
0
10
20

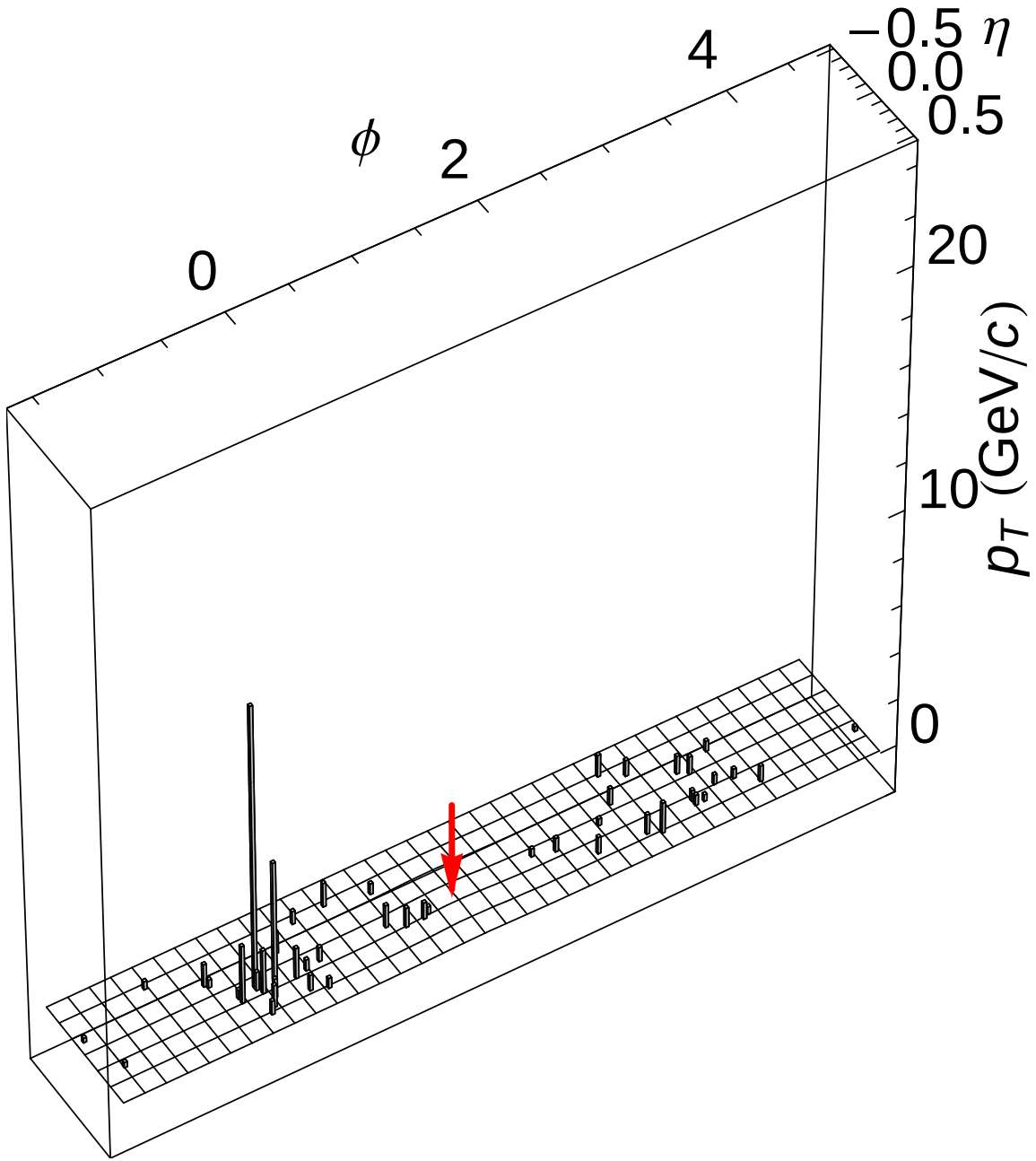
ϕ
0
2
4
η
−0.5
0.0
0.5
p_T (GeV/c)
0
10
20

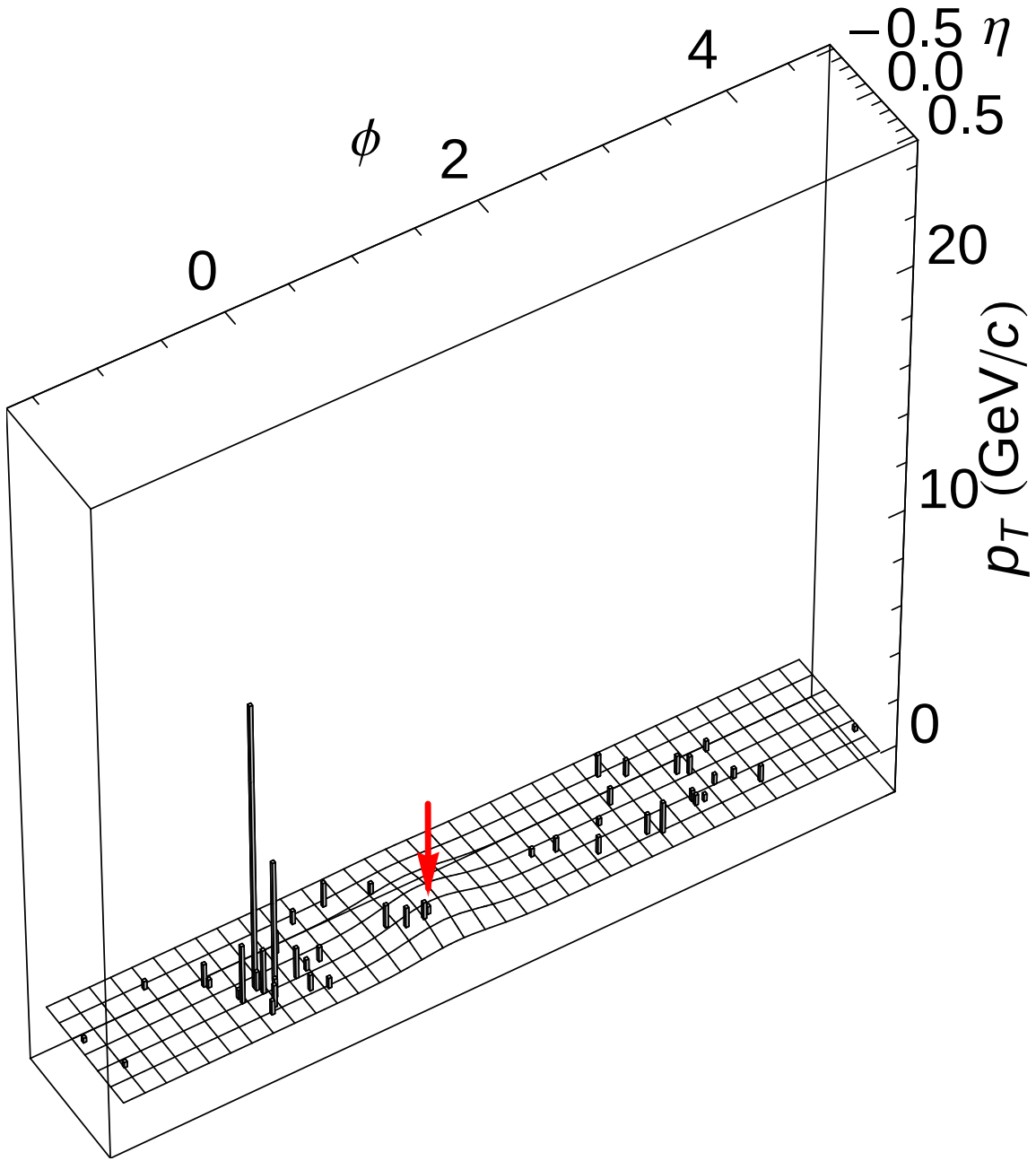
ϕ
0
2
4
η
−0.5
0.0
0.5
p_T (GeV/c)
0
10
20

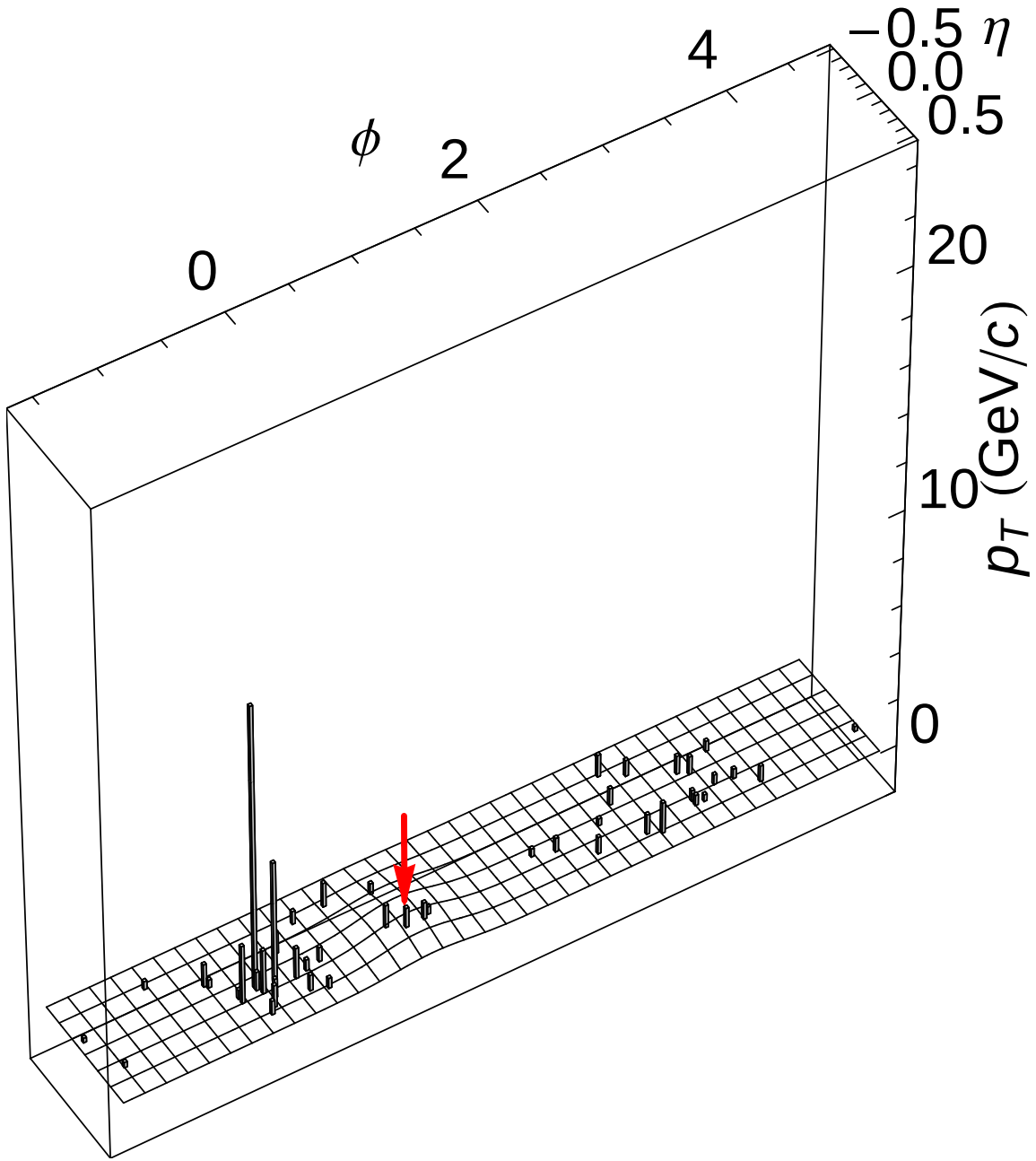
ϕ
0
2
4
η
−0.5
0.0
0.5
p_T (GeV/c)
0
10
20

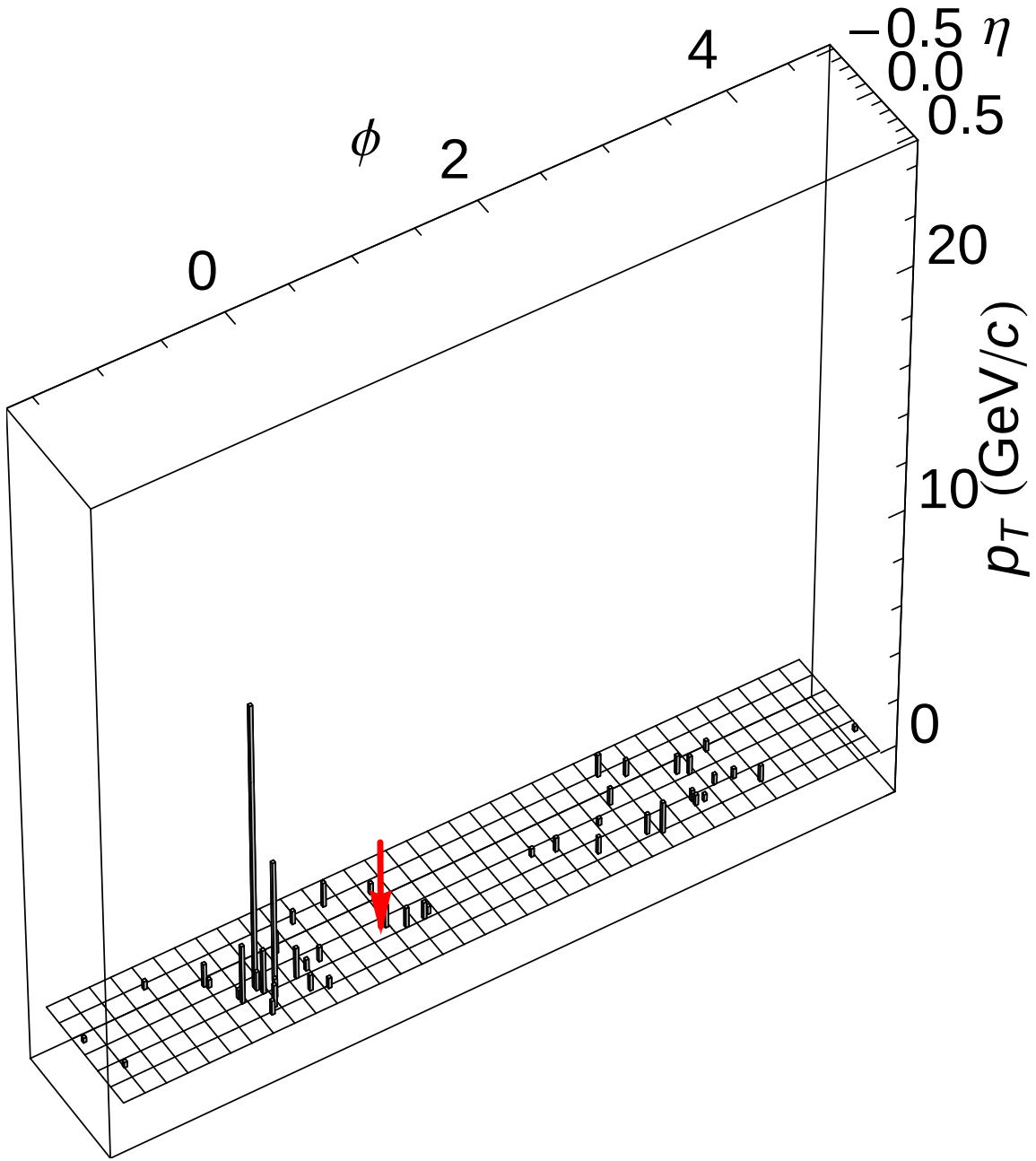
ϕ
0
2
4
η
−0.5
0.0
0.5
p_T (GeV/c)
0
10
20

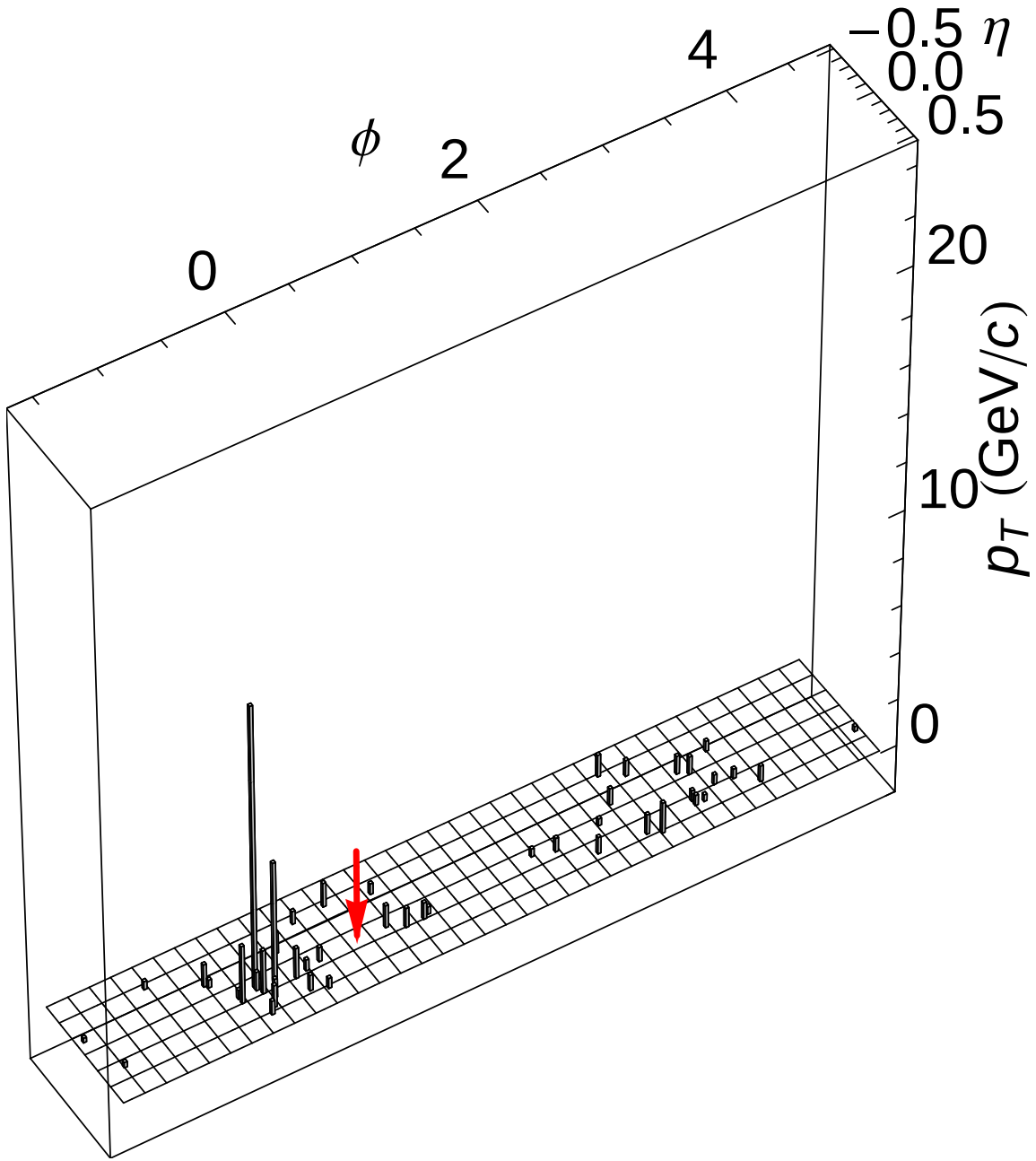
ϕ
0
2
4
η
−0.5
0.0
0.5
p_T (GeV/c)
0
10
20

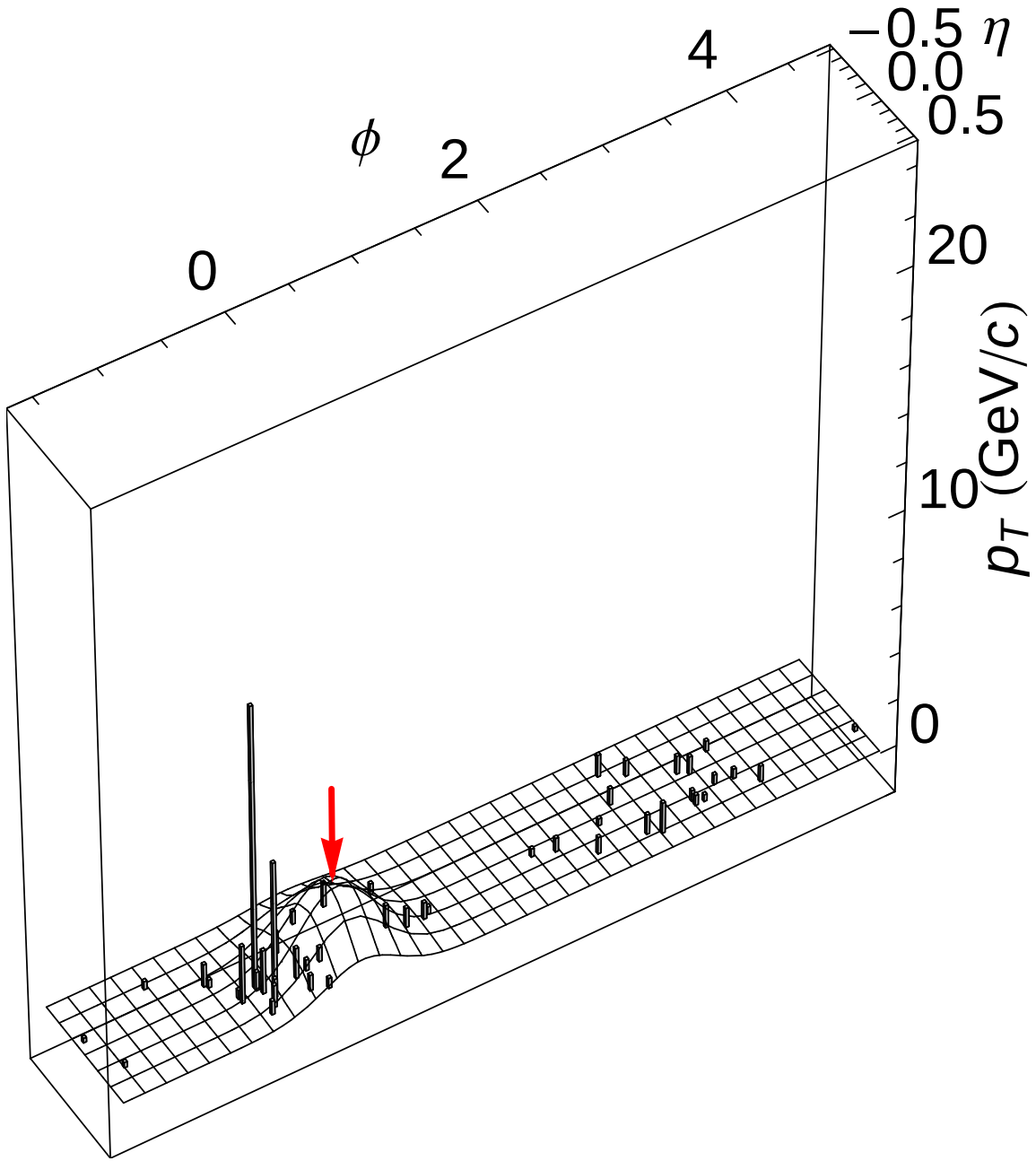
ϕ
0
2
4
η
−0.5
0.0
0.5
p_T (GeV/c)
0
10
20

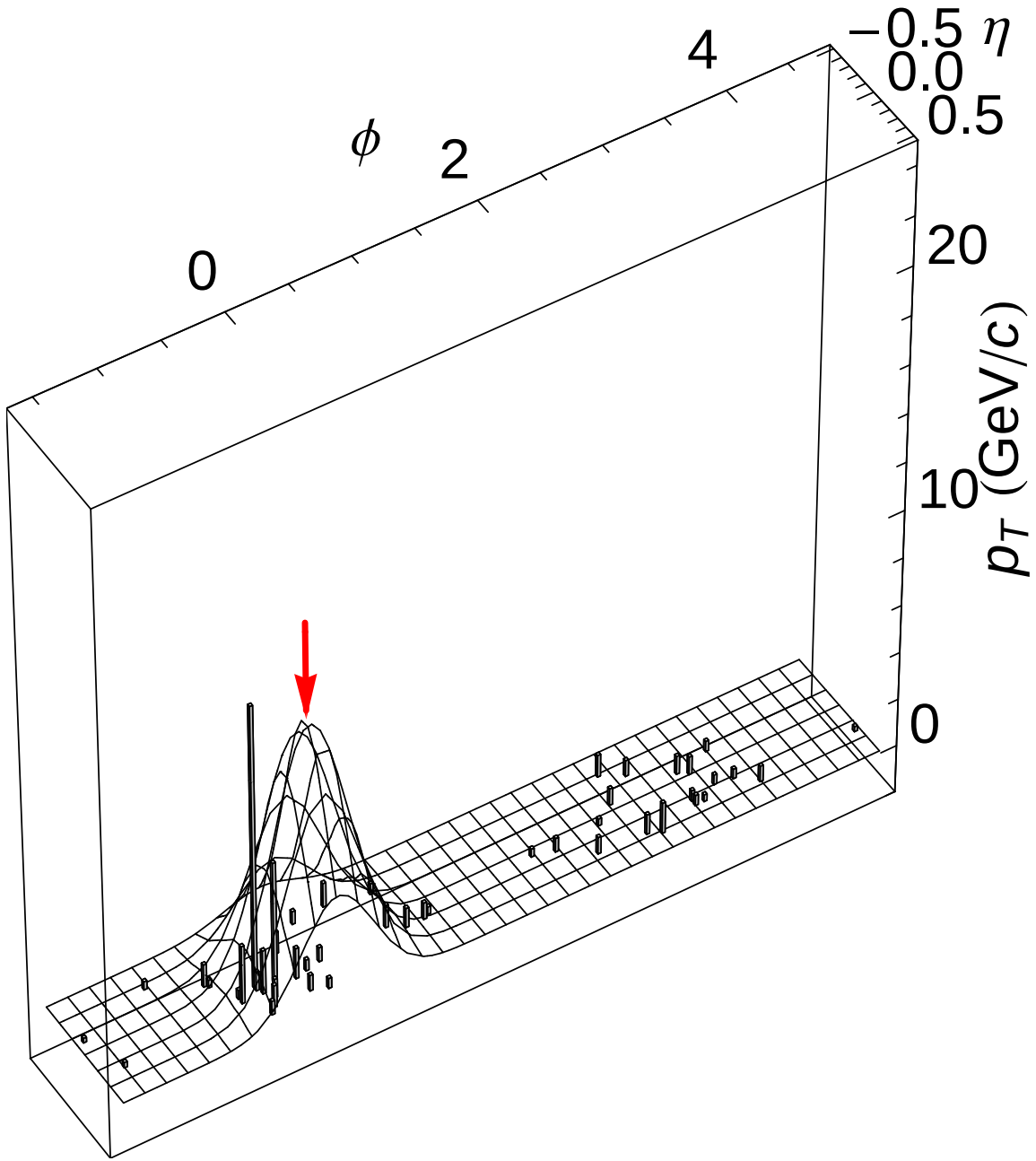
ϕ
0
2
4
η
−0.5
0.0
0.5
p_T (GeV/c)
0
10
20

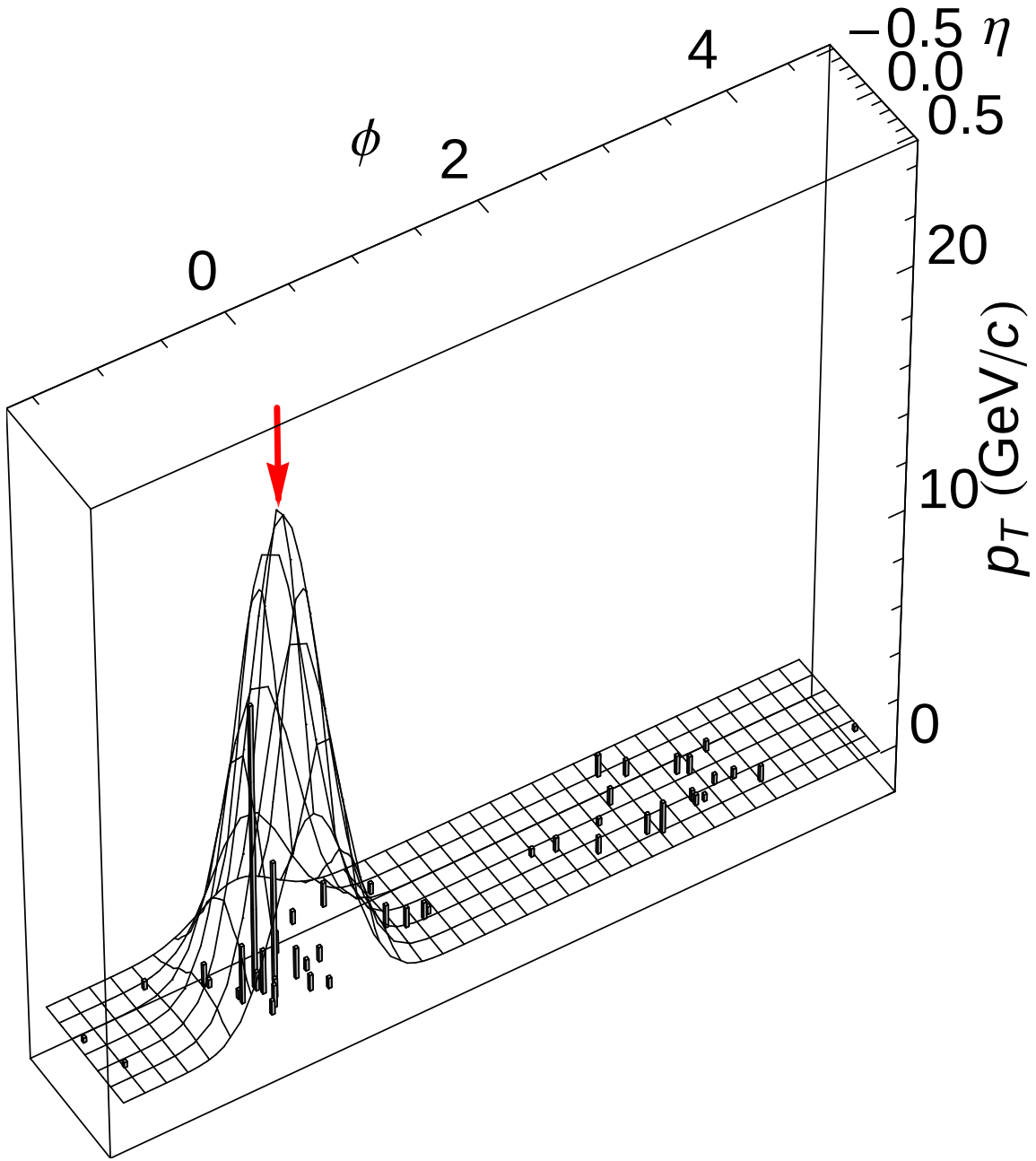
ϕ
0
2
4
η
−0.5
0.0
0.5
p_T (GeV/c)
0
10
20

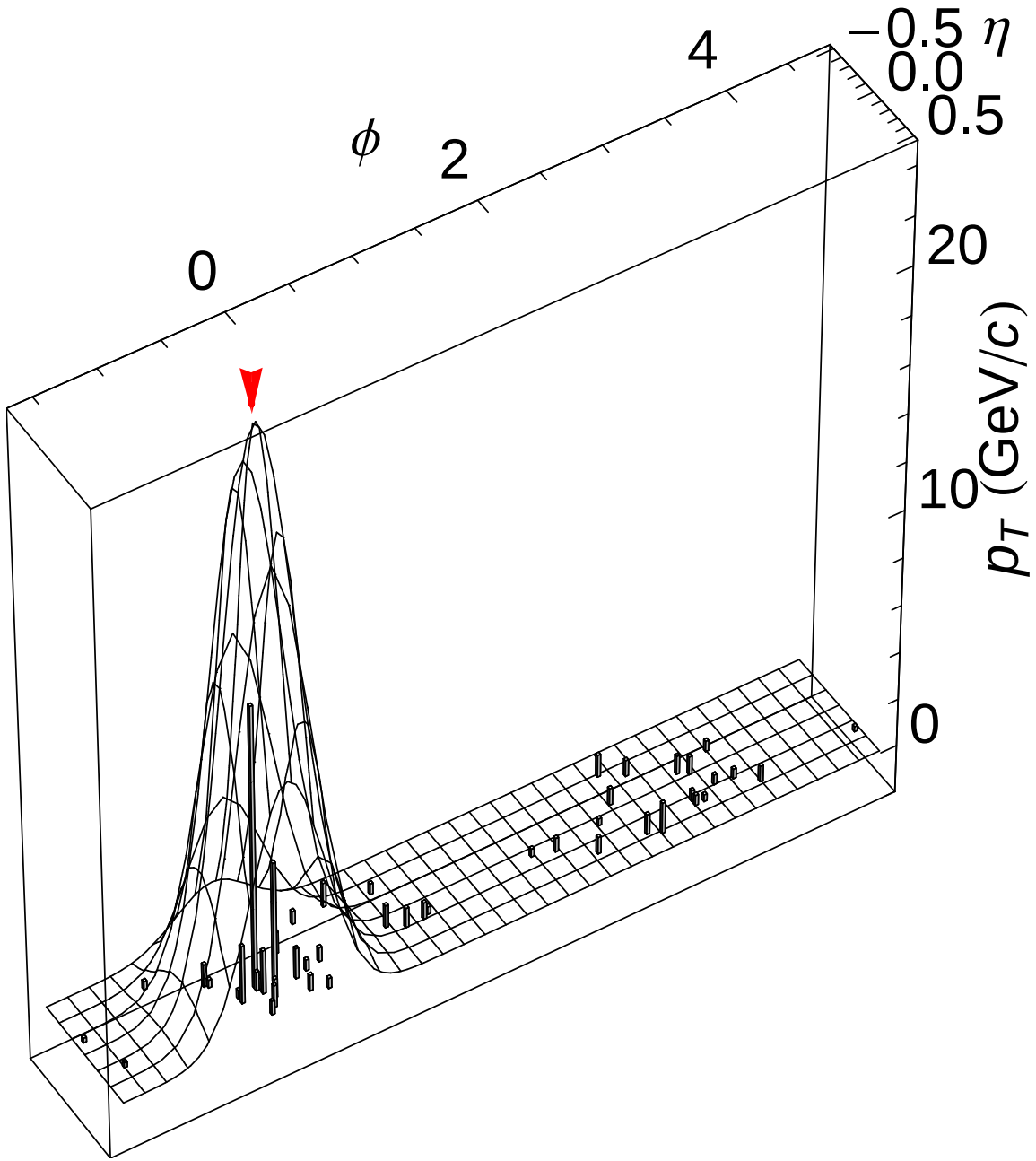
ϕ
0
2
4
η
−0.5
0.0
0.5
p_T (GeV/c)
0
10
20

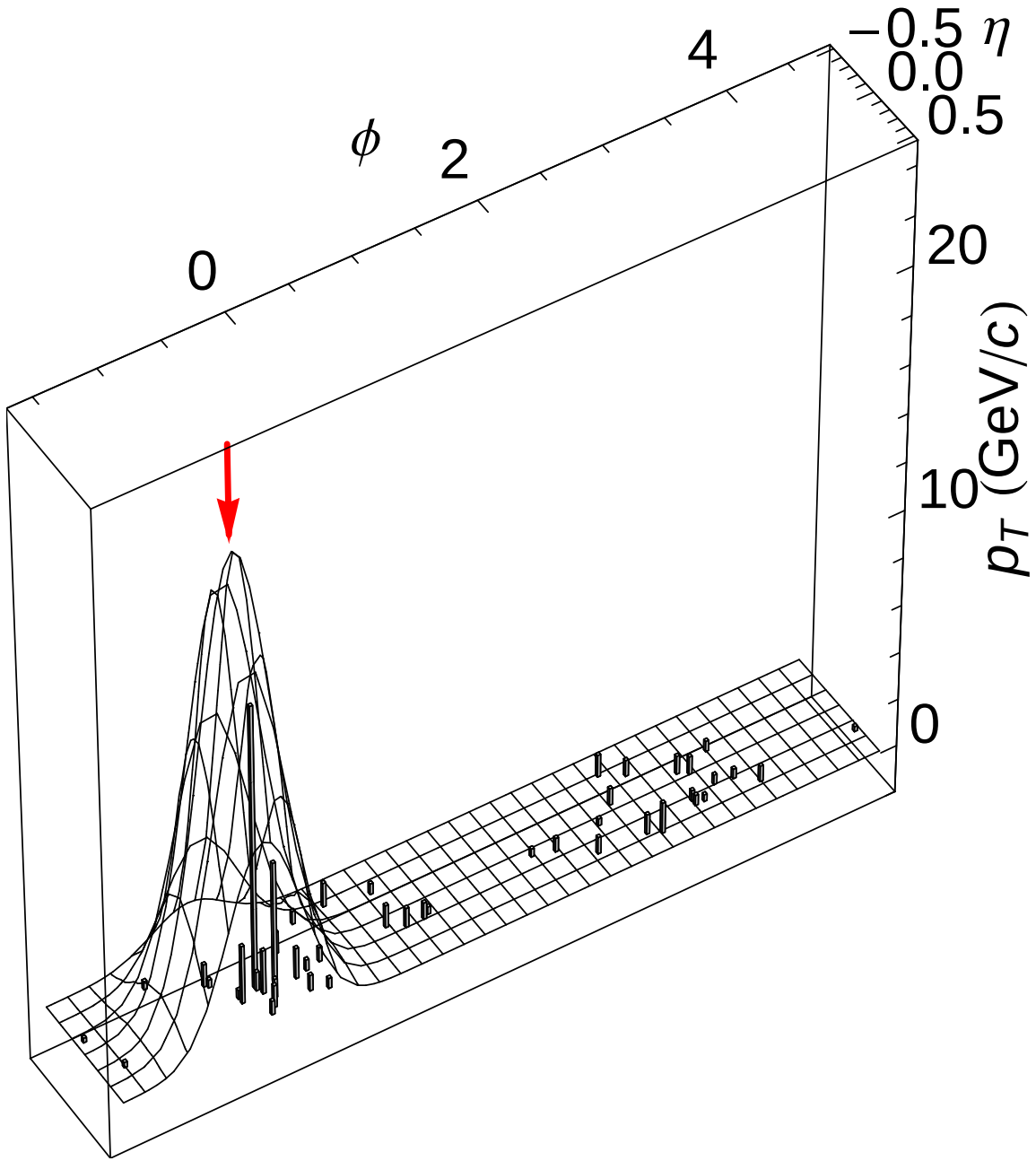
ϕ
0
2
4
η
−0.5
0.0
0.5
p_T (GeV/c)
0
10
20

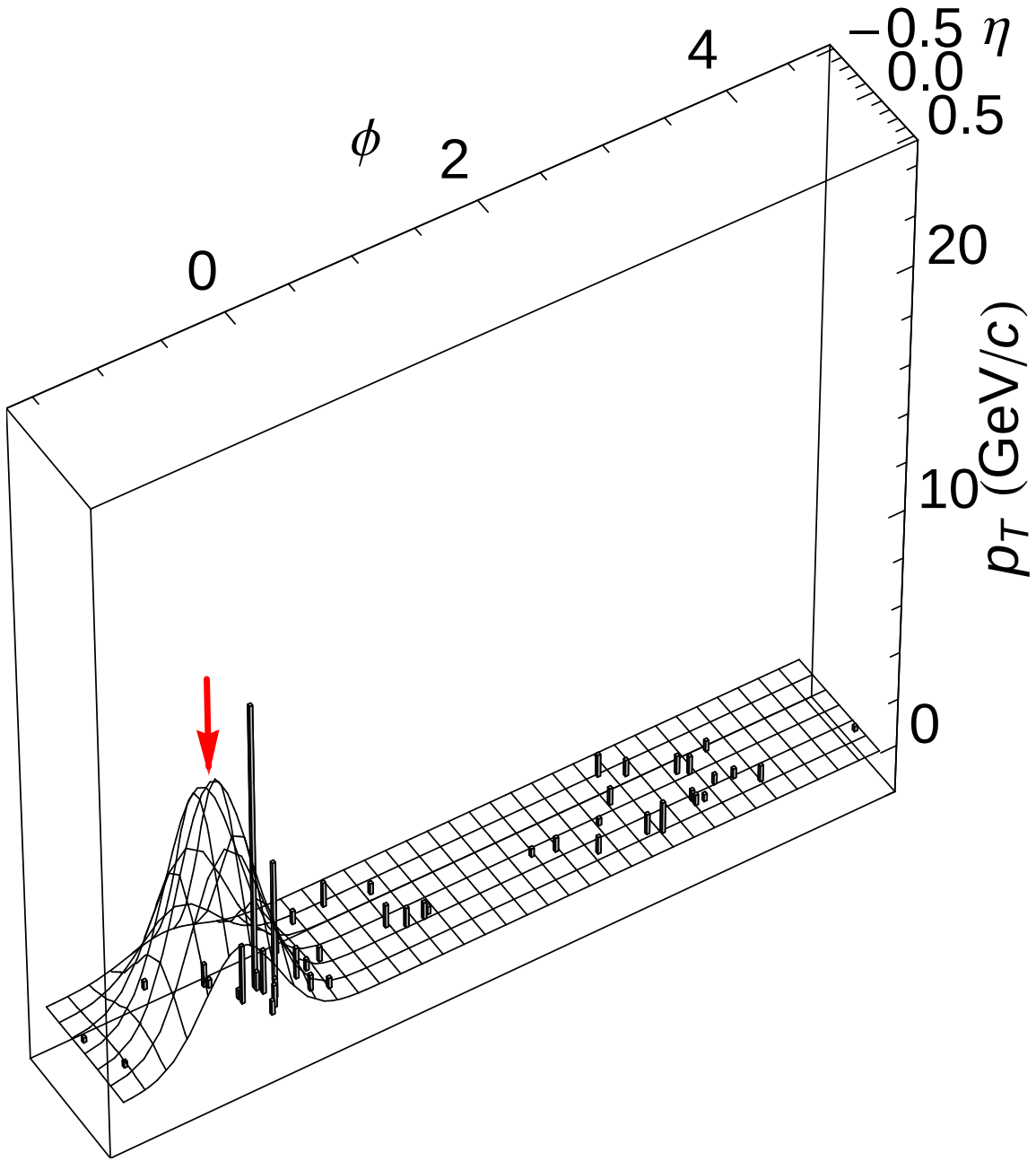
ϕ
0
2
4
η
−0.5
0.0
0.5
p_T (GeV/c)
0
10
20

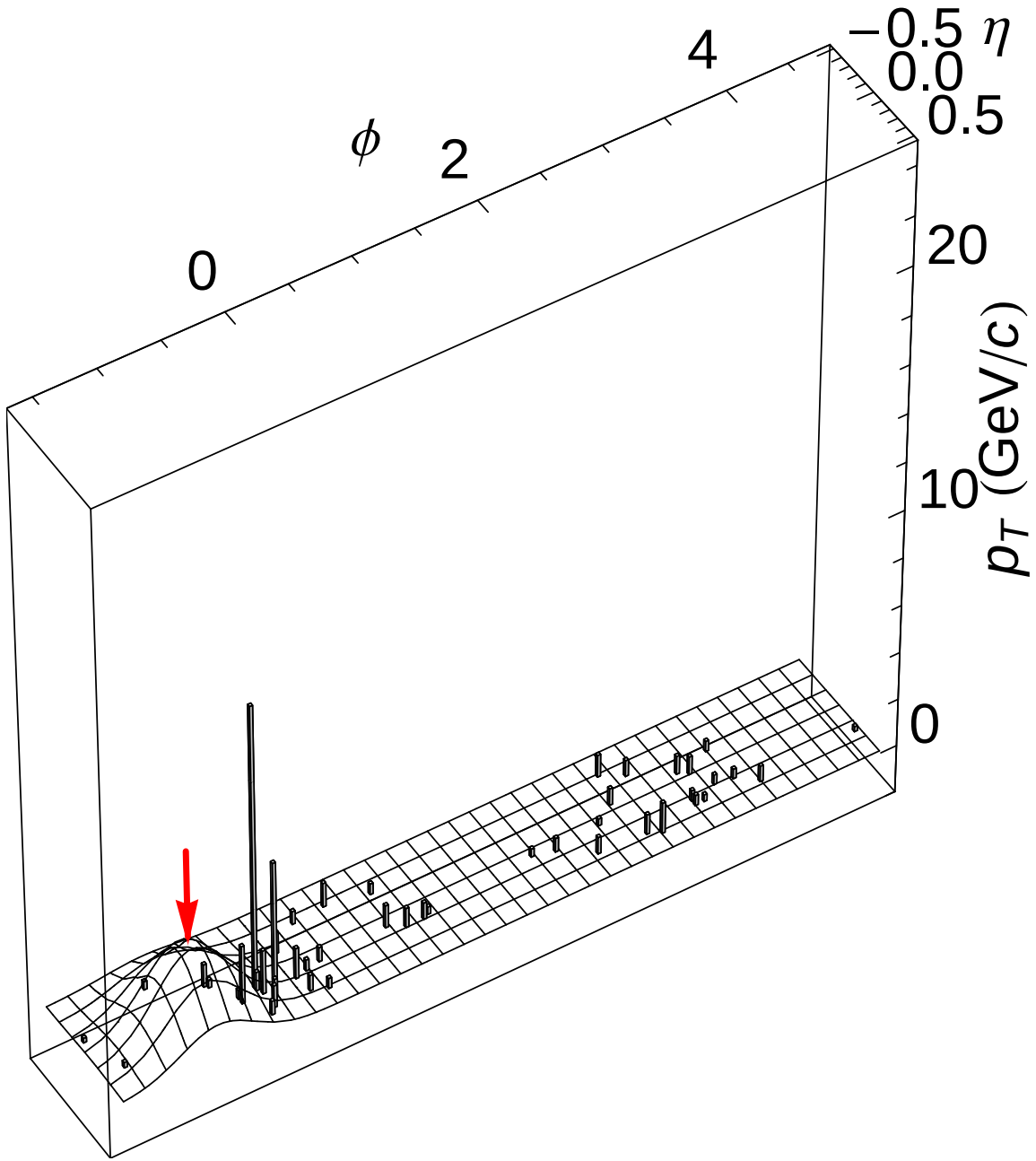
ϕ
0
2
4
η
−0.5
0.0
0.5
p_T (GeV/c)
0
10
20

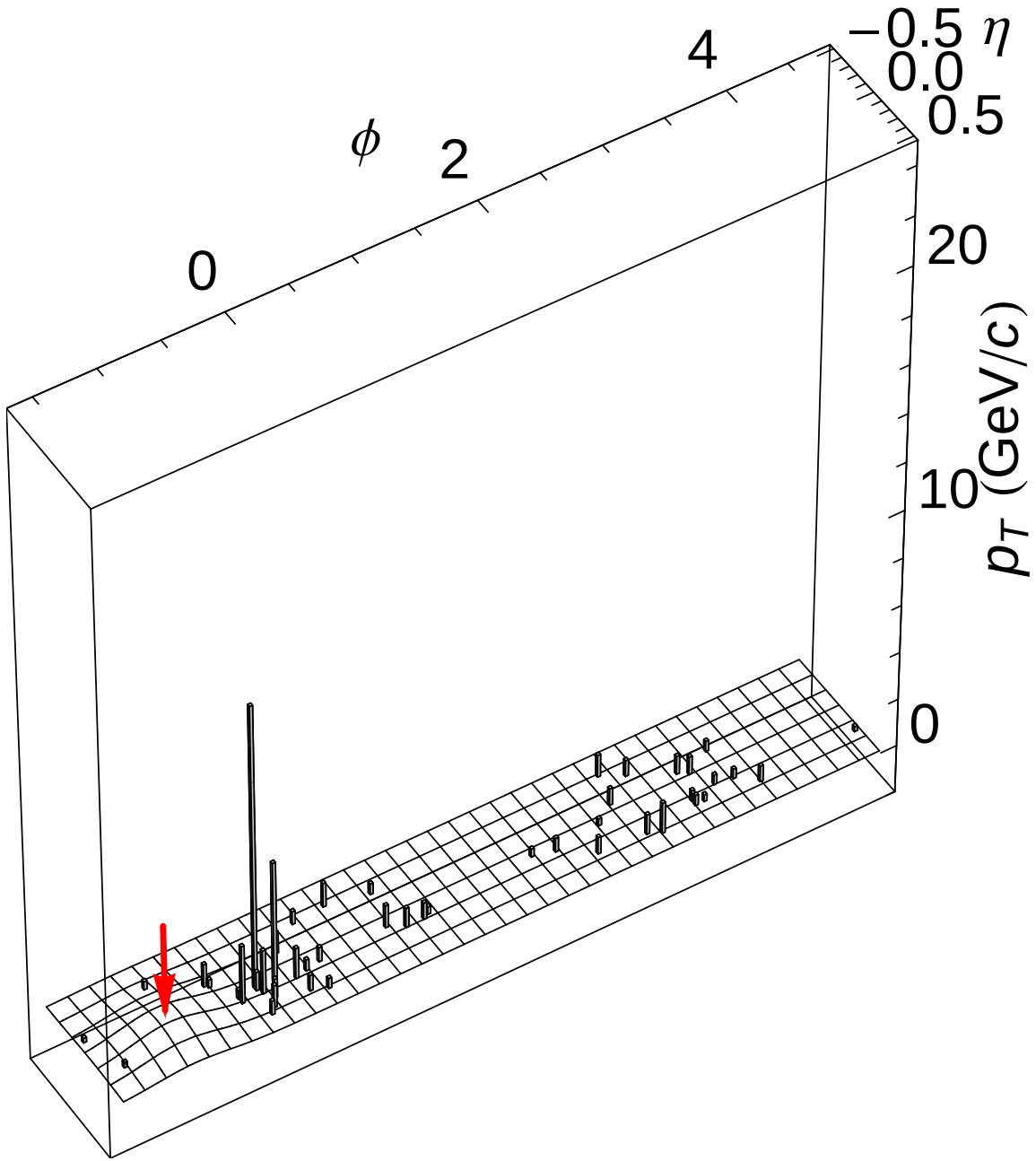
ϕ
0
2
4
η
−0.5
0.0
0.5
p_T (GeV/c)
0
10
20

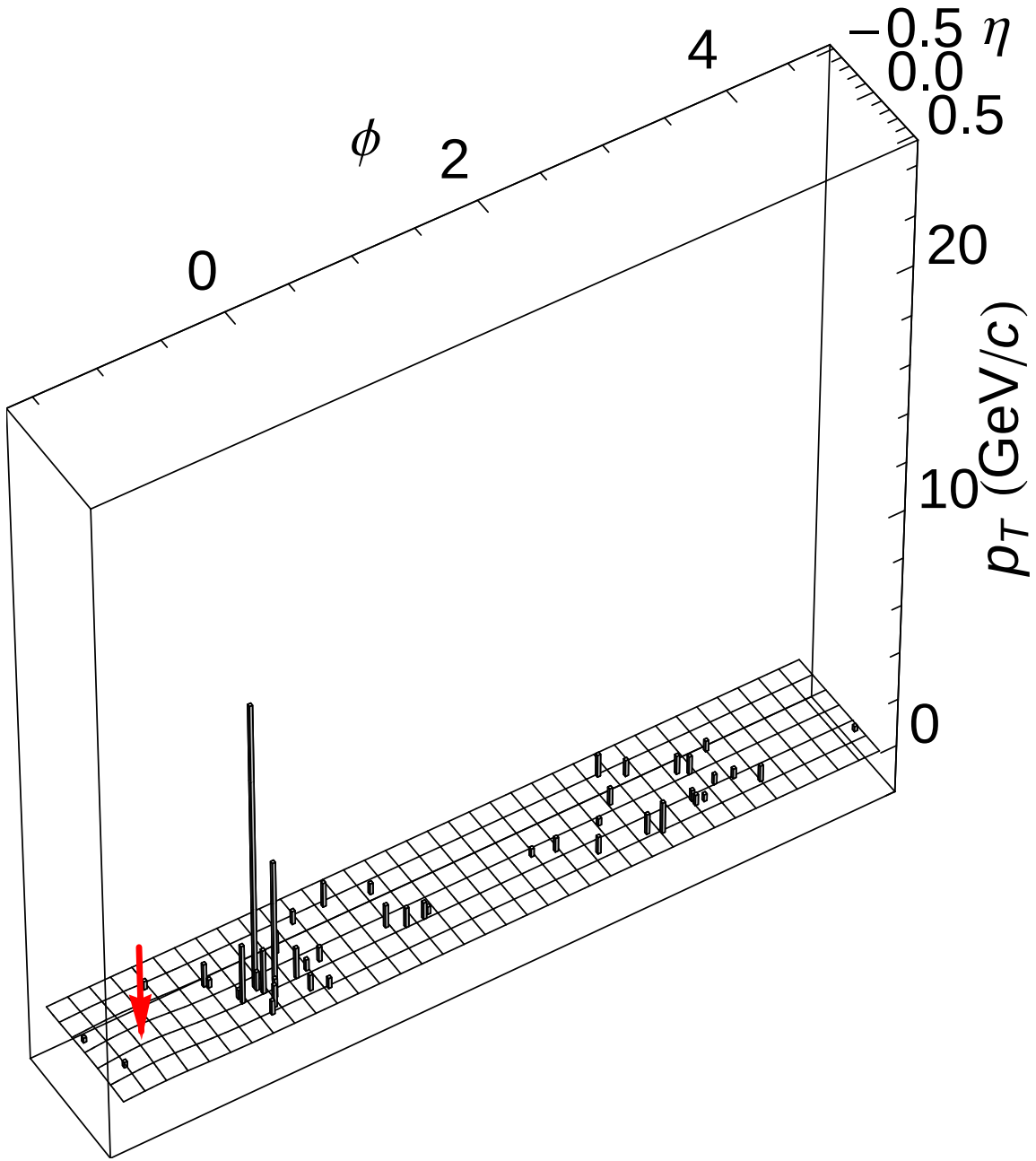
ϕ
0
2
4
η
−0.5
0.0
0.5
p_T (GeV/c)
0
10
20

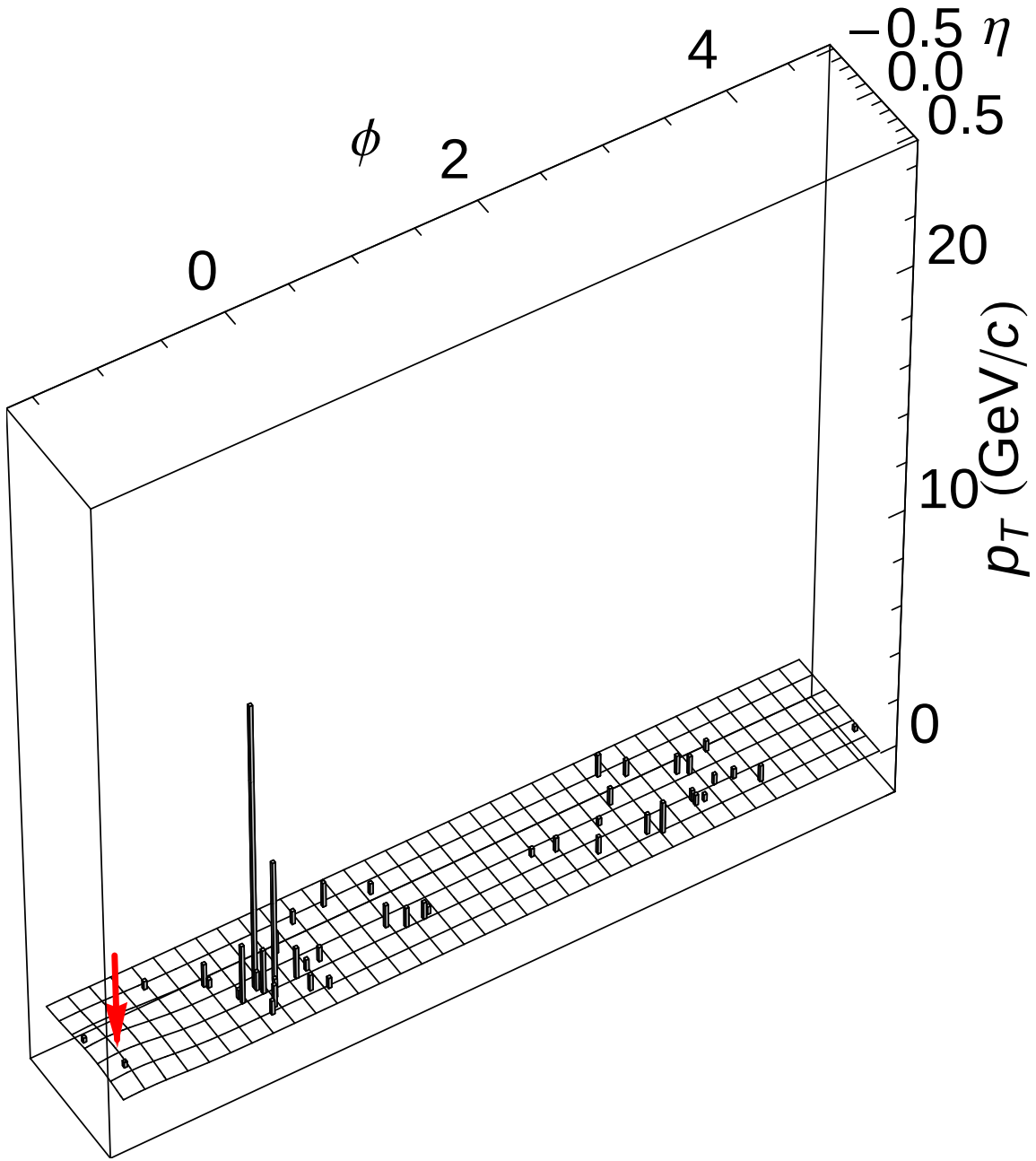
ϕ
0
2
4
η
−0.5
0.0
0.5
p_T (GeV/c)
0
10
20

Implementing the Gaussian Filter

- Stage 1: Calculate a discrete (η, φ) histogram from all particles in the event (usually the calorimeter already sets a minimum meaningful discretization)
- Stage 2: Apply a recursive digital Gaussian filter
  - Filter is a recursive (IIR) design for efficiency
  - Obtains an approximate ($\Delta R \approx 0.03$) position of the jet
- Stage 3 (for heavy ion): Subtract the underlying event
  - Underlying event is pre-convolved with the Gaussian filter
  - Resulting function is parametrized (L_∞ approximation) using Chebyshev polynomials
  - 5×17 order polynomial is accurate to $\Delta E < 30$ MeV for PHENIX and Cu + Cu
- Stage 3: Continuously optimize the discrete maxima
  - Robust trust-region/line search algorithm

Gaussian filter implemented this way is $\approx 1.9\times$ as fast as FastJet at $dN_{\mathrm{ch}}/d\eta = 858$ (HIJING central Au + Au)!

RHIC Complex

- Two independent intersecting storage rings
- Accelerates p up to $E = 250$ GeV
- Accelerates d, Cu, Au, U up to $E = 100\,A$ GeV

PHENIX Subsystems

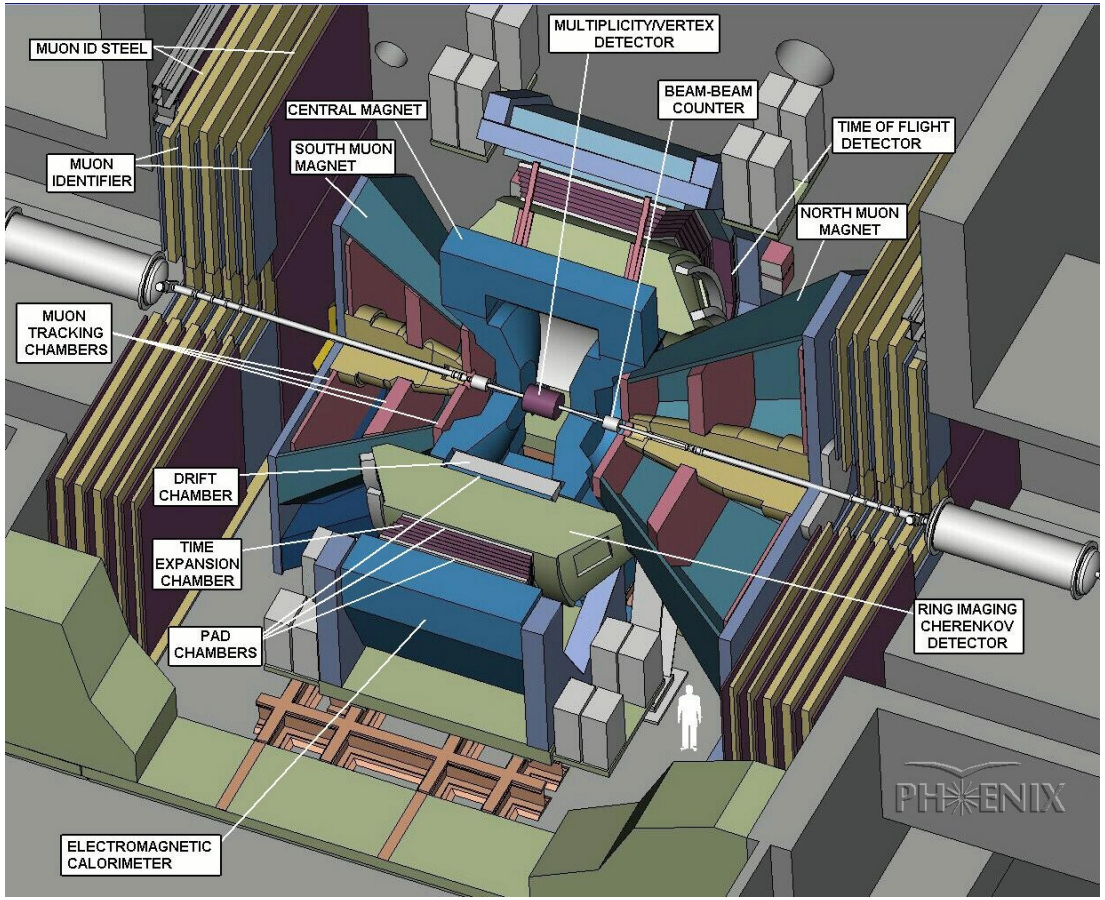

- Nonhermetic detector, dipole field
- Tracking + electromagnetic calorimeter only
- Central arms $\Delta\varphi = \pi, |\eta| < 0.35$, projective except for pad chambers

Particle Identification

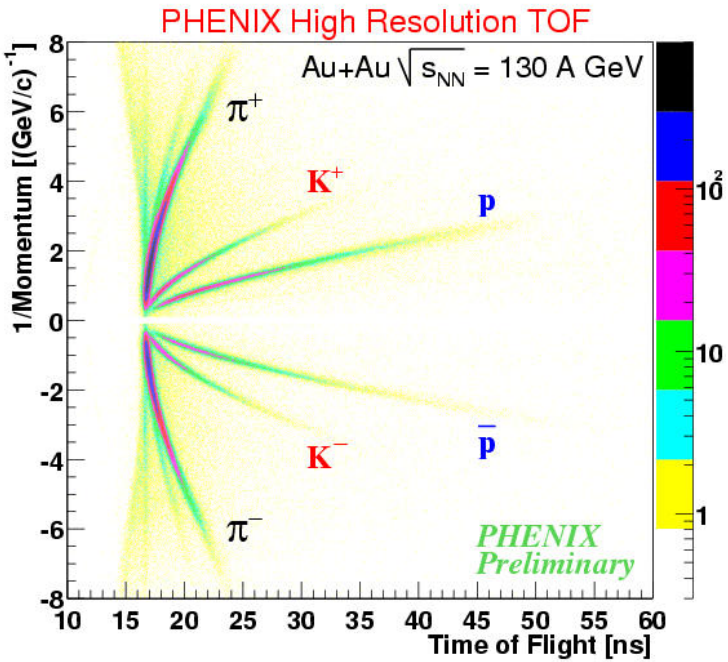

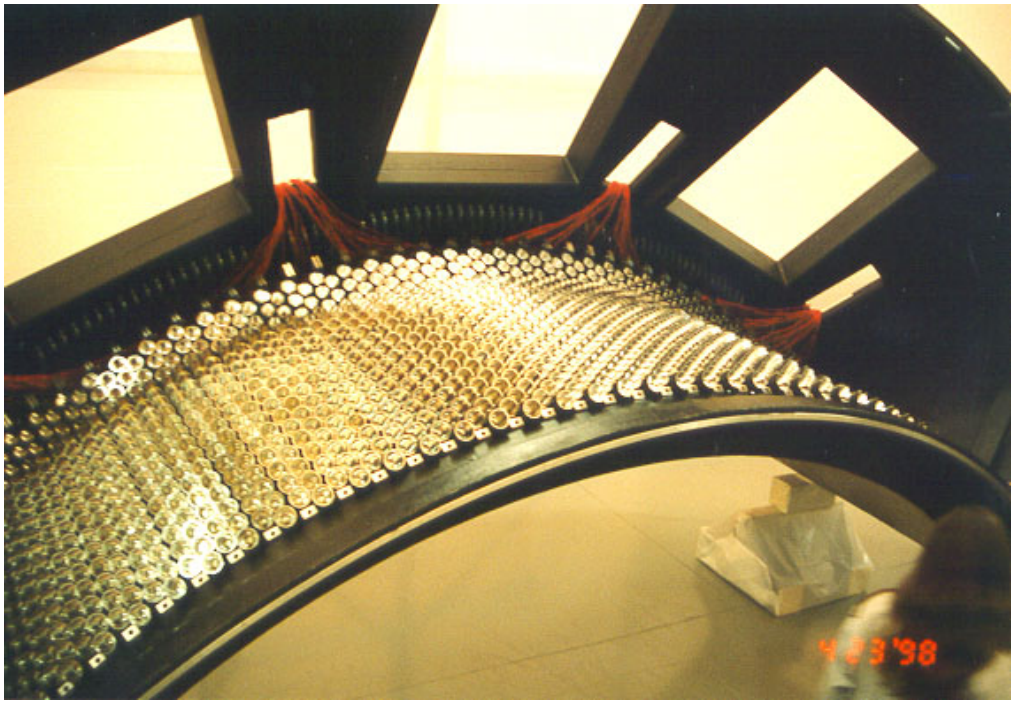

- High-resolution time-of-flight with 100 ps resolution, determines the tracking momentum scale with $\pi^{\pm}, K^{\pm}, p/\bar{p}$
- Ring-imaging Cherenkov detects $e^{\pm}$ up to the $\pi^{\pm}$ threshold of $p = 4.9$ GeV$/c$

Drift Chamber/Pad Chamber

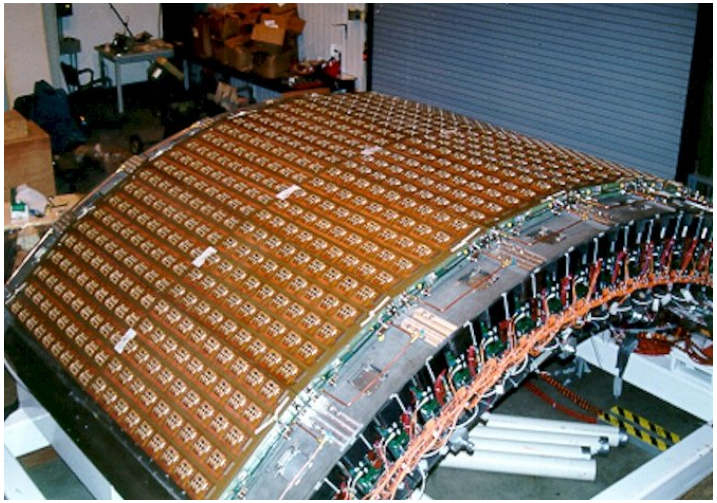

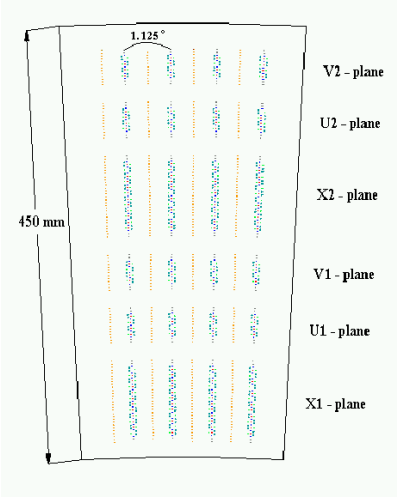

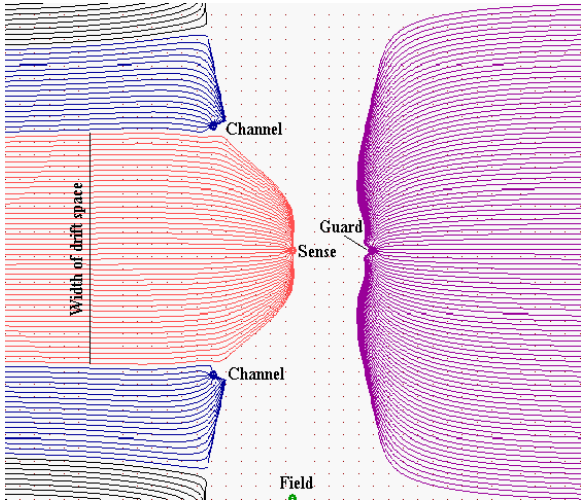

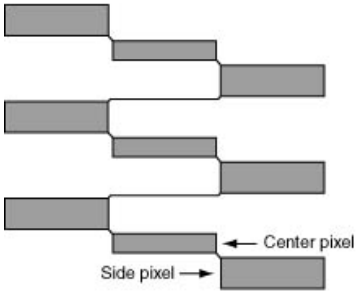

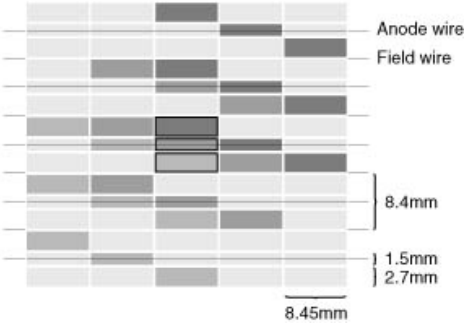

- DC using a focusing geometry
- Energy scale determined by high-resolution time-of-flight
- Pad chambers are nonprojective

Electromagnetic Calorimeter

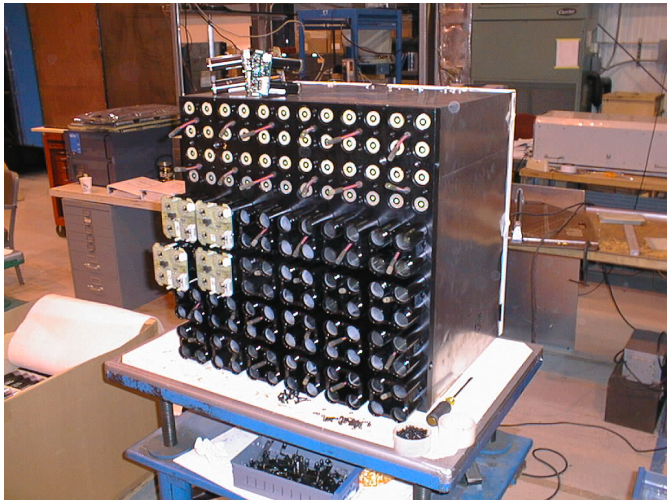

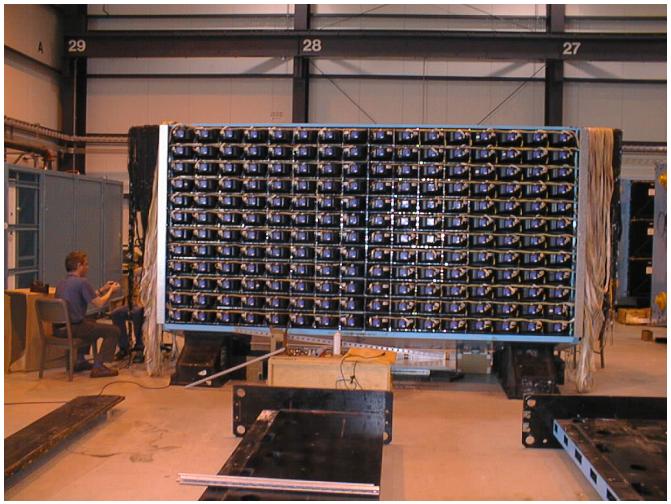

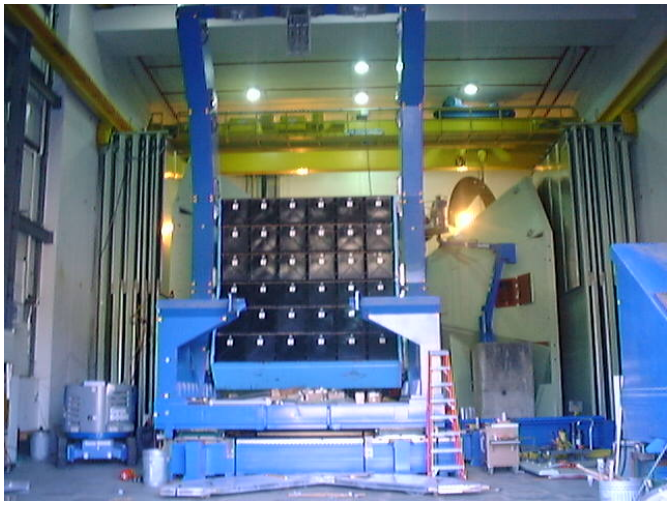

- 6 sectors sampling Pb–scintillator (PbSc), $18X_0$, $\Delta\eta \times \Delta\varphi \approx 0.01 \times 0.01$
- 2 sectors Cherenkov Pb–glass (PbGl), $16X_0$, $\Delta\eta \times \Delta\varphi \approx 0.0075 \times 0.0075$

Minimum Bias Trigger

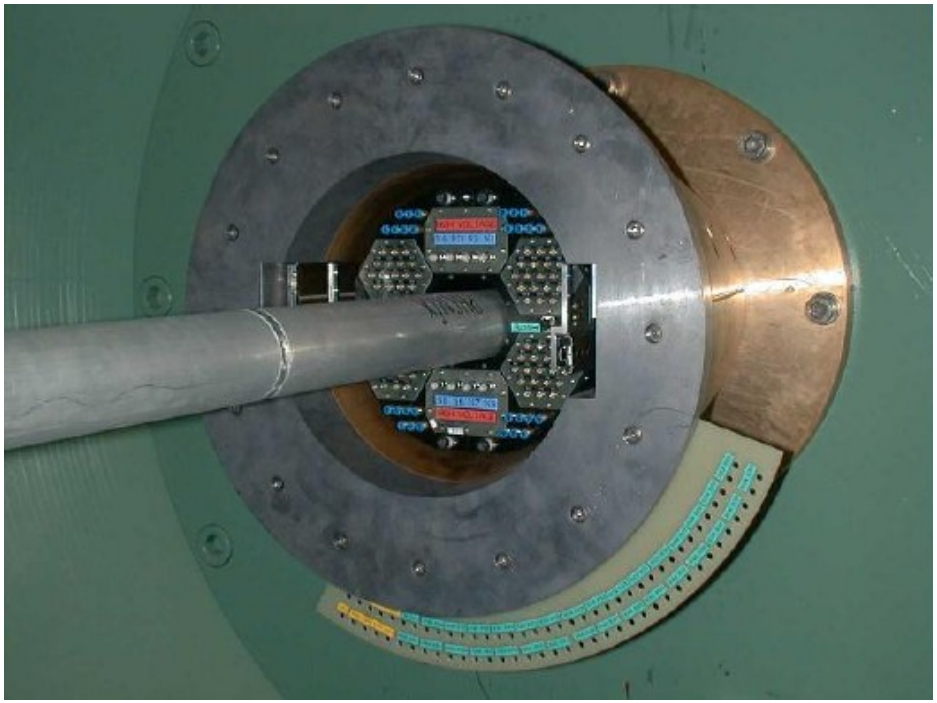

- PHENIX minimum bias trigger: Coincident phototube firing (threshold $\approx$ 0.125 GeV) in the north/south BBC
- Trigger sees $\approx$ 50% of the σ_{inel}
- Trigger sees $\approx$ 90% of high-p_T jets
- Cross section determination using BBC + wall current monitor (WCM) with vernier scan

Electromagnetic Calorimeter–RICH Trigger

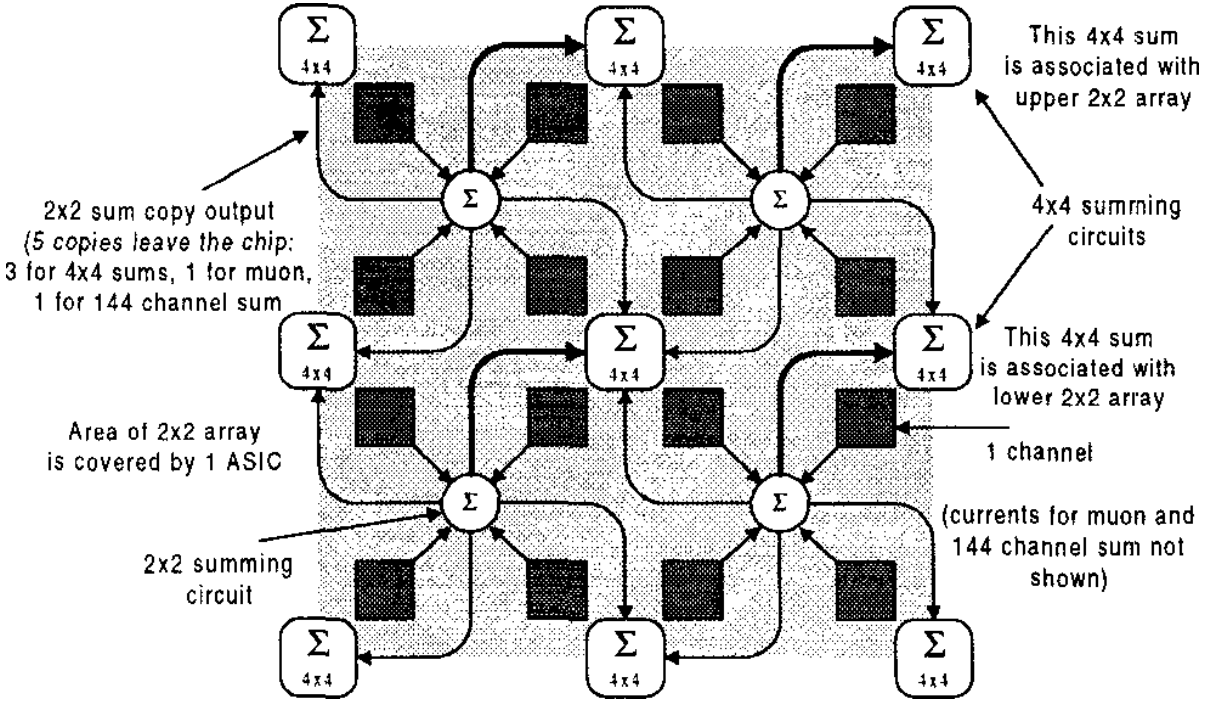

- Nonstaggered analog 2×2 and staggered analog–digital 4×4 sum
- 2×2 threshold: $\approx$ 800 MeV
- 4×4 thresholds: $\approx$ 1.4, 2.1, 3.5 GeV

S.S. Frank, IEEE Nuclear Science Symposium 1997

Centrality Determination

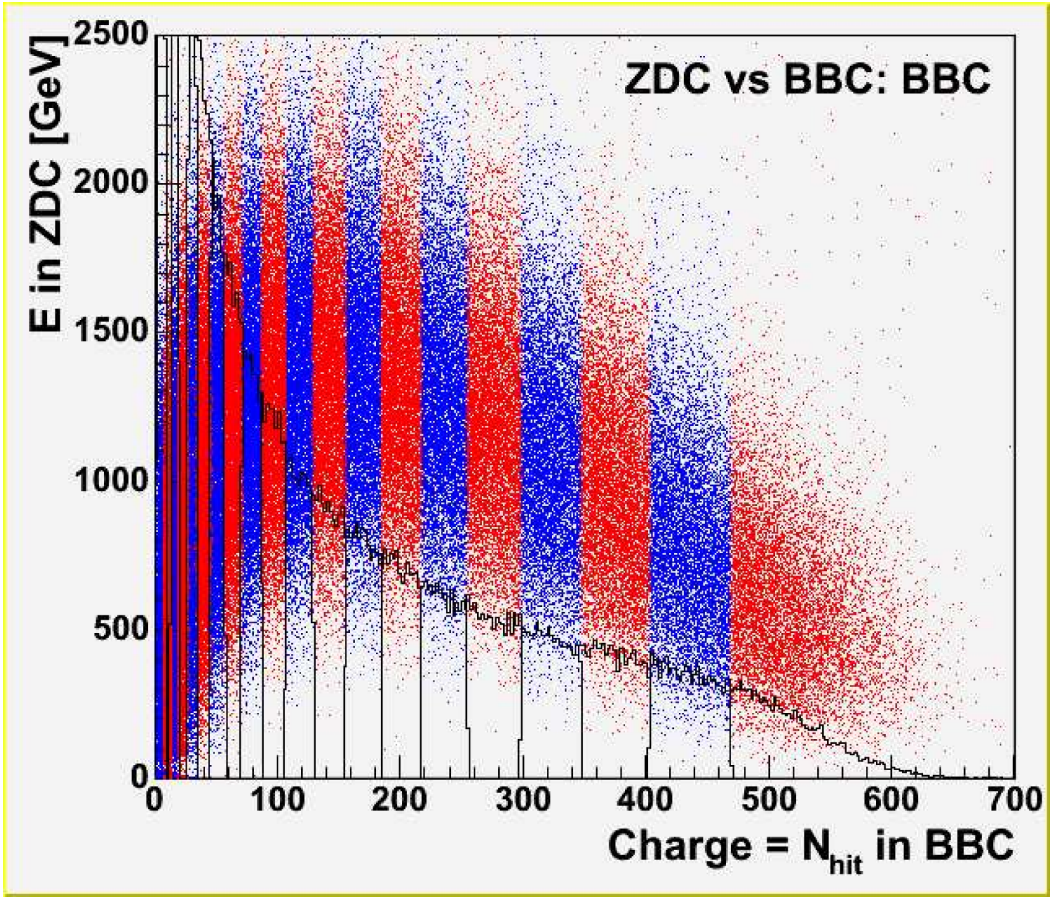

- Centrality is sliced into fractions of the total minimum bias trigger count
- Centrality in Cu + Cu determined by BBC only

Heavy Ion Collision

Glauber model: nuclear overlap function T_{AB} convolution of two thickness functions

$$T_{AB}(\underline{\mathbf{b}}) = \int d^2\underline{\mathbf{s}}\, T_A(\underline{\mathbf{s}}) T_B(\underline{\mathbf{b}} - \underline{\mathbf{s}})$$

T_{AB} can be used to define the number of collisions

$$N_{\text{coll}} = T_{AB}\sigma_{\text{inel}}$$

Nuclear modification factor (centrality class averaged $\langle T_{AB} \rangle$)

$$R_{AA} = \frac{N_{\text{evt}}^{-1} dN_{\text{CuCu}}/dp_T}{\langle T_{AB} \rangle d\sigma_{pp}/dp_T}$$

Center-to-peripheral modification factor

$$R_{CP} = R_{AA}(\text{central})/R_{AA}(\text{peripheral})$$

Reaction Plane Determination

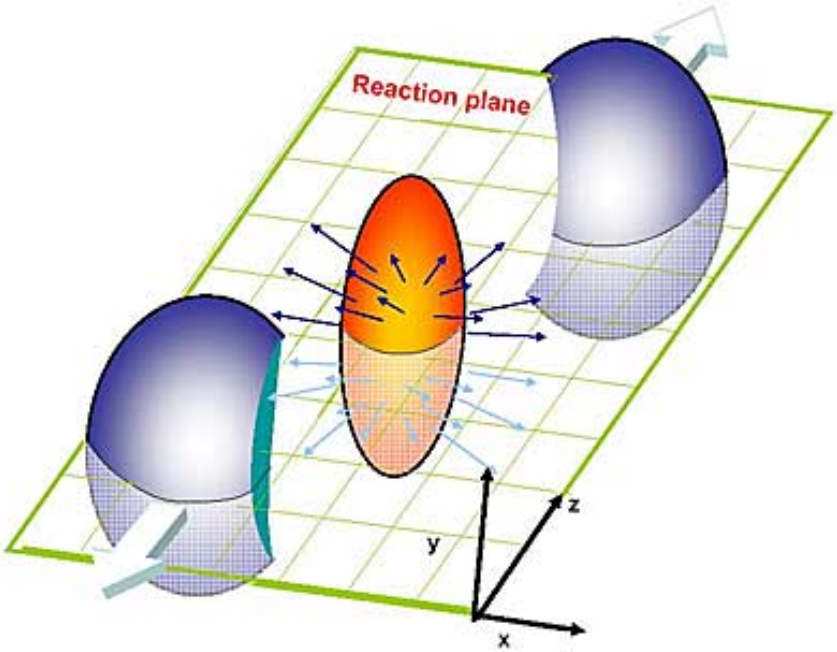

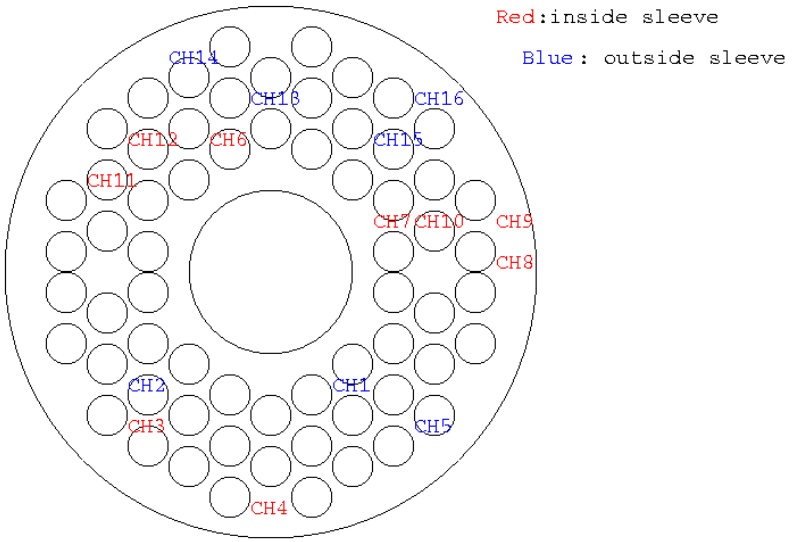

$$Q_x + iQ_y = \sum_{k=1}^{64} q_i e^{2i\varphi_i}$$

$$\Psi = \frac{1}{2}\arg(Q_x + iQ_y).$$

Why Does Jet Reconstruction Work at PHENIX?

- We would like to measure jet variable in a certain $|\eta|$, here $|\eta| < 0.3$
- Jets can have its axis
  - inside PHENIX
    - $\Rightarrow$ Reconstructed inside PHENIX, normal detector energy response (corrected using unfolding)
  - outside PHENIX
    - $\Rightarrow$ Zero to small energy deposit in PHENIX
    - $\Rightarrow$ Has the cross section of a high-p_T jet, but energy of a low-p_T jet
    - $\Rightarrow$ Contribute negligibly to low-p_T jet cross section (and correctable using unfolding)

Particle to Jet

- There is no hadronic calorimeter
  - Long-lived neutral hadrons (n, K_L^0, ...) completely lost
  - Tracking needed to reconstruct charged hadrons
  - Tracking has a background constant with p_T (exacerbated by no in-field tracking)
- Ring-imaging Cherenkov detector used to reject conversion $e^{\pm}$, inefficiency for $\pi^{\pm} > 4.9$ GeV$/c$
- Clusters matching tracks are ignored
- Remaining clusters are merged with tracks
- Apply jet reconstruction

Event display, $p + p$

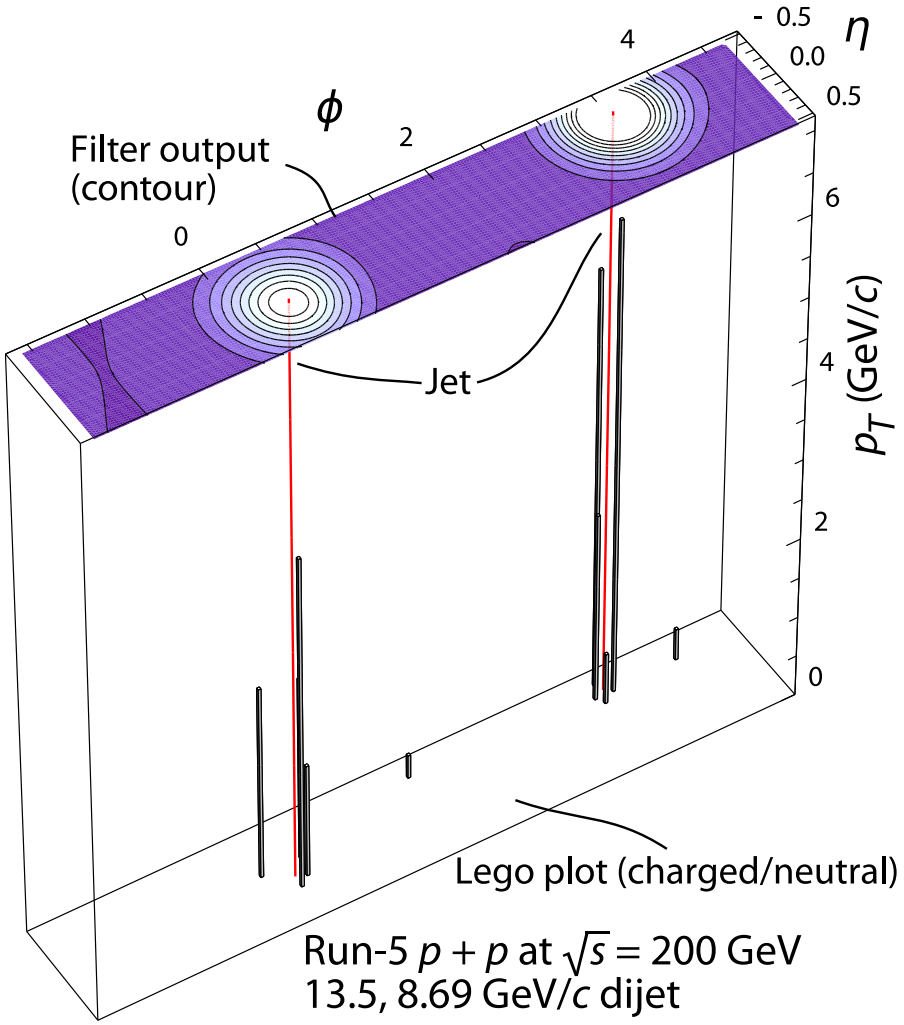

Run-5 $p + p$ at $\sqrt{s} = 200$ GeV
13.5, 8.69 GeV/c dijet

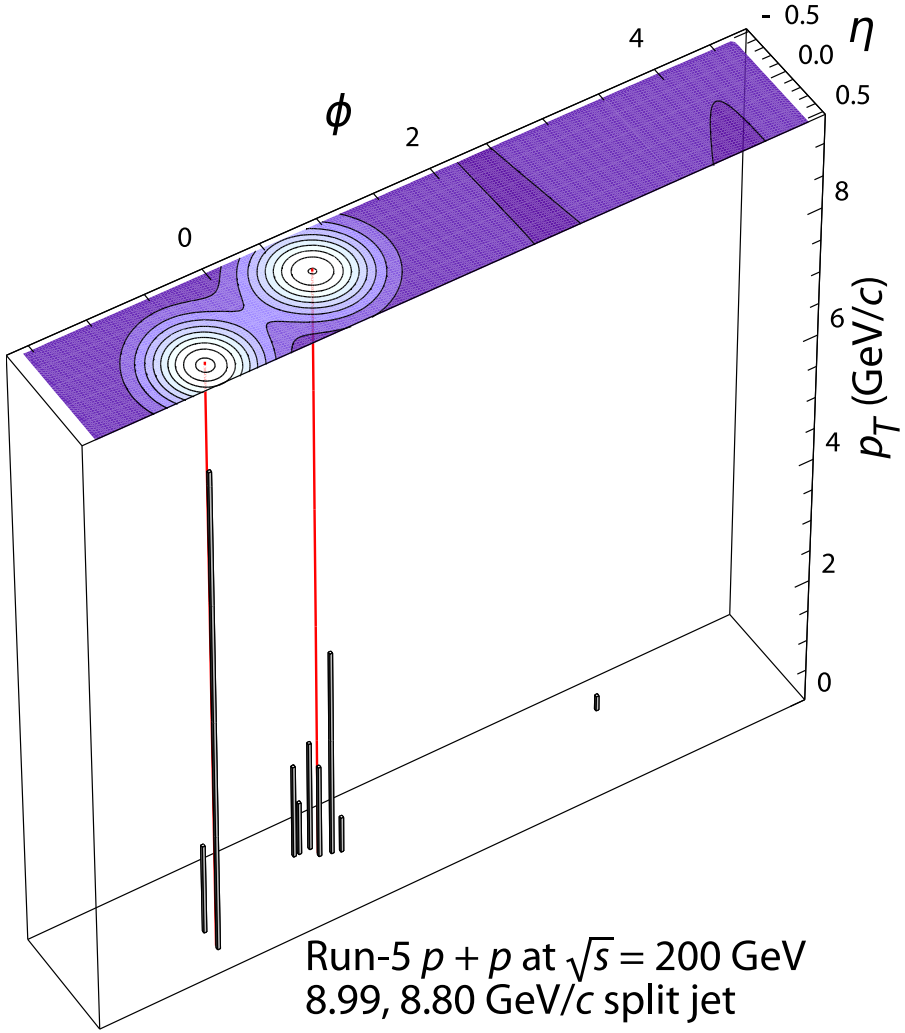

Run-5 $p + p$ at $\sqrt{s} = 200$ GeV
8.99, 8.80 GeV/c split jet

Jet Energy Scale

p_T

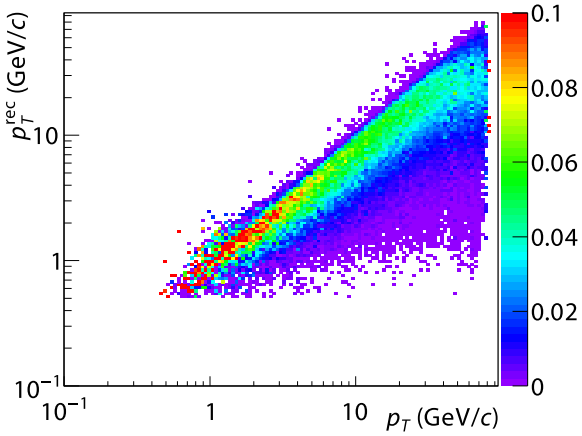

p_T^{pp}

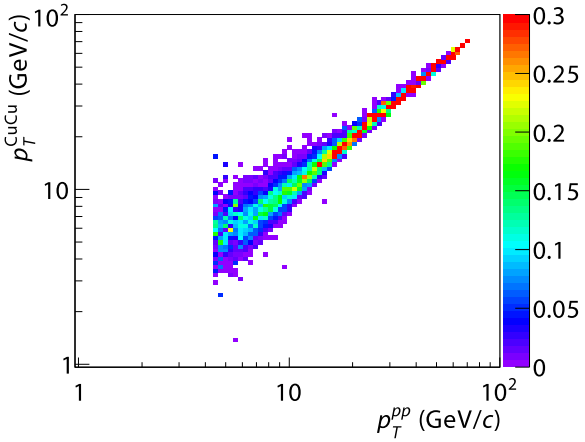

p_T^{CuCu}

- p_T: Particle level, hadronized particles in a perfect detector
- p_T^{pp}: Detector level, with PHENIX acceptance and inefficiencies
- p_T^{CuCu}: Detector level, with PHENIX acceptance and inefficiencies plus Cu + Cu underlying event

(Truth to) $p+p$ Jet Energy Scale

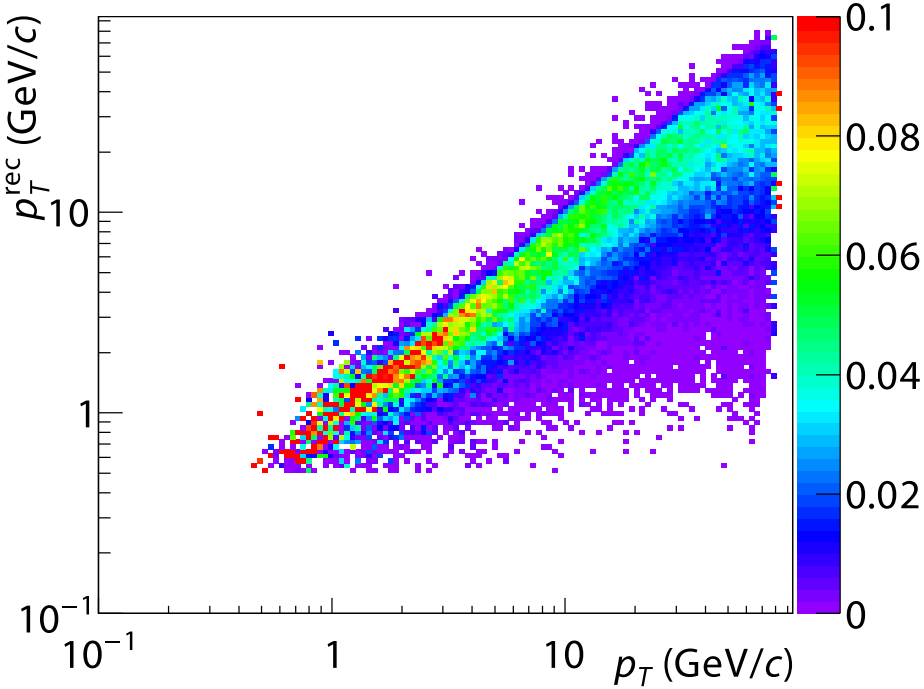

Gaussian filter, $\sigma = 0.3$

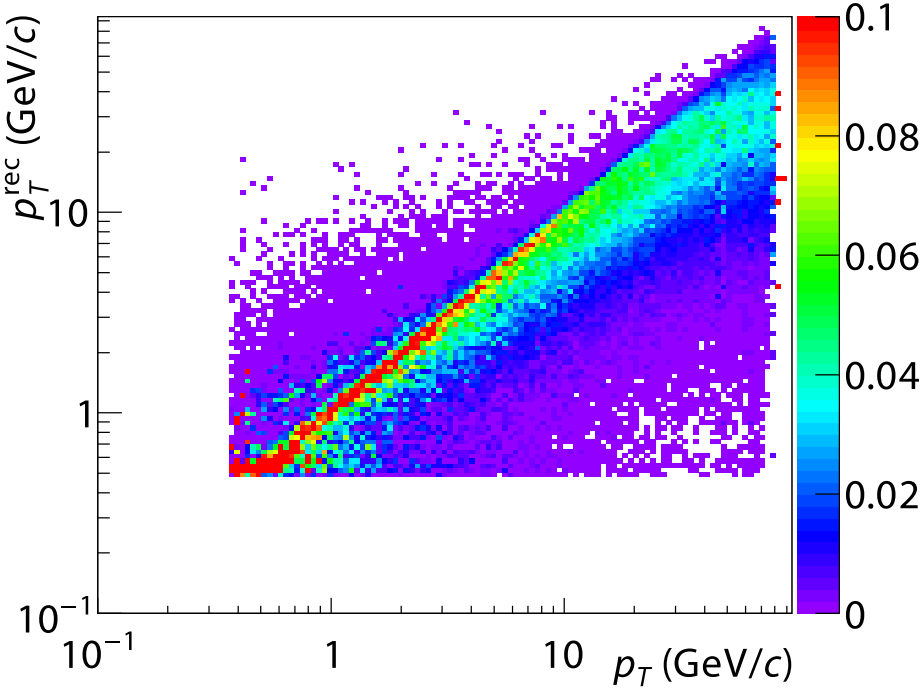

Anti-$k_\perp$, $D = 0.3$

- Gaussian filter has little $p_T^{rec} > p_T$ fluctuation (good for unfolding with a limited acceptance)
- Anti-$k_\perp$ is narrower at low p_T due to discrete particles/no weighting

Unfolding: Phillips–Tikhonov Regluarization

- Notation:
  - A: transfer matrix
  - x: unfolded spectrum
  - b: measured spectrum
  - B: covariance matrix of measurement
  - τ: regularization parameter (related to singular values of A)
  - C: 2nd order finite derivative (rows $= 0, \ldots, 0, -1, 2, -1, 0, \ldots, 0$)
- Simple least square: $\|Ax - b\|_2 = \min$
- Least square with errors: $\|Ax - b\|_2^{B^{-1}} = (Ax - b)^T B^{-1} (Ax - b) = \min$
- Least square with regularization: $\|Ax - b\|_2^{B^{-1}} + \tau \|Cx\|_2^{B^{-1}} = \min$
- Scaled least square with regularization: Replace $x_i = w_i x_{\mathrm{ini},i}$

Unfolding: Other Types

- Richardson–Lucy
  - Iterated, multiplicative ratio correction with reblurring
  - Systematic uncertainty hard to quantify (since iterated)
  - Widely mislabeled as "Bayesian unfolding" after G. D'Agostini's 1994 paper – it is not, and shown to be maximum-likelihood by L. A. Shepp, Y. Vardi 1982 (!)
- Van Cittert and Landweber algorithm
  - van Cittert is the iterative (Neuman series) direct inversion, highly unstable with (Poisson) noise in the transfer matrix
  - Landweber algorithm modifies van Cittert by reblurring using $\mathbf{A}^T$
  - I developed a x_{ini} scaled Landweber algorithm for unfolding steep spectra
  - Problem: PHENIX $\mathbf{A}$ asymmetric $\Rightarrow$ low-p_T drop and high-p_T artifacts

Evaluation of unfolding errors

- Unfolding result $x = (N_1, \ldots, N_n)$
- $P(p_T)$ a polynomial in p_T
- k in range of "meaningful" number of regular equations, typically $k \geq 4$, $k < K_N \approx \frac{K}{2}$ by Nyquist argument, K total number of regular equations
- Nyquist is a guess for the best case
- Statistical error: $\sigma^2_{\text{stat},i} = \sum_j \rho_{ij} N_j$
- Systematic error from $p_T^P(p_T)$ fit, evaluate $(p_T^P(p_T))_k$ for each bin and each s_k, $\sigma^2_{\text{syst},i} = \text{Var}((p_T^P(p_T))_k)$

Run-5 $p+p$ Jet Spectrum

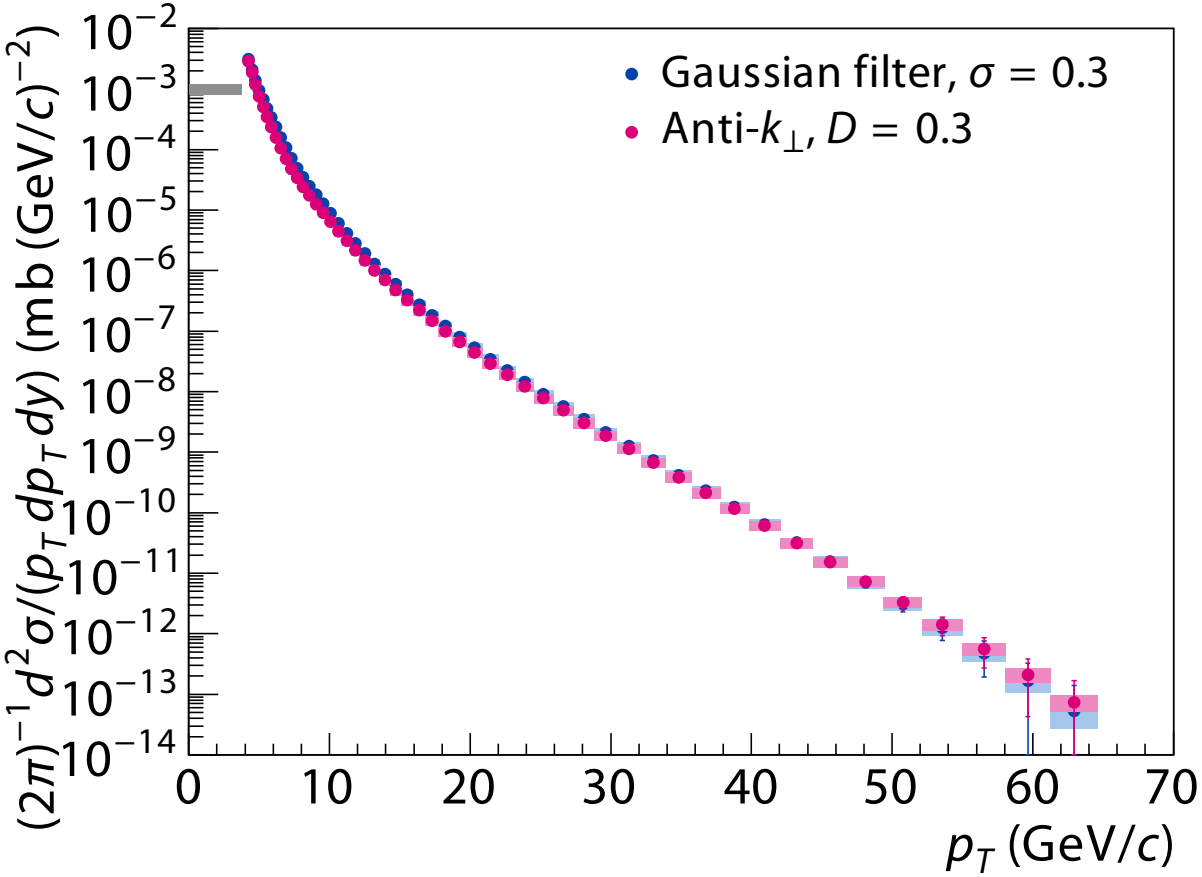

- $\int \mathscr{L} dt = 2.2\,\mathrm{pb}^{-1}$
- Large angle summing of Gaussian filter gives a higher cross section at low p_T
- Lack of angular weighting gives anti-$k_\perp$ a higher cross section at high p_T

Run-5 $p+p$ Jet Spectrum

No.	Description	Magnitude
1	BBCLL1 cross section	10%
2	BBCLL1 efficiency	5%
3	$p+p$ ERT efficiency saturation level	3%
4	minimum bias/ERT normalization matching	5%
5	global energy scale	15%
	quadrature sum	20%

Run-5 $p+p$ Fragmentation Function

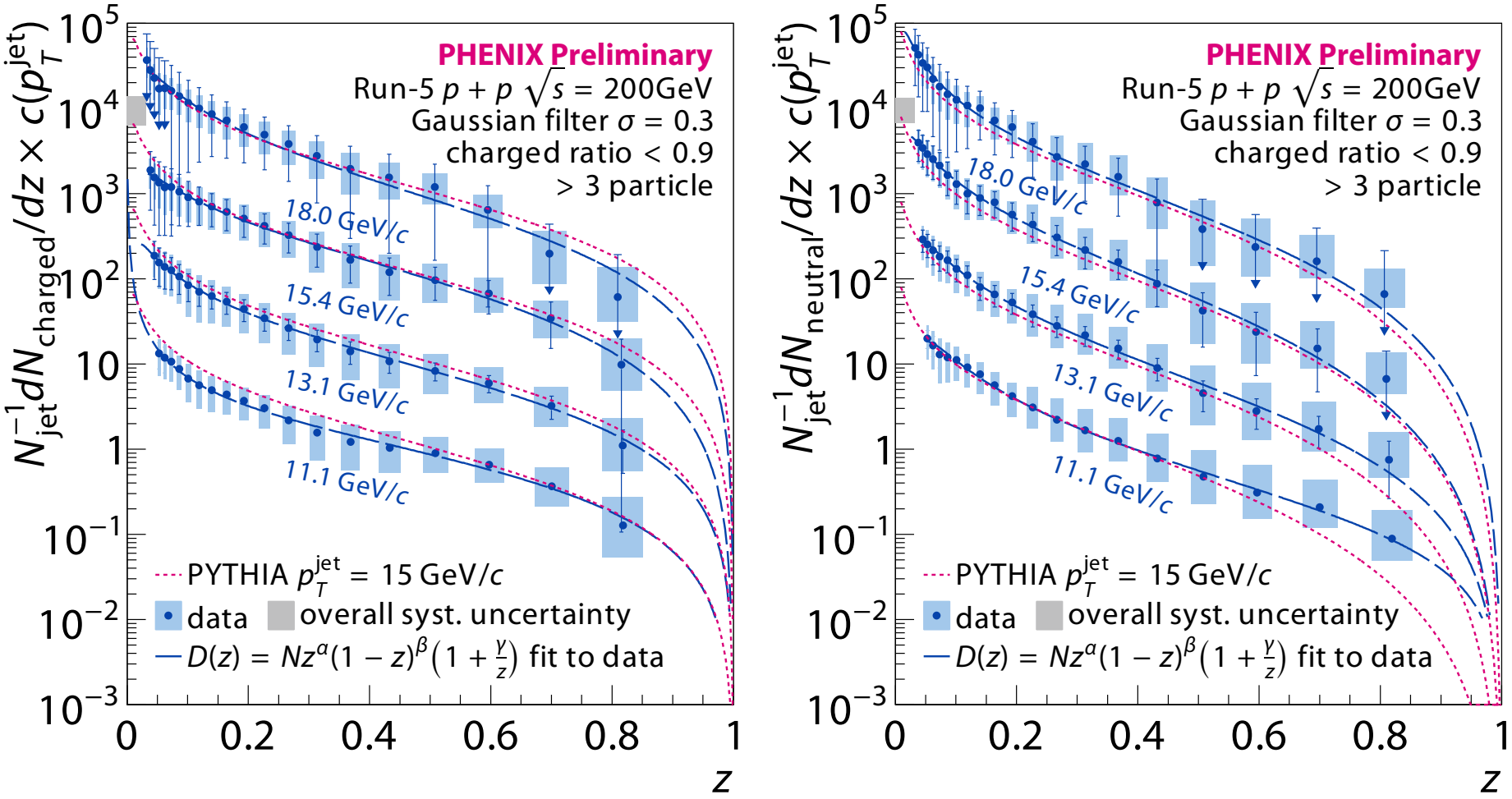

- First time 2D regularized unfolding applied in HEP/NP
- First time any RHIC experiment produced a jet fragmentation function

Run-5 $p+p$ Fragmentation Function

No.	Description	Magnitude
1	Tracking efficiency (z dependence)	10%
2	DC efficiency run dependence	2.6%
	quadrature sum	19%

No.	Description	Magnitude
1	Cluster efficiency (z dependence)	5%

$p+p$ to Cu + Cu Jet Energy Scale (Underlying Event)

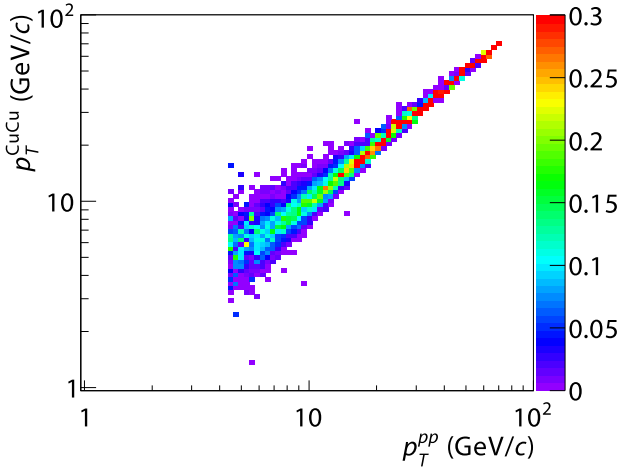

0–10% centrality

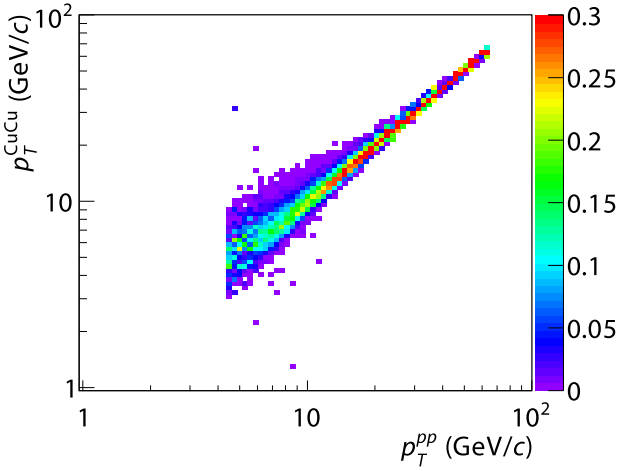

10–30% centrality

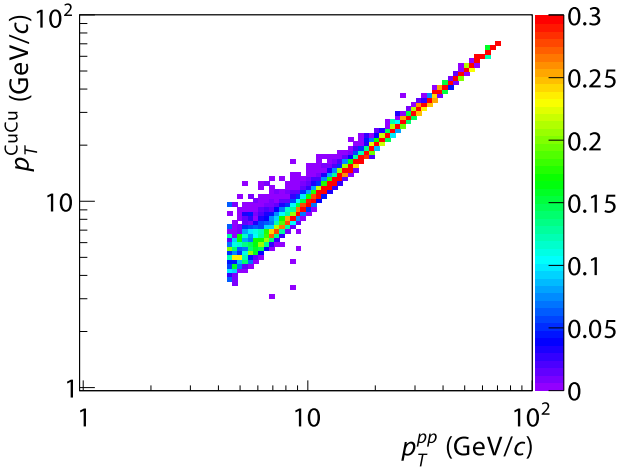

30–50% centrality

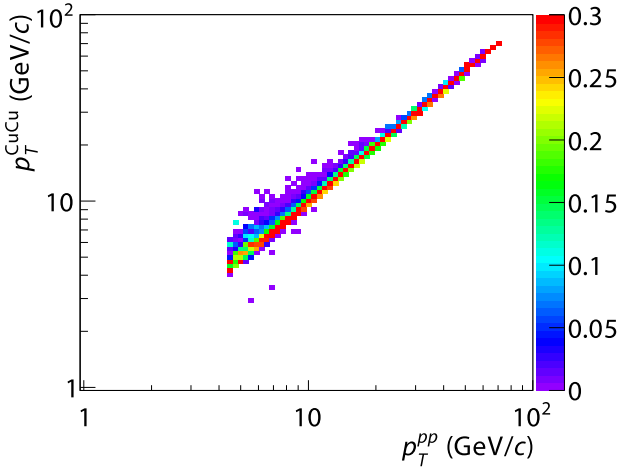

0–10% centrality

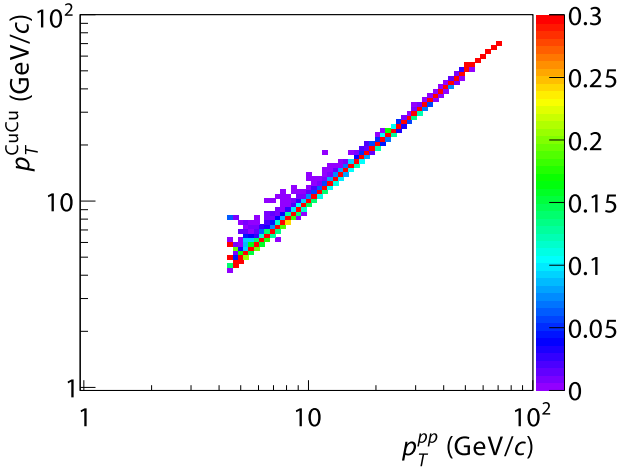

30–50% centrality

$p+p$ to Cu + Cu Jet Energy Scale (Underlying Event)

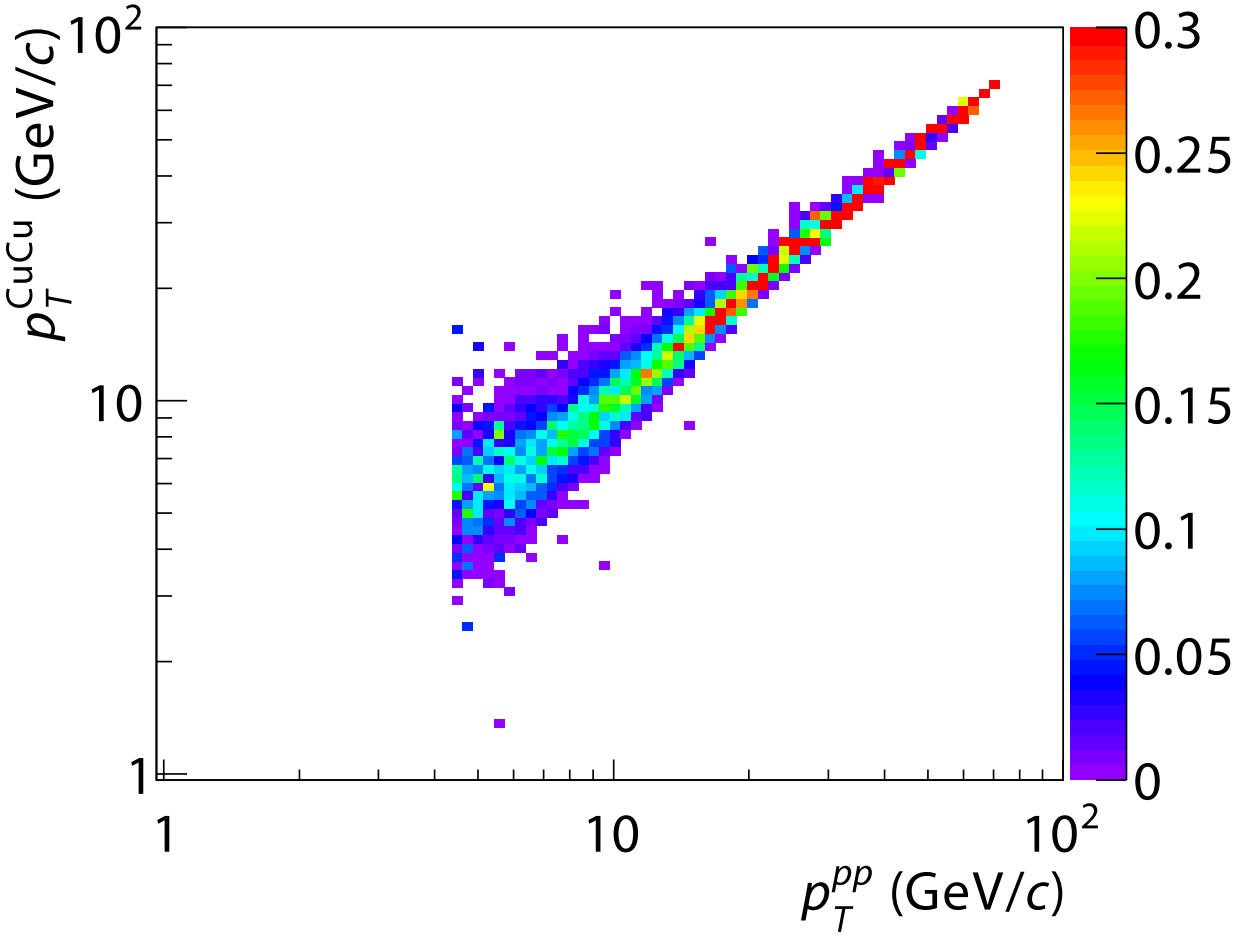

0–10% centrality

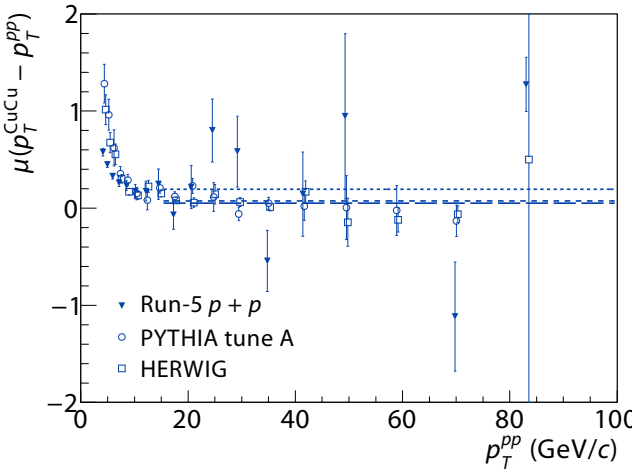

Mean

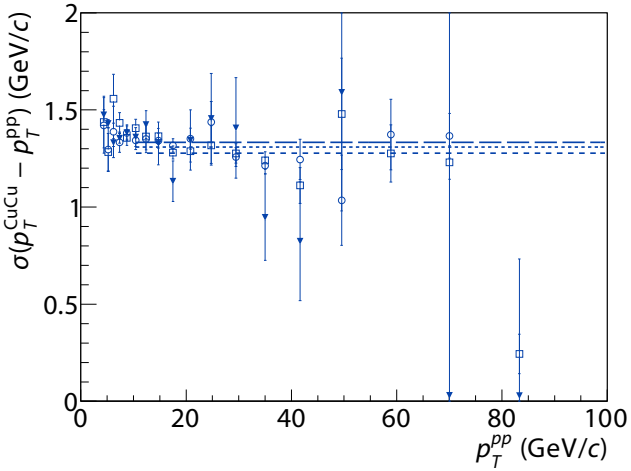

Standard deviation

- Gaussian filter a linear jet definition (constant energy smearing, modulo fake rejection)

Fake Jet Rejection

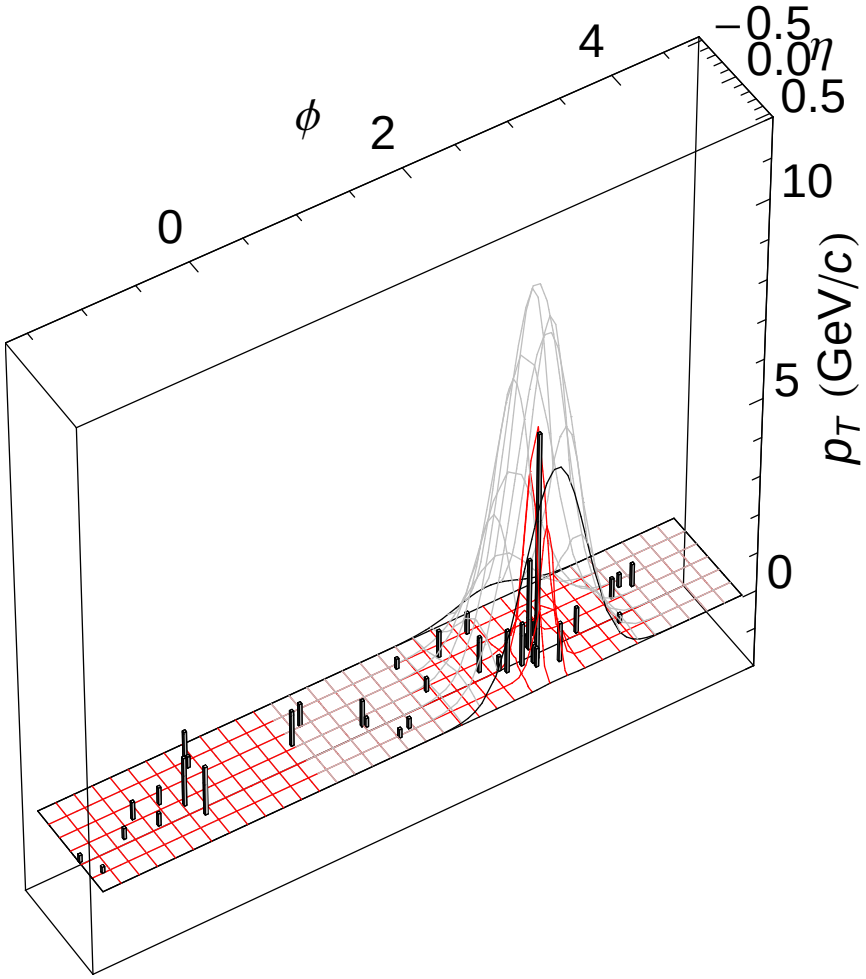

9.6 GeV/c jet passing fake rejection

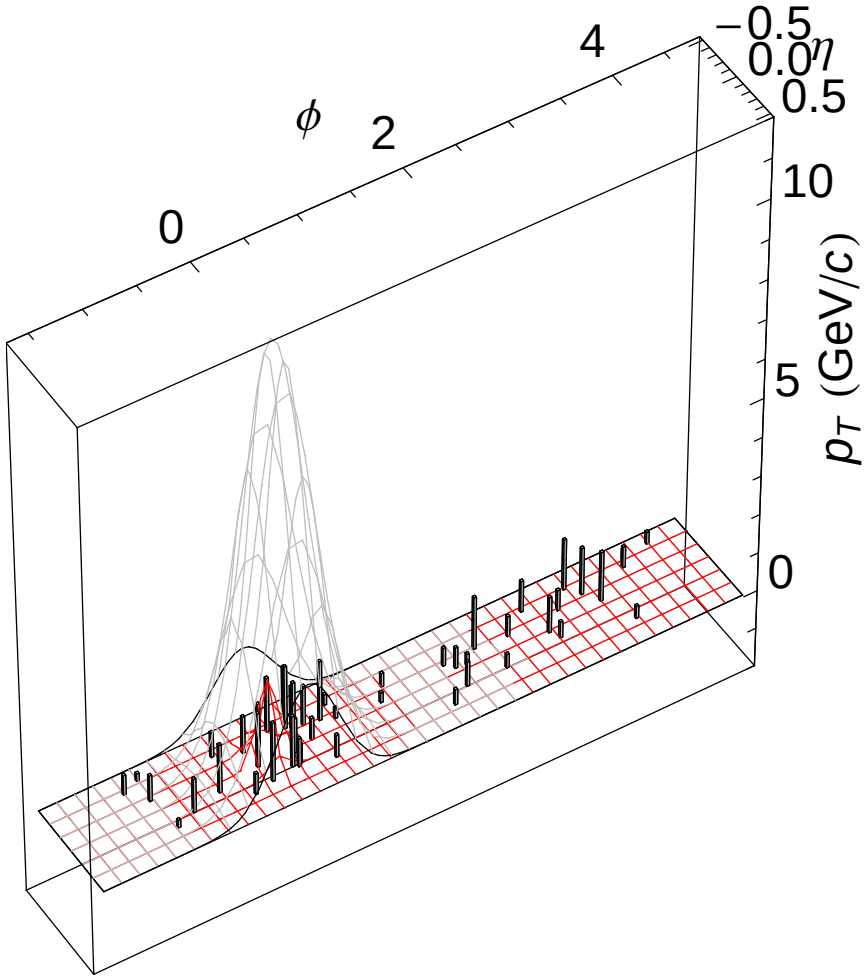

Rejected 10.8 GeV/c background fluctuation

Gaussian Fake Rejection

- Cut on the overall shape of the jet
- Inspired by the principle of Gaussian filter
- Strategy:
  1. Sum p_T^2 inside a Gaussian kernel to obtain a discriminant:

$$g_{\sigma_{\text{dis}}}(\eta, \varphi) = \sum_{i \in \text{fragment}} p_{T,i}^2 \exp\left[-\frac{(\eta_i - \eta)^2 + (\varphi_i - \varphi)^2}{2\sigma_{\text{dis}}^2} \right],$$

  2. Gaussian kernel $\sigma_{\text{dis}} \approx 0.1$
  3. (Technical detail: allow adaption for jets with very close maxima, obtain an updated $g'_{\sigma_{\text{dis}}}$)
- Cut on $g'_{0.1}$ = weighted p_T^2-sum
- In central Au + Au HIJING simulation proves to be more effective than $\sigma/\sqrt{\langle A \rangle}$ (Cacciari & Salam, Phys. Lett. B **659**, 119, 2008) and Σj_T (Grau *et al.*, arXiv:0810.1219, 2008)

Fake Rejection in Cu + Cu

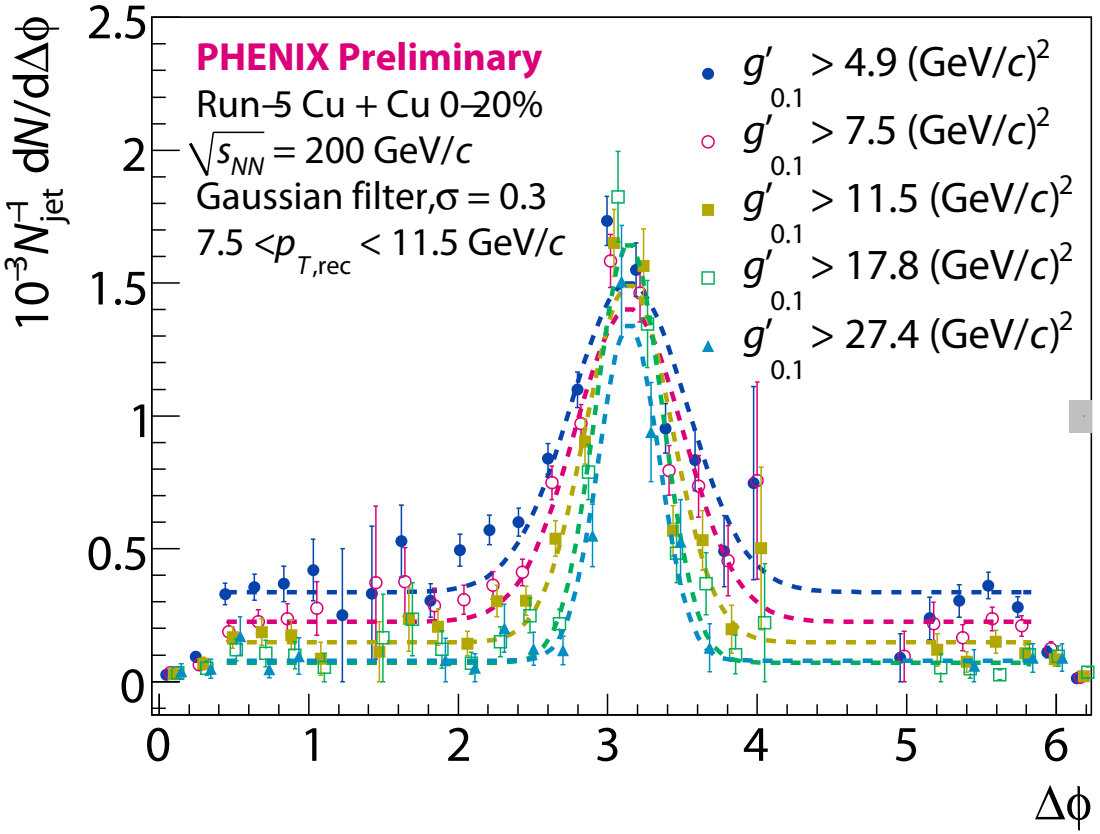

- Pedestal $\approx 0.3 \times 10^{-3}$ translates into $\frac{1}{2\pi}\frac{1}{N_{evt}}\frac{dN}{p_T dp_T dy} \approx 10^{-5}(\mathrm{GeV}/c)^{-2}$, substantial contamination for 7.5 GeV/c
- 17.8 $(\mathrm{GeV}/c)^2$ used as standard fake rejection cut level:
  $\Rightarrow$ $<$ 10% contamination at 7.5 GeV/c

Run-5 Cu + Cu Dijet Azimuthal Correlation

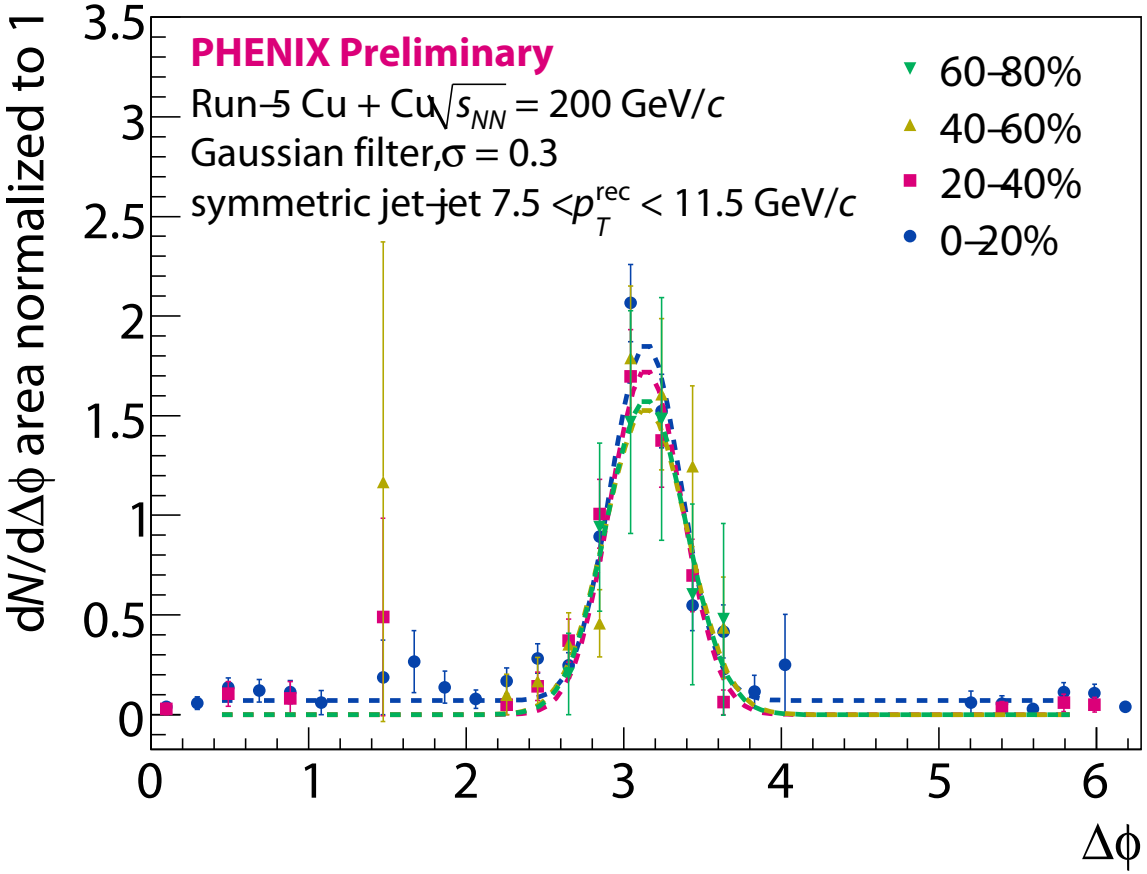

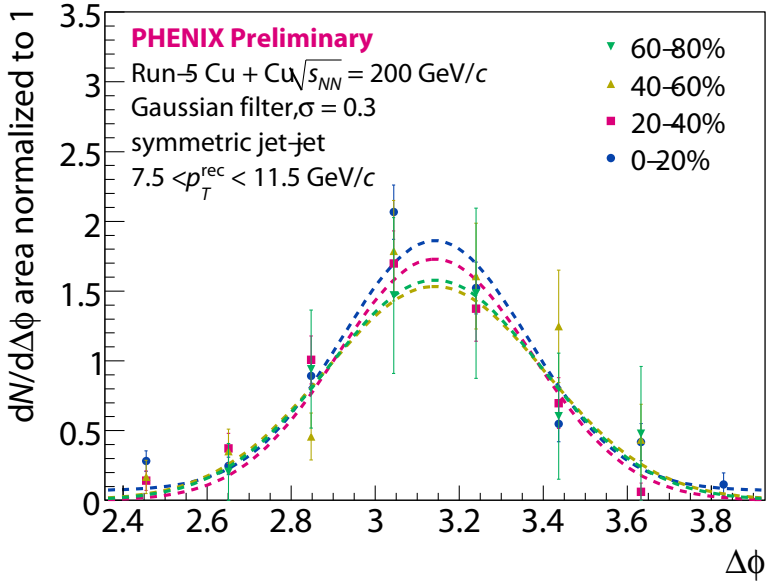

Centrality	$\Delta\varphi \approx \pi$ width σ
0–20%	0.223 ± 0.017
20–40%	0.231 ± 0.016
40–60%	0.260 ± 0.059
60–80%	0.253 ± 0.055

Stages of the Cu + Cu Spectrum

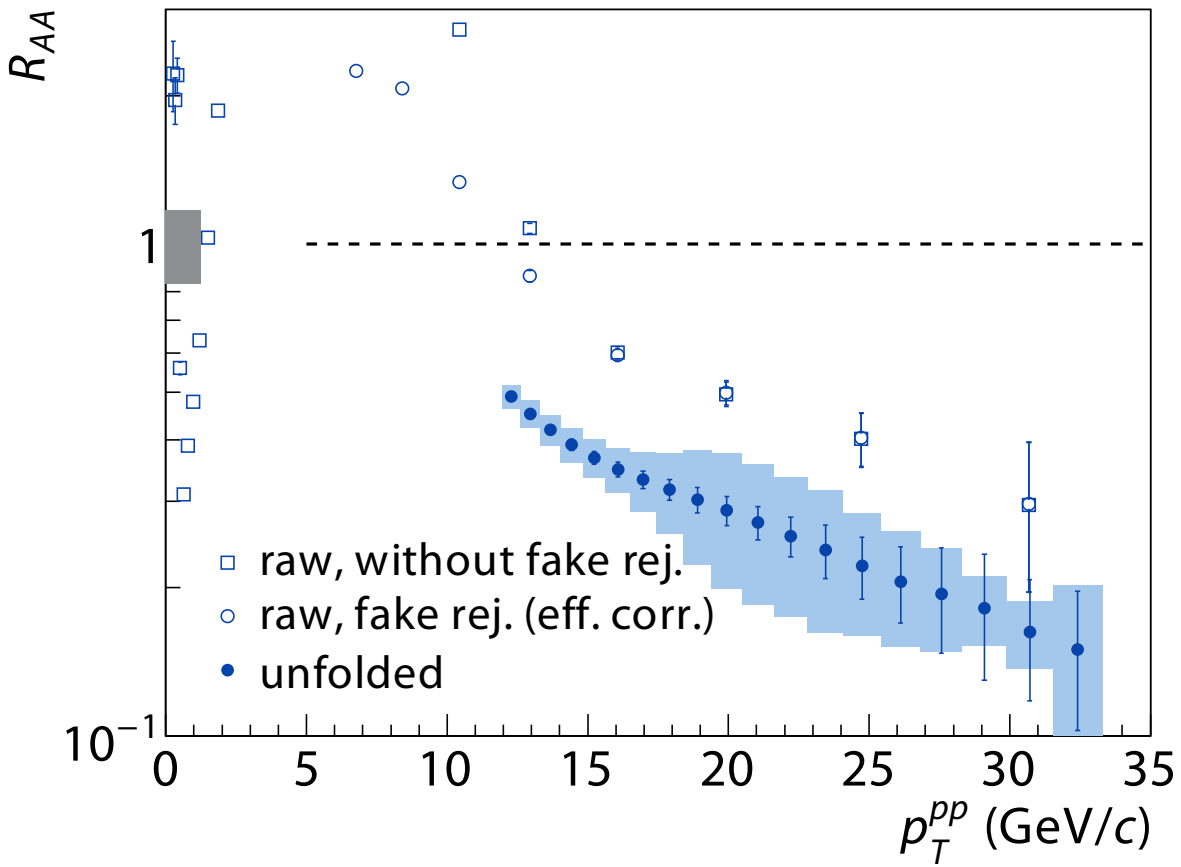

- $p+p$ spectrum divided out for clarity
- Large fake rate without fake rejection
- Fake rejection has no effect $>$ 17 GeV/c

Run-5 Cu + Cu R_{AA}

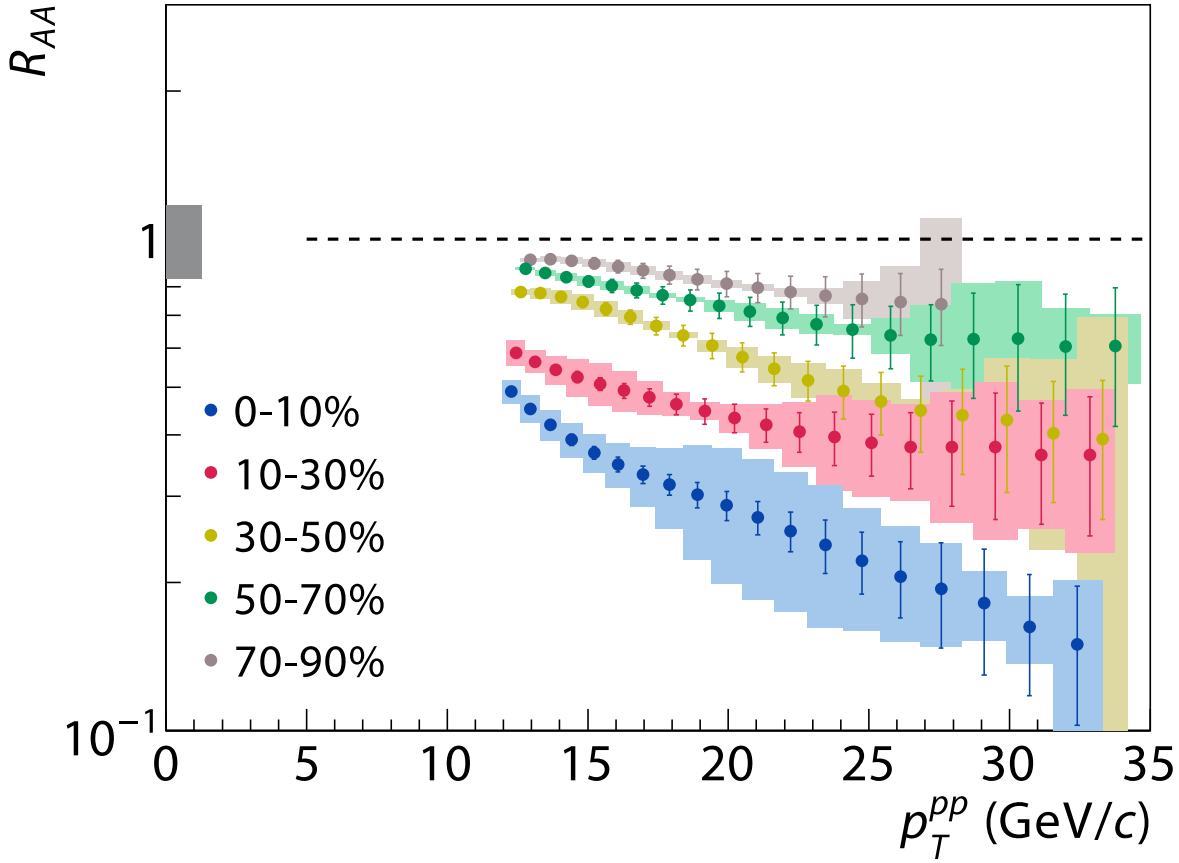

- Central 0–10% is strongly suppressed
- Some (statistically marginal) initial state effect may be observable

Run-5 Cu + Cu R_{AA}

No.	Description	Magnitude
1	BBCLL1 cross section	10%
2	Cu + Cu vs. $p + p$ EMCal/DC acceptance difference	5%
3	BBCLL1 efficiency	5%
4	$p + p$ ERT efficiency saturation level	3%
5	minimum bias/ERT normalization matching	5%
6	Cu + Cu vs. $p + p$ energy scale difference	10%
	quadrature sum	17%

Run-5 Cu + Cu R_{AA} 0–10% against π^0

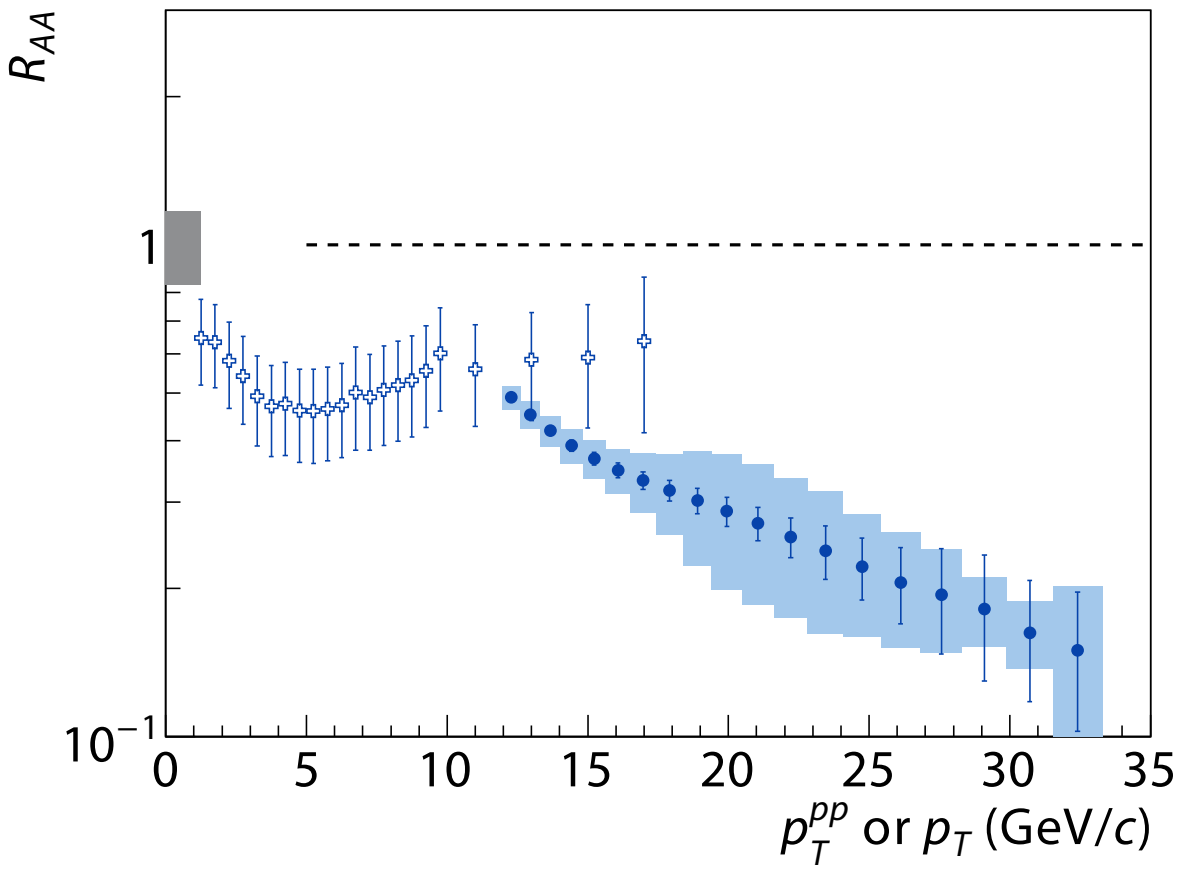

- Apples-to-oranges comparison! Cu + Cu not fully unfolded, energy scale are different.
- Low-p_T suppression level are comparable

Run-5 Cu + Cu R_{CP}

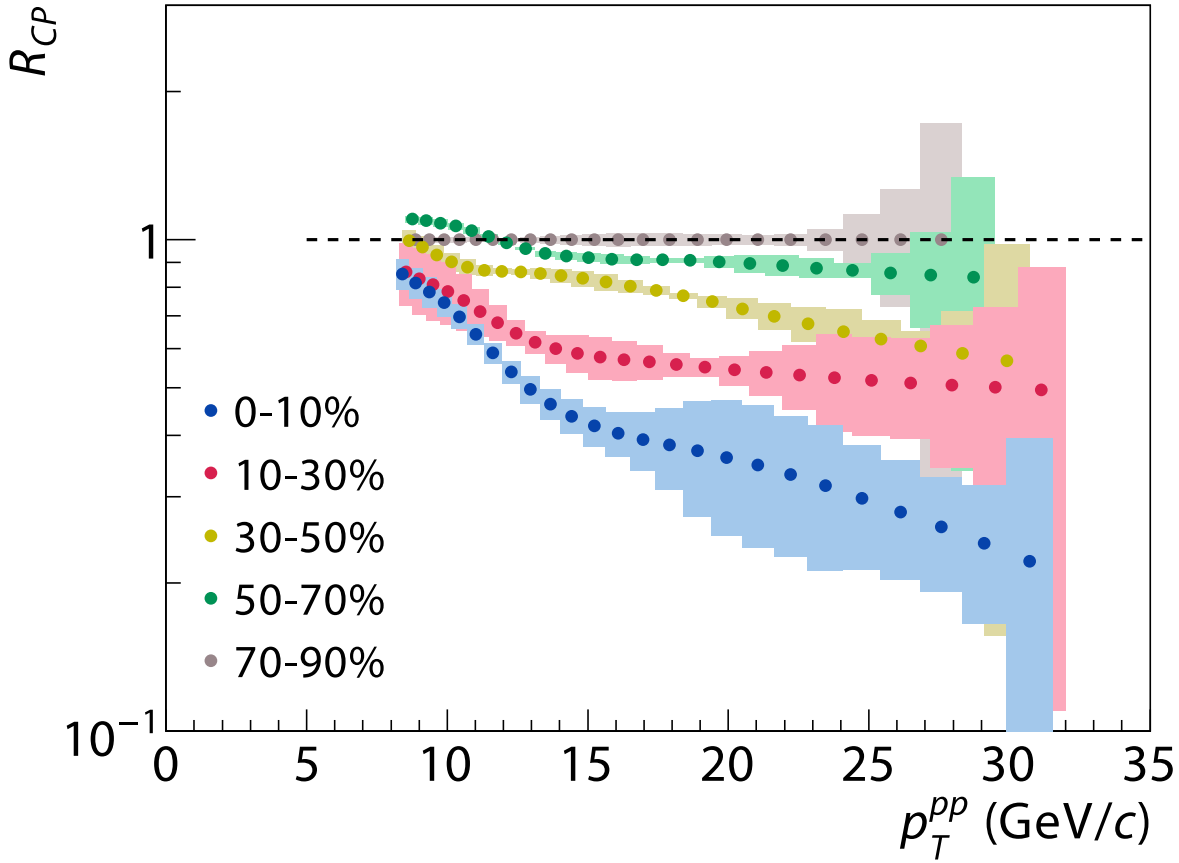

- Removes $p+p$-to-Cu + Cu normalization systematics
- Removes potential initial state effects

Dijet Azimuthal Correlation and BDMPS-Z

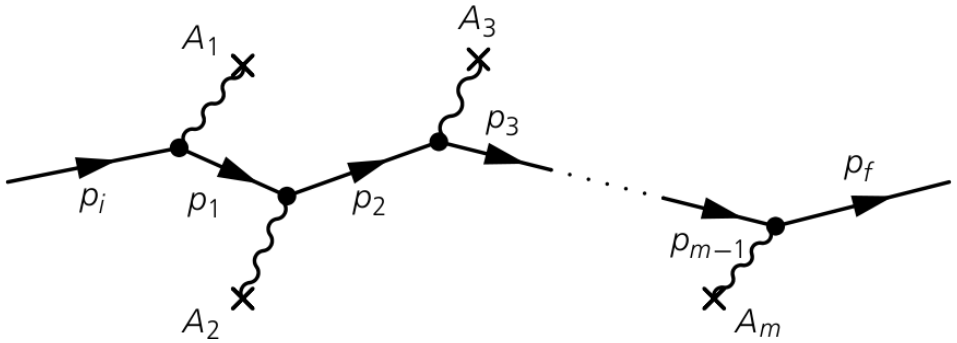

- A first attempt to quantify the constraint on radiative energy loss
- If radiative energy loss (e.g. BDMPS-Z) from multiple scattering holds: $\langle k_\perp^2 \rangle = \hat{q}L$
- No $k_\perp$ broadening was observed at $\langle k_\perp \rangle = 0.06$ rad $\times$ 8 GeV$/c \approx 0.5$ GeV$/c$
- $\langle k_\perp \rangle < 0.5$ GeV$/c$ for $L \approx 1$ fm strongly constrains $\hat{q} < 0.3$ GeV$^2/fm$

Hadronization Timescale

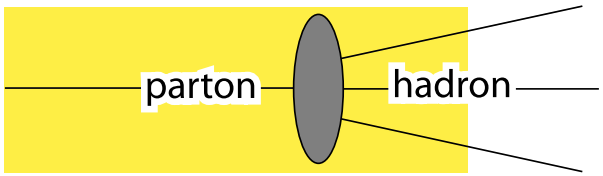

or

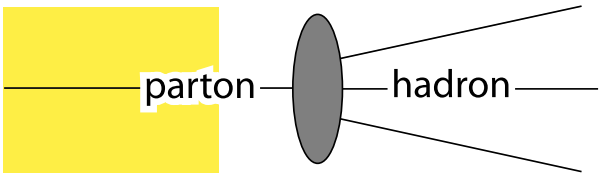

- R_{AA} comparable to single particle
- Energy loss carried by parton, not fragmentation
- Exit time of parton > hadronization time scale

Comparison to STAR

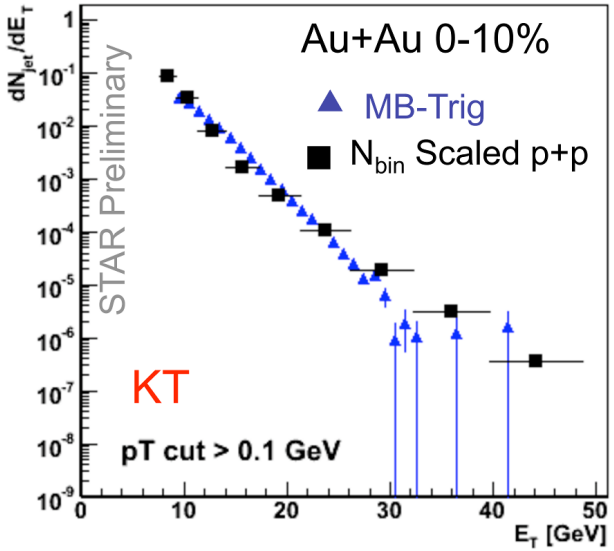

2008

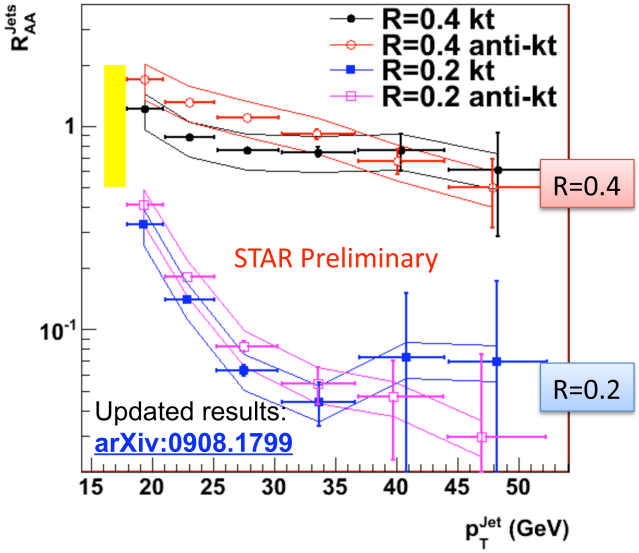

2009

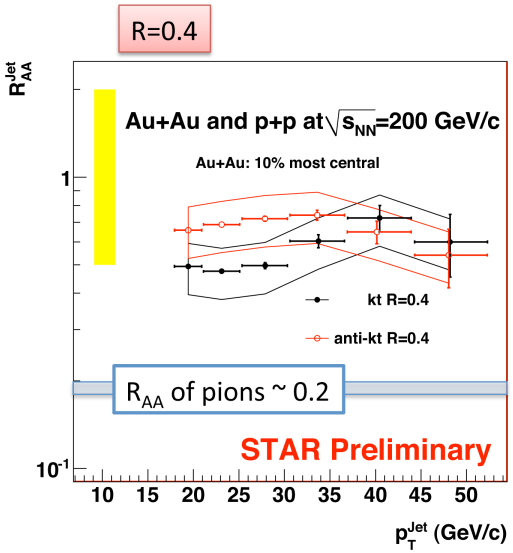

2010

- 2008 results has no fluctuation/fake jet correction at all, is apple to oranges (spin group's $p+p$ CDF midpoint true energy vs. HI group's Au + Au $k_\perp$ detector energy), $R_{AA} \approx$ 2–3 if accounted for energy scale
- 2009 $R = 0.2$ jet $R_{AA} \approx$ 0.2–0.4 $R_{AA}^{\pi^0}$ using azimuthal randomization/sub-$\sqrt{N}$ combinatorics subtraction
- 2010 R_{AA} evaluated using single particle energy response ($z = 1$ "jet")

S. Salur, Hard Probes 2008; M. Ploskon, Quark Matter 2009; M. Ploskon, INT 10-2A 2010

Comparison to LHC

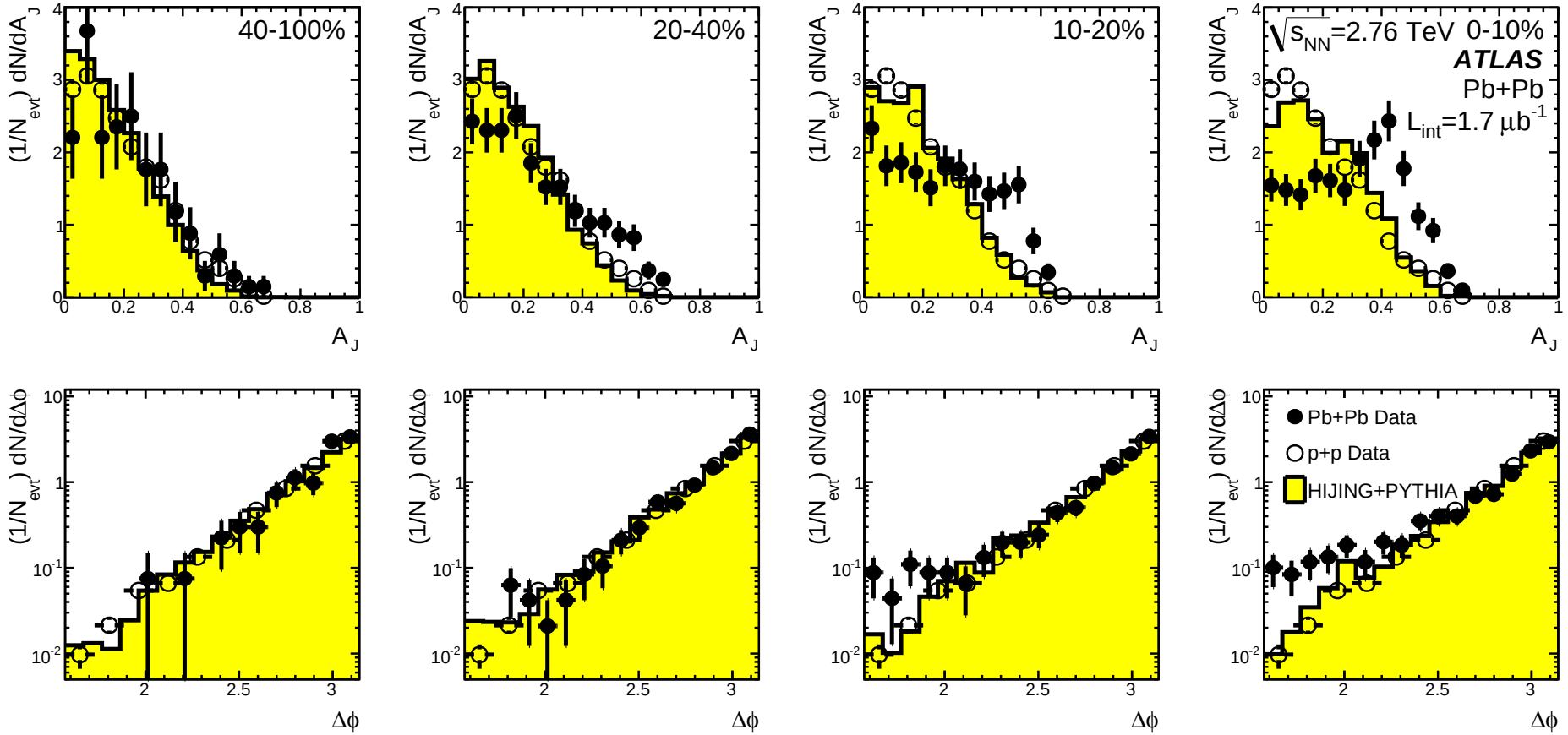

- Strong modification of the away side jet
- Large asymmetry vs. small $k_\perp$ implies a nonradiative energy loss mechanism

ATLAS, Phys. Rev. Lett. 105 252303

Comparison to LHC

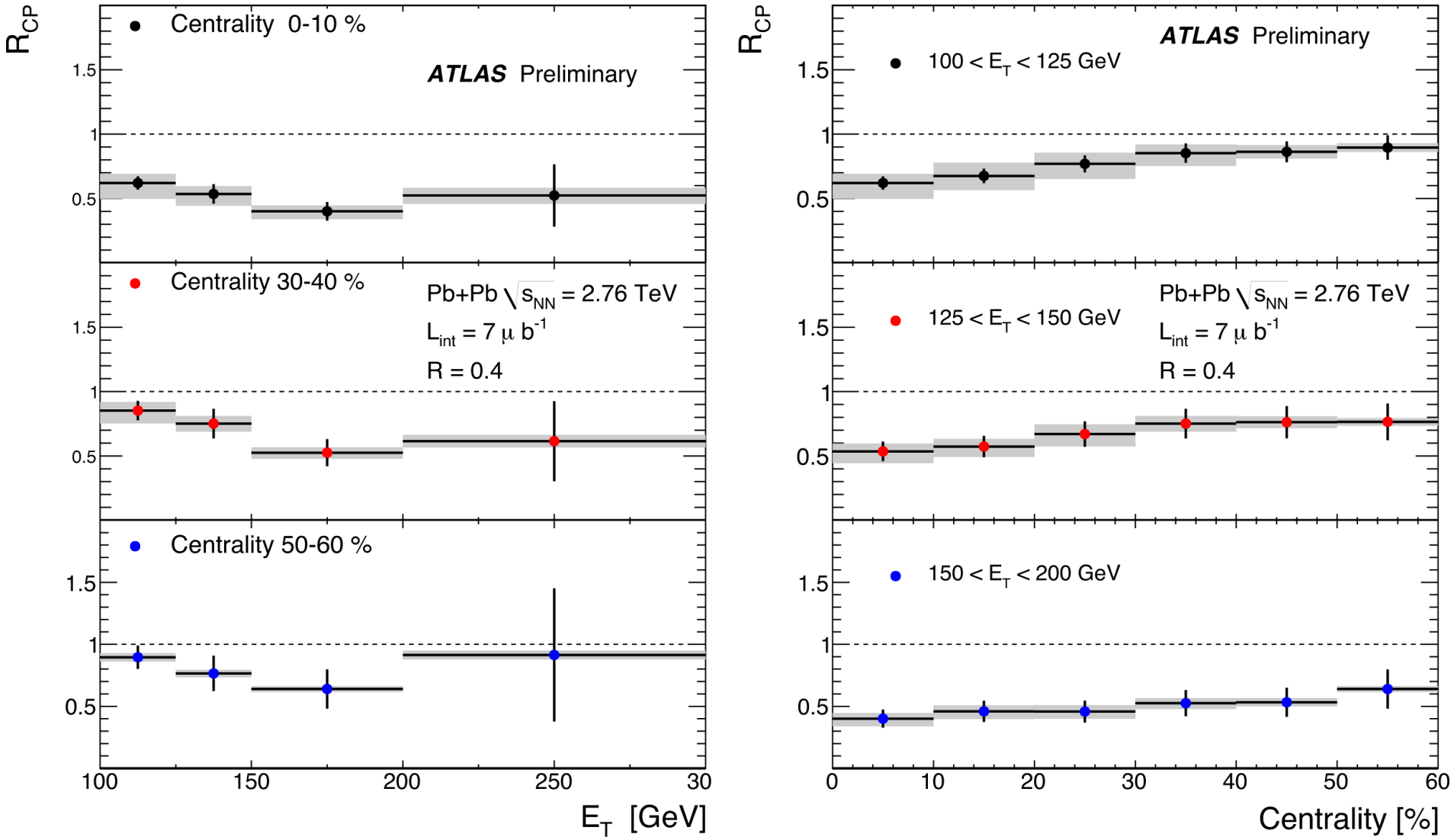

A. Angerami, Quark Matter 2011

Summary

- Developed a Gaussian filter with corresponding fake rejection method for $p+p$ and heavy ion collisions
- After three years, still the only RHIC algorithm with
  - All centrality jet reconstruction
  - Complete treatment of elliptic flow
- Obtained the first measurement of $p+p$ spectrum at RHIC up to $x \approx 0.6$
- Obtained the first measurement of $p+p$ jet fragmentation function at RHIC, inclusive and up to $z \approx 0.8$
- Obtained the first measurement of the dijet angular correlation in Cu + Cu collisions
  - $\Rightarrow$ With the p_T range of RHIC, can provide strong constraint for radiative energy loss such as BDMPS-Z and AdS/CFT–Wilson loop

  (and still the only RHIC + LHC heavy ion dijet correlation)
- Obtained the first measurement of the jet R_{AA} in Cu + Cu collisions
  - $\Rightarrow$ With implication on hadronization time scale
- Developed unfolding tools
  - Multidimensional unfolding for fragmentation properties
  - Scaled Landweber algorithm as cross check
  - Evaluation method of unfolding systematics
  - Full covariance ratio extraction

Outlook

- Crucial measurement for the field
  - PHENIX Run-5 Cu + Cu R_{AA} unfolded to the true energy scale
  - Run-5 Cu + Cu j_T and fragmentation function (potential modification at very low, LHC inaccessible E_T)
  - Dijet angular correlation for RHIC and LHC would strongly (and quantitatively) constrain the radiative energy loss mechanism
  - Extend to d + Au, p + Pb to quantify initial state effects
  - Use flavor tagged jets to further constrain whether PQCD or strongly interacting (e.g. AdS/CFT) energy loss dominates
- PHENIX long term
  - Vertex detector will improve jet energy scale by extending the clean tracking momentum range
  - Vertex detector will allow flavor tagging of jets
  - Compact electromagnetic/hadronic calorimeter will provide calorimetric jets, further improve energy scale, extend kinematic range

Part I

Backup

Experimental Cuts, $p + p$

- Cuts attempts to remove all conversions, but keep as much jet p_T as possible
- Tracking:
  - Maximum $|p|$
  - Quality (p_T dependent)
  - PC3 matching (p_T dependent)
  - $e^{\pm}$ pair (PC3/RICH/$\Delta\eta/\Delta\varphi$ dependent)
  - Ghost (complex shape)
  - Cluster-unassociated $e^{\pm}$
- EMCal
  - Tower E/p balancing, reject E/p outliers
  - Tower spectrum fit, cut on χ^2 (abnormal spectra)
- Combined
  - Replace p_T by E (assuming $m^2 = 0$) for abnormally low E/p track/clusters

PYTHIA/HERWIG, Gaussian Filter

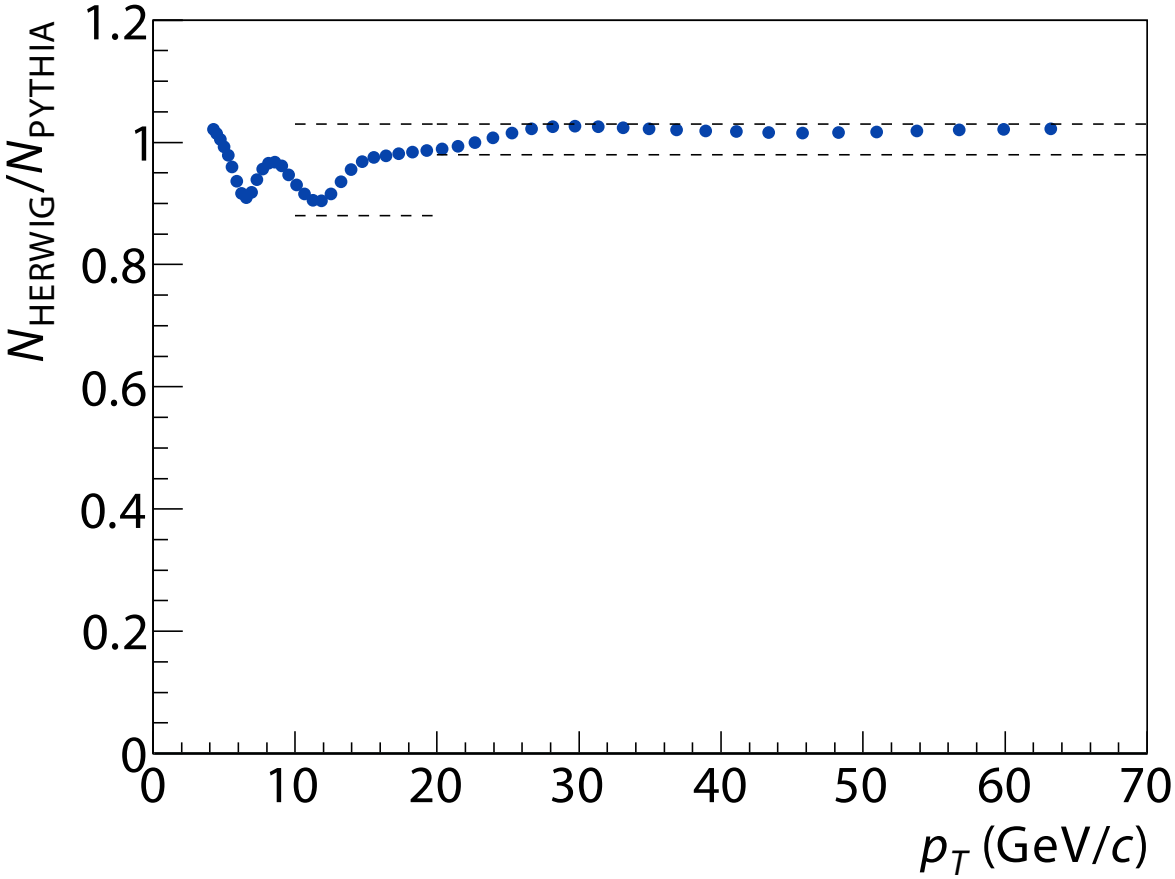

- Really consistent for high p_T

PYTHIA/HERWIG, Anti-k_T

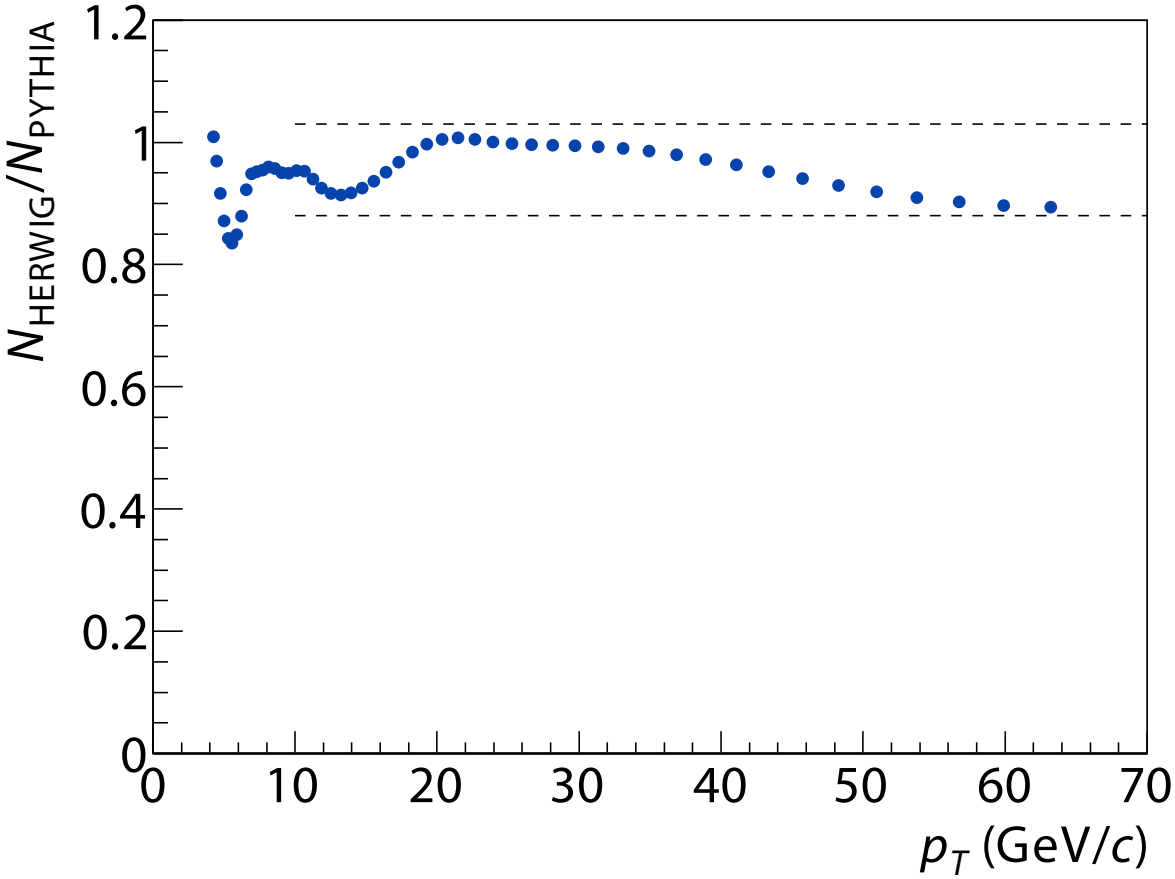

- Larger uncertainty than filter

η_{rec} Dependence

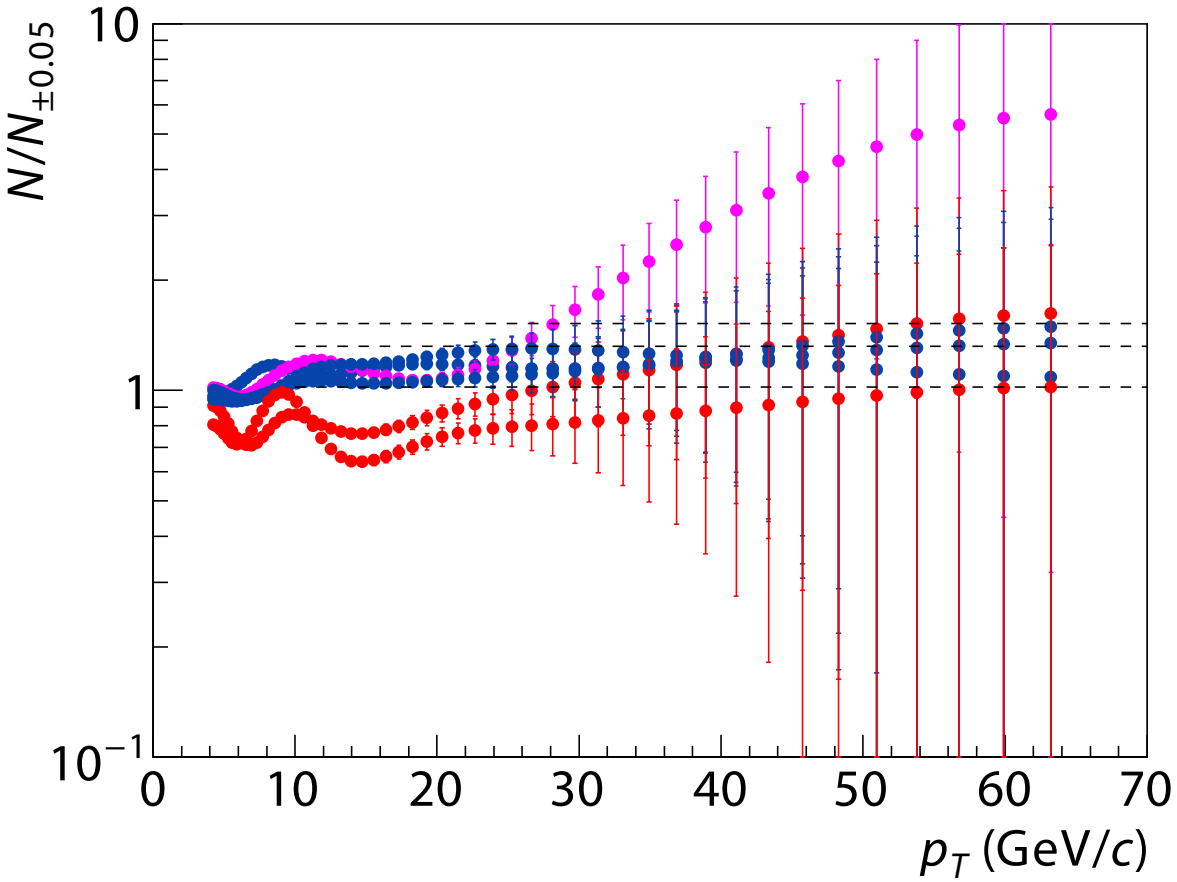

- Acceptance cut in $\Delta\eta = 0.1$ slices and individually unfolded
- Red: $|\eta| > 0.25$, some effect expected
- Magenta: $-0.15 < \eta < -0.05$, located to be in PbSc and $p_T^{\text{rec}} \approx 30\,\text{GeV}/c$, proximity to some large, known hot patches, possibly a almost-normal tower firing rarely

η_{truth} Dependence

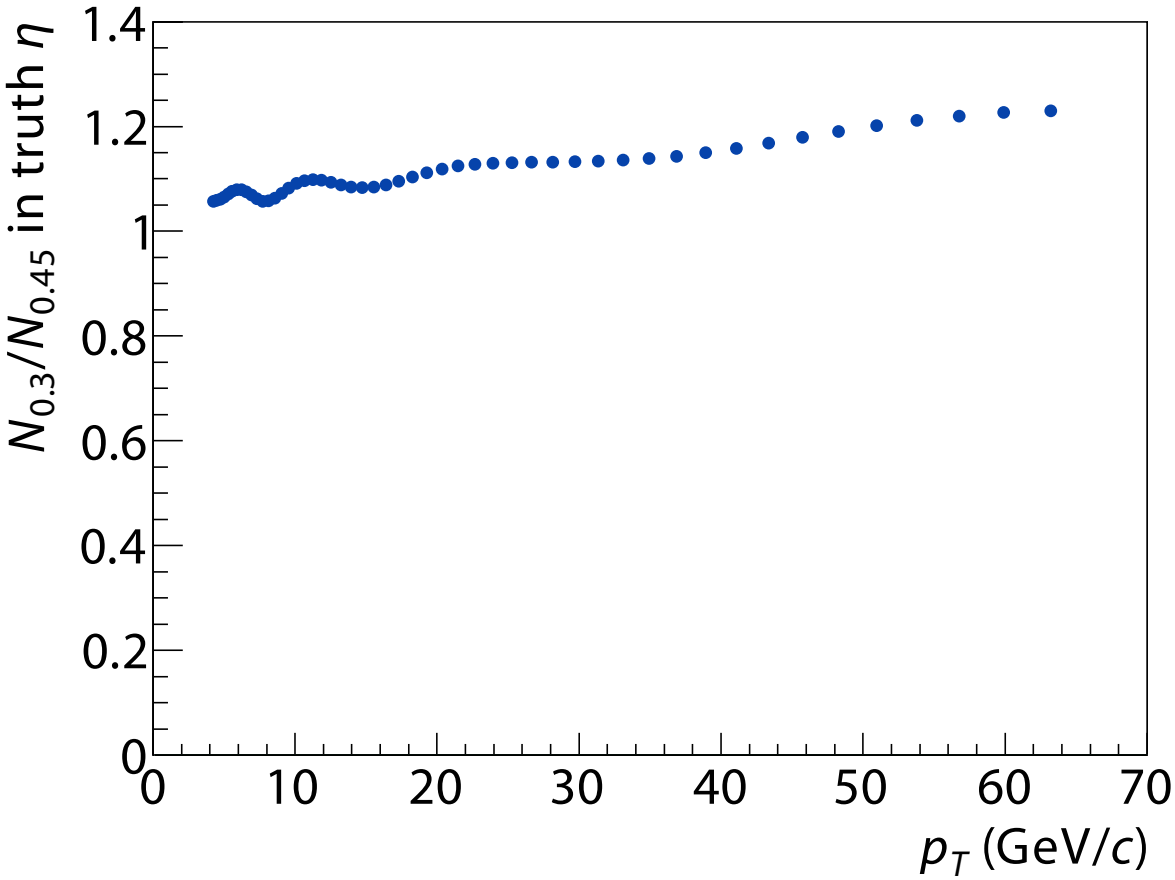

- Check when unfold, what effect the target (η_{truth}) region may have
- Some out of acceptance jets dump particles into the detector and can be unfolded with energy/efficiency sacrifice
- Plotted ratio: truth $|\eta| < 0.3$ divided by $|\eta| < 0.45$, corrected by geometric factor and inefficiency

Two Unfolding Methods

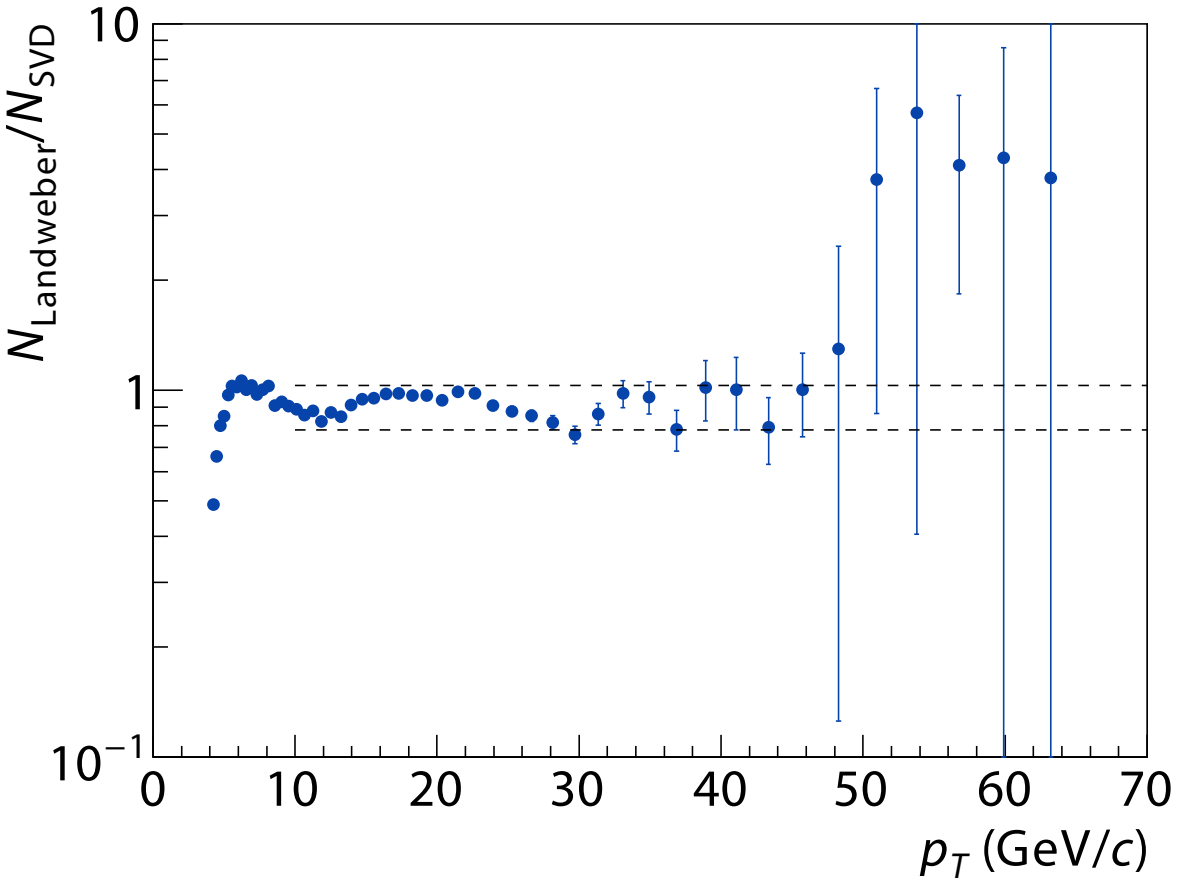

- Landweber method (modified for HEP spectra) vs regularized unfolding
- There are two artifacts in the Landweber method, the sharp drop to the left and rise to the right correspond to the asymmetry in PHENIX detector response
- This should not be doubly counted with the uncertainty we already obtained

$p + p$ Multi-Unfolding

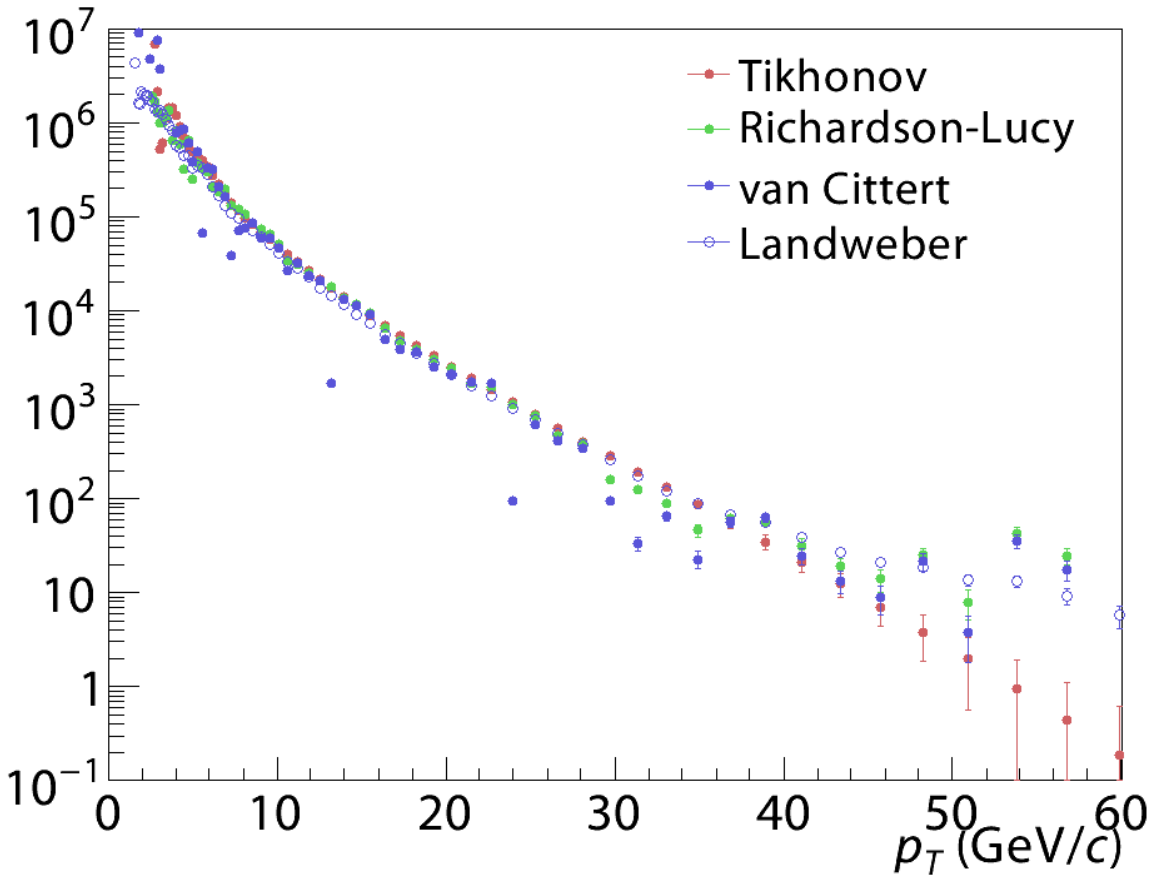

$p + p$ Unfolding Residual Gaussian Filter

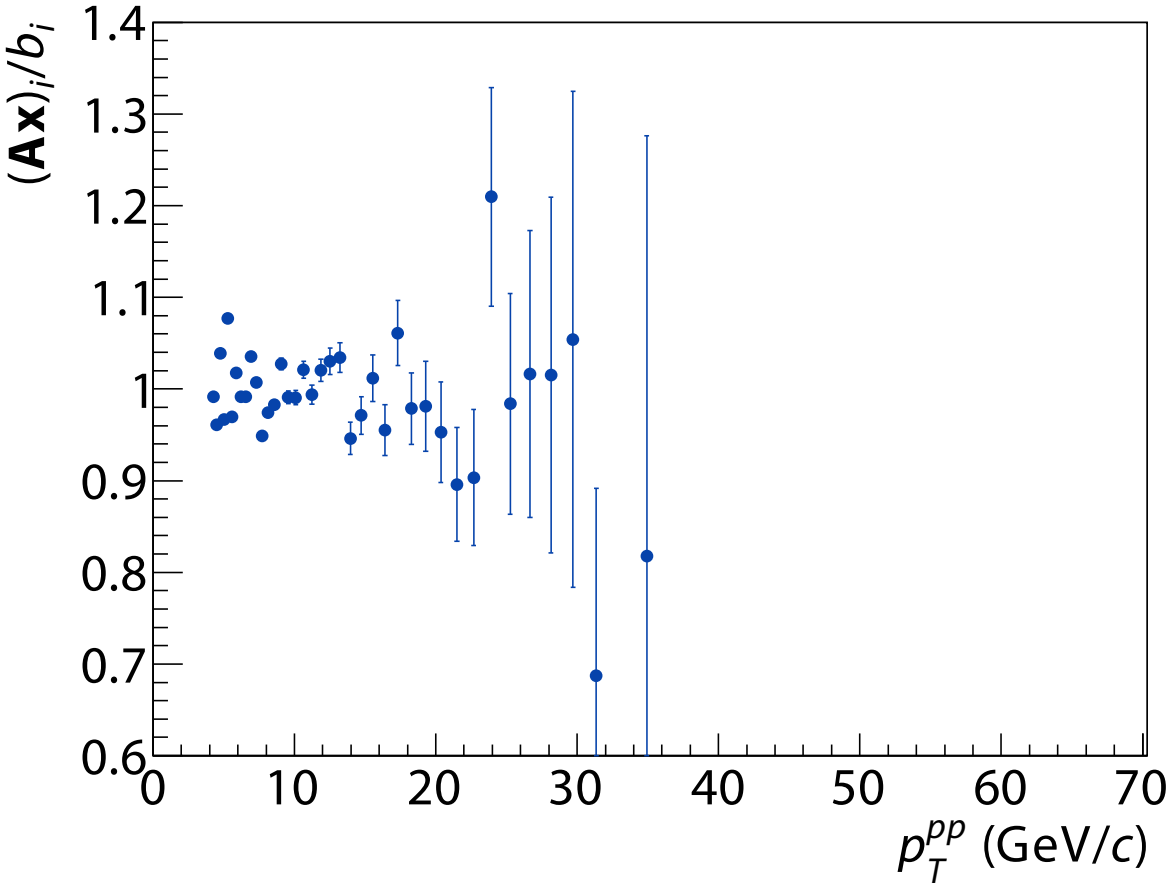

$p+p$ Unfolding Residual Anti-$k_\perp$

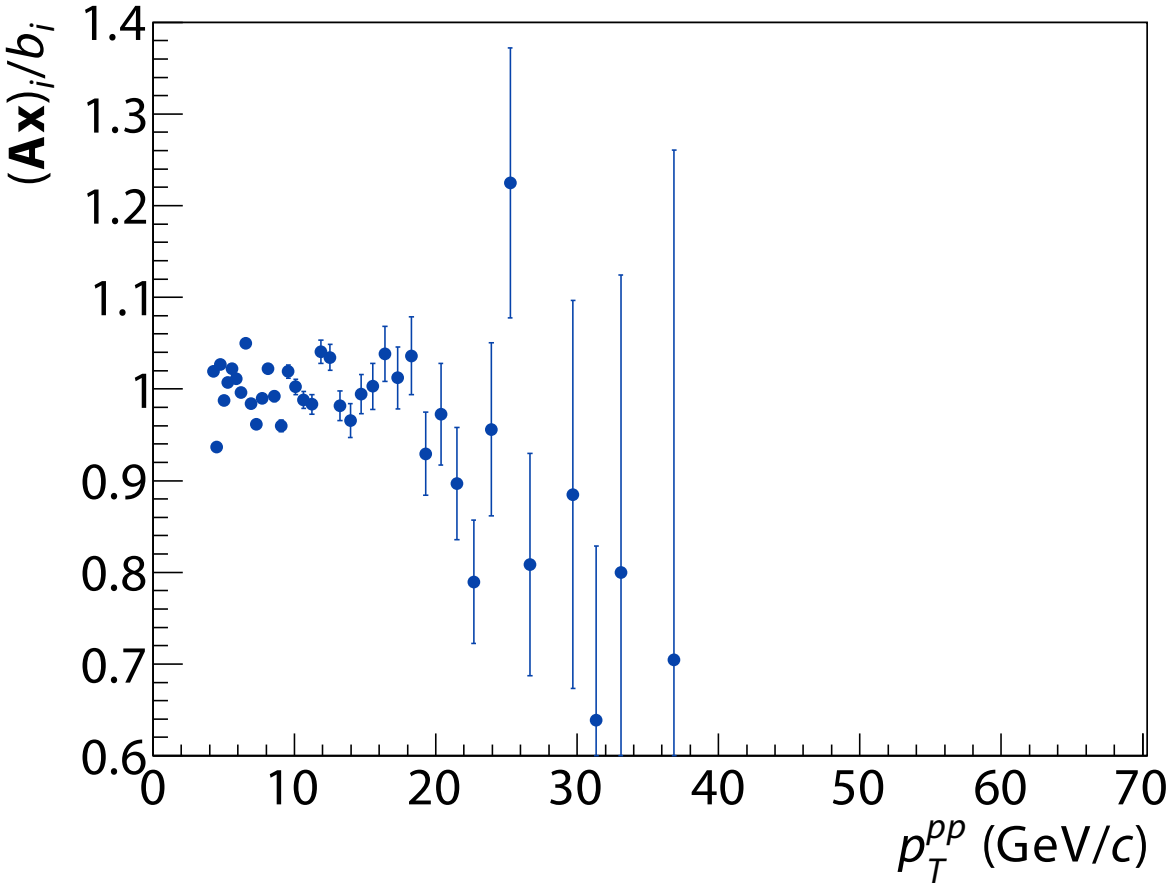

Cu + Cu Unfolding Residual 0–10%

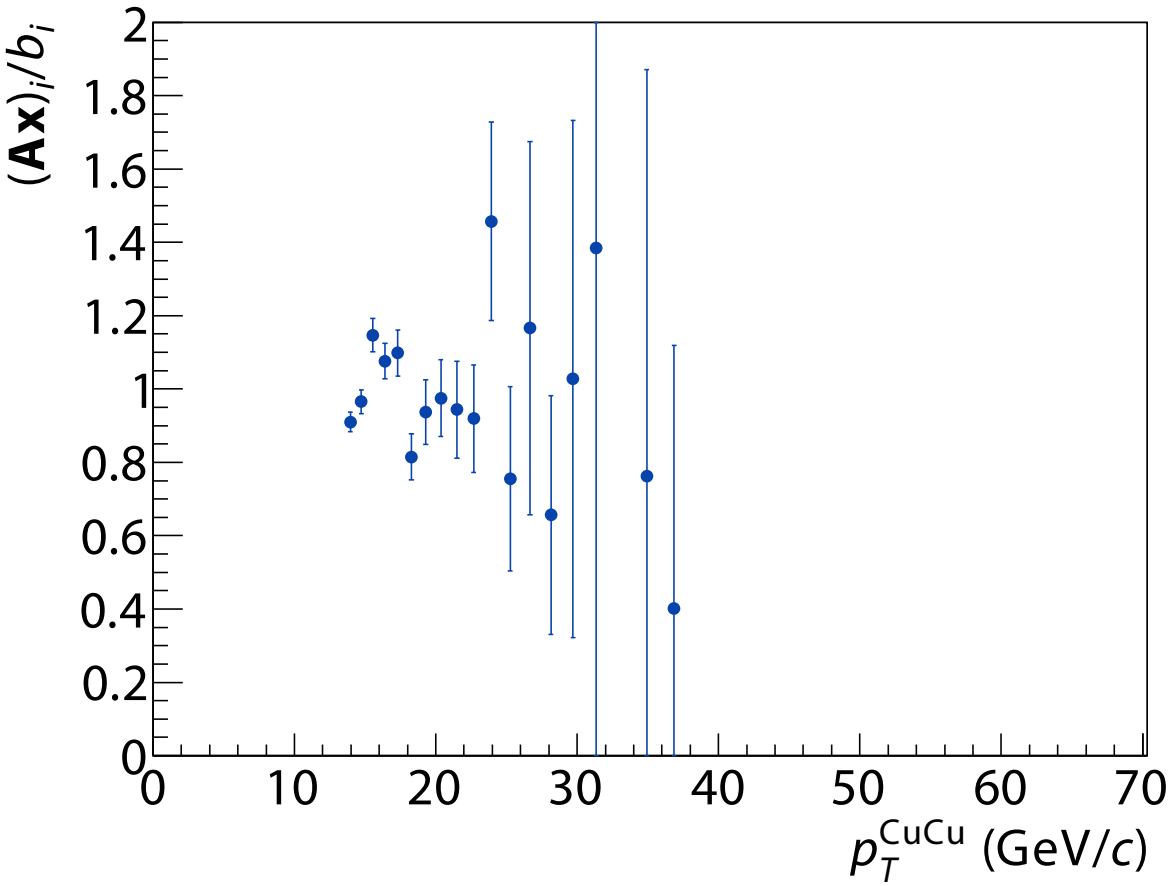

Cu + Cu Unfolding Residual 10–30%

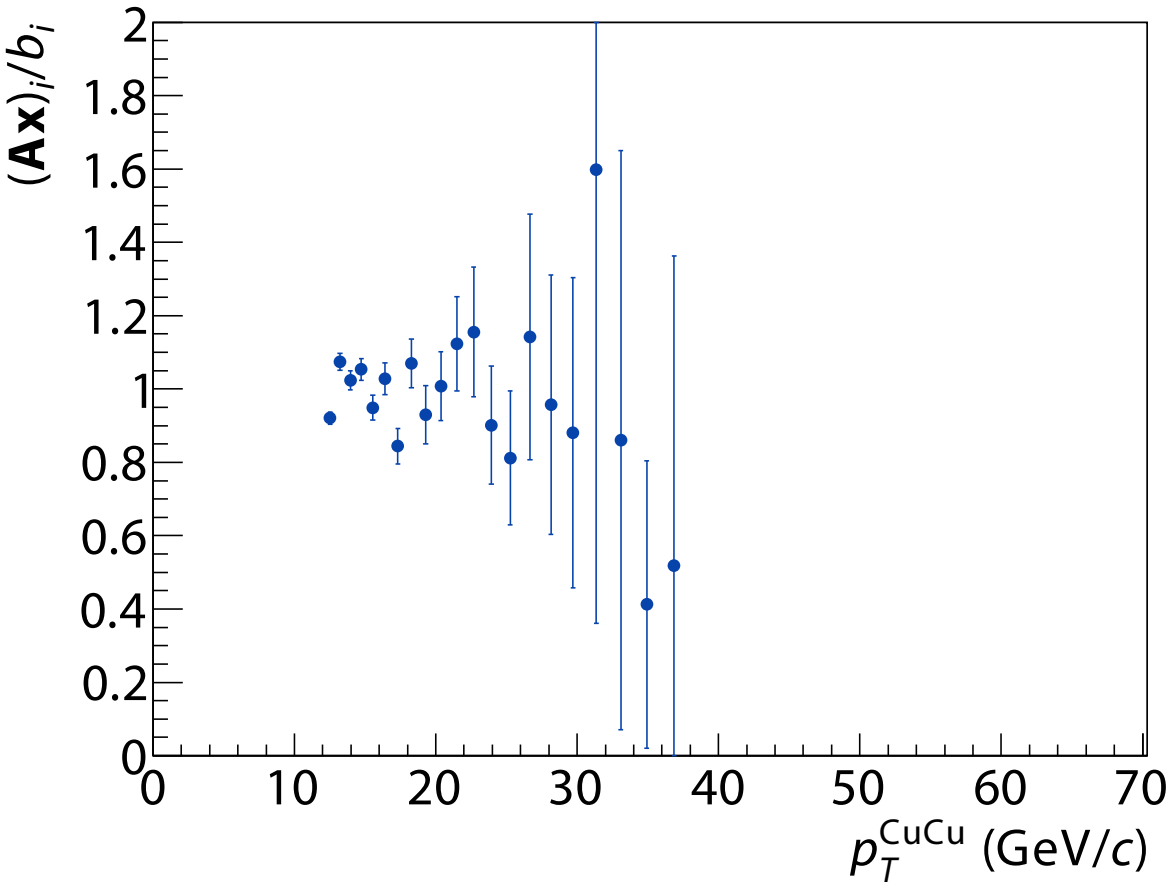

Cu + Cu Unfolding Residual 30–50%

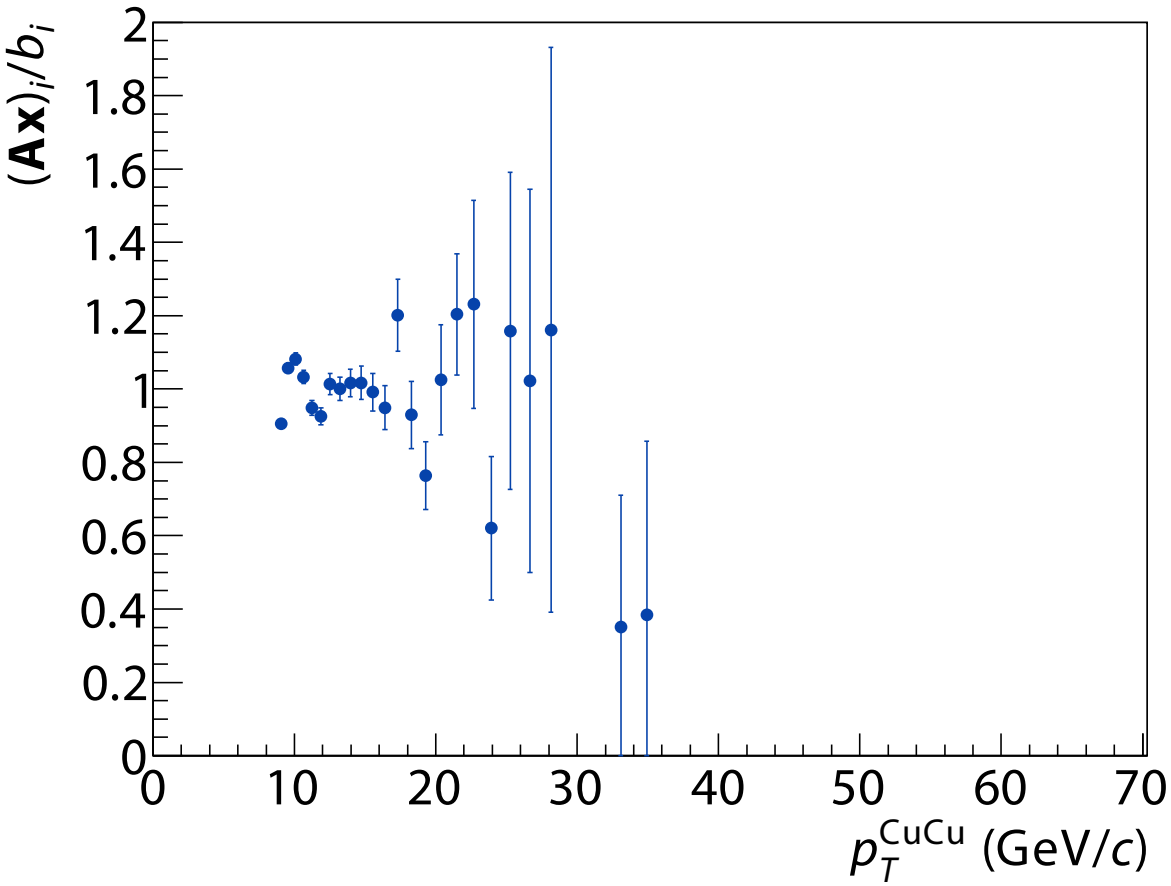

Cu + Cu Unfolding Residual 50–70%

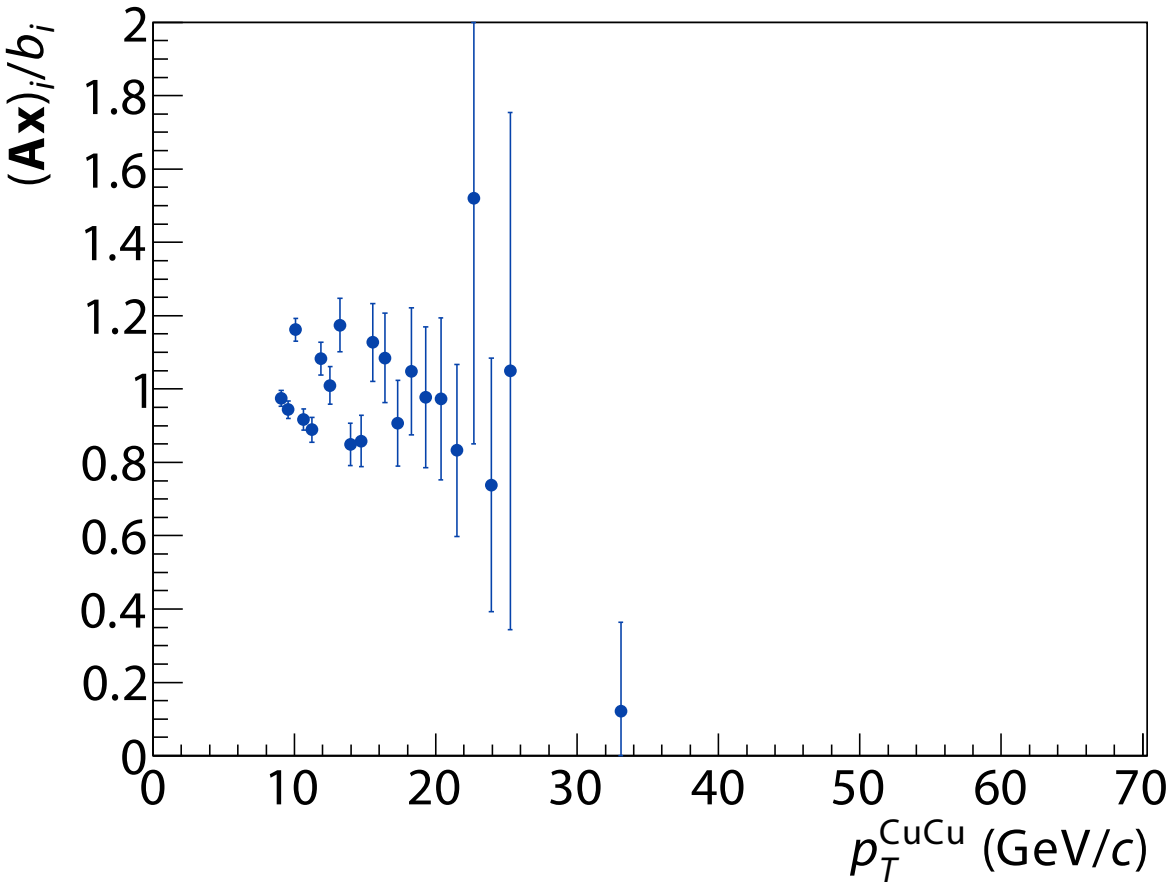

Cu + Cu Unfolding Residual 70–90%

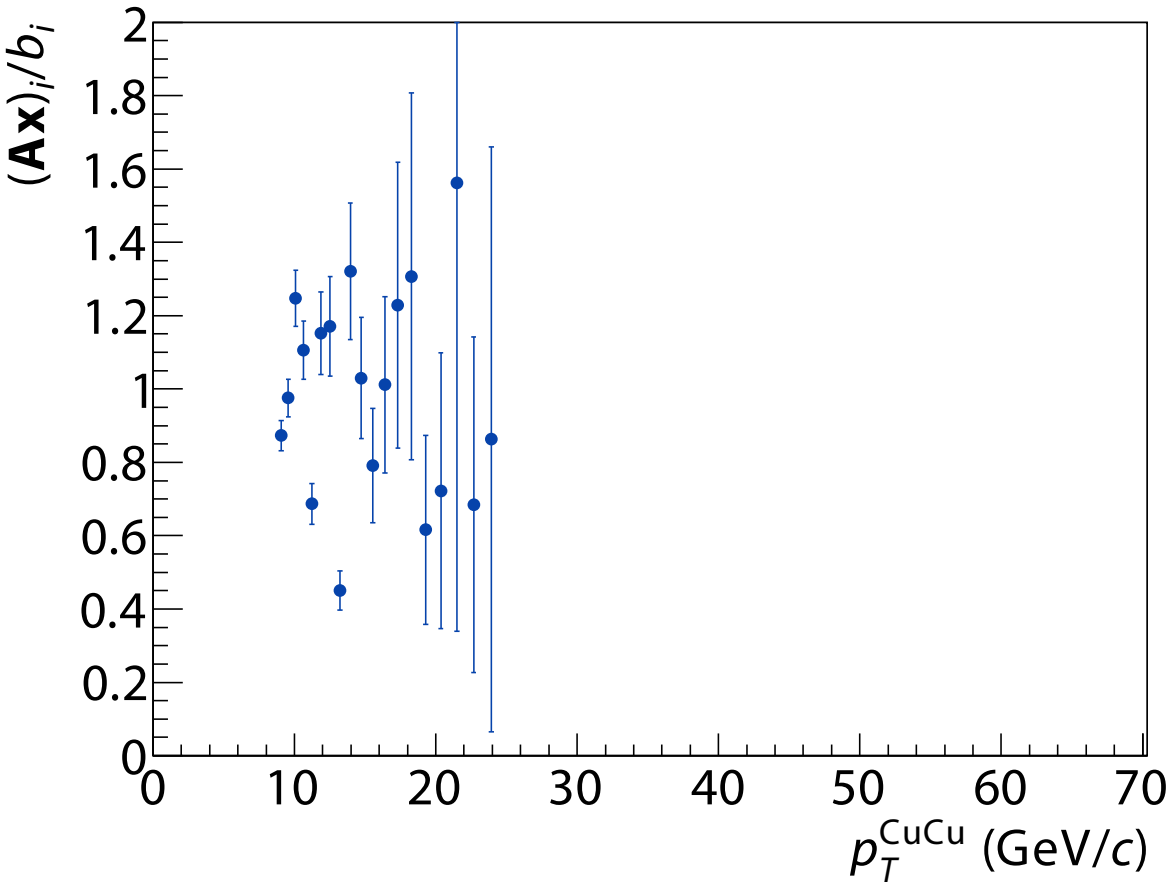

Run-5 $p + p$ DC Dead/Hot Region

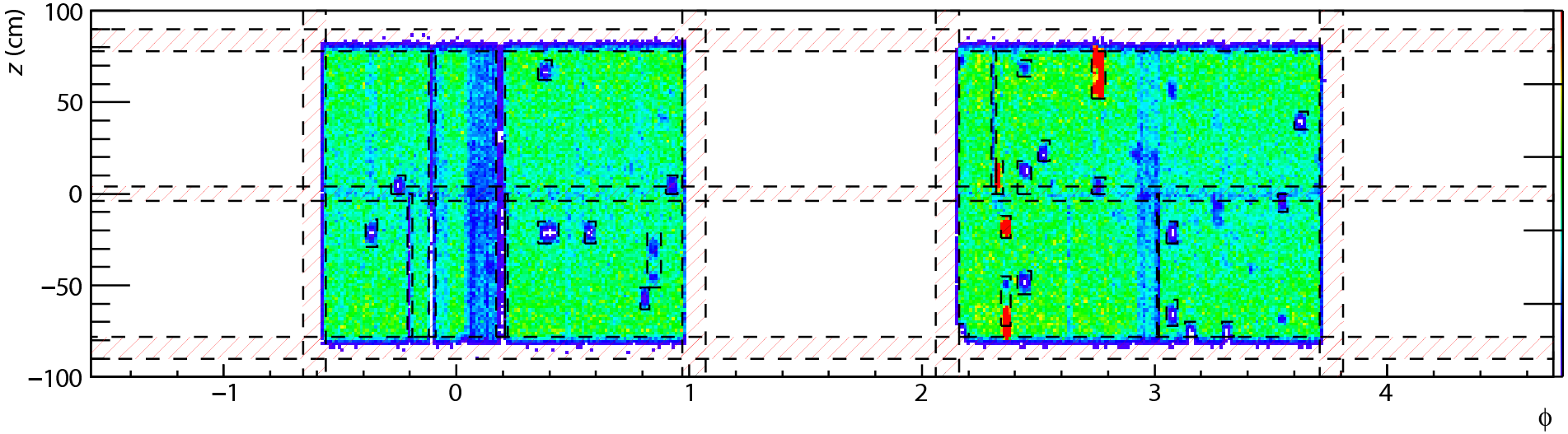

Run-5 $p + p$ EMCal Tower Map

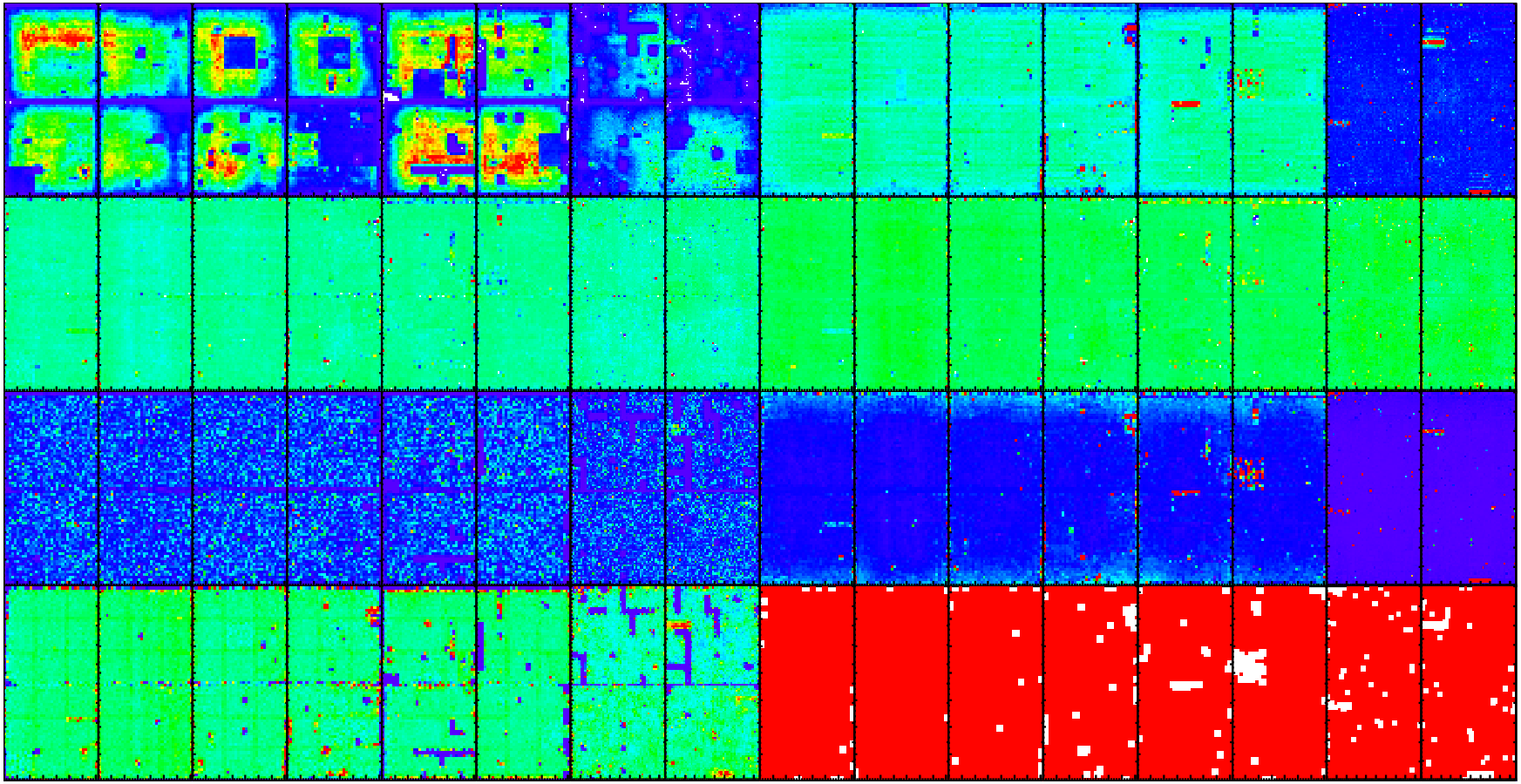

Run-5 Cu + Cu EMCal Tower Map

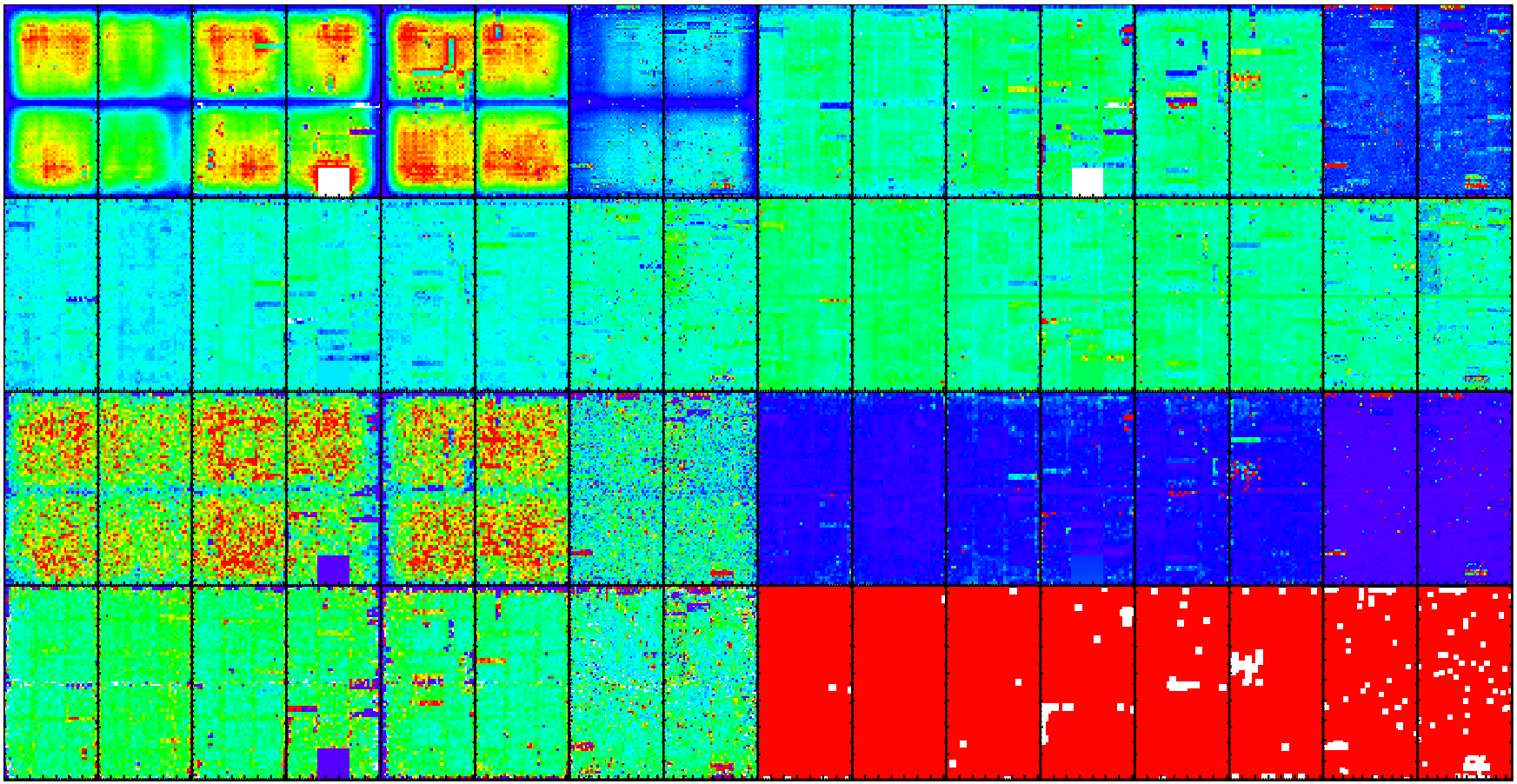

Cu + Cu 0–10%

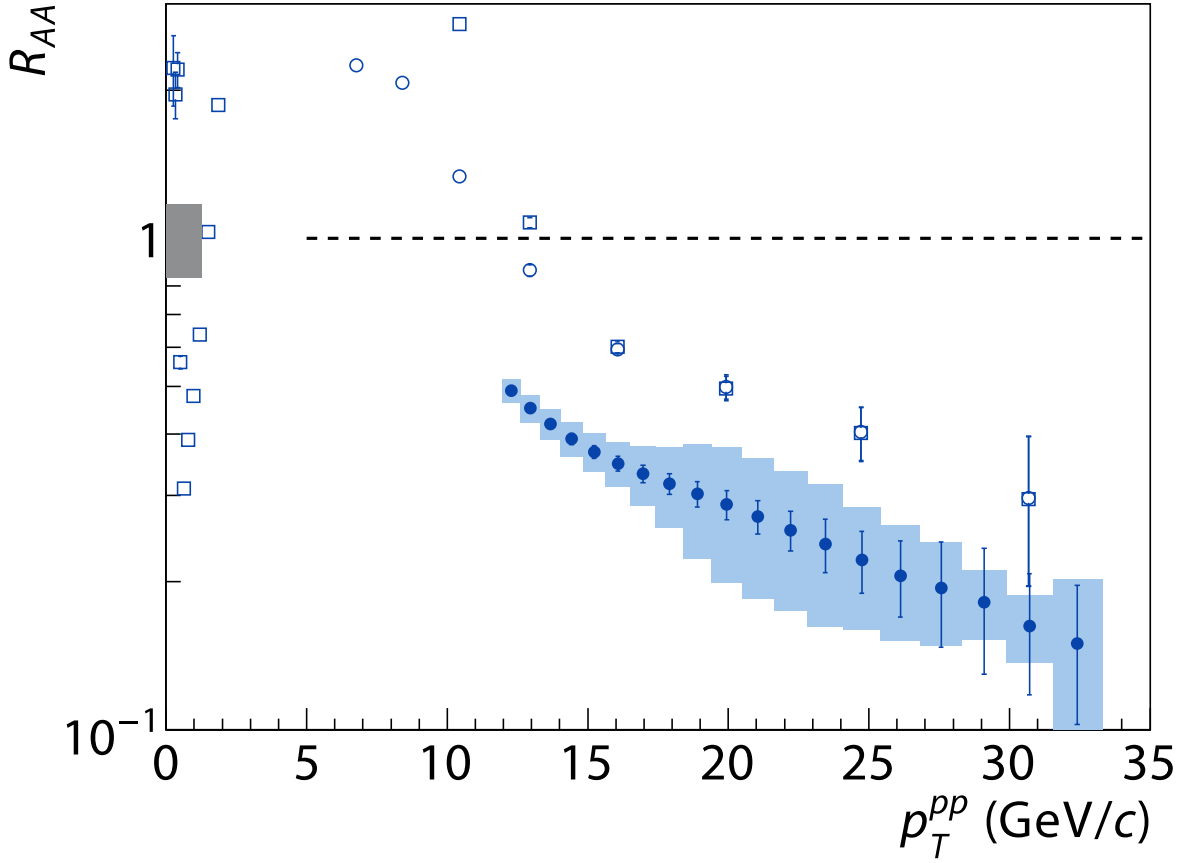

Cu + Cu 10–30%

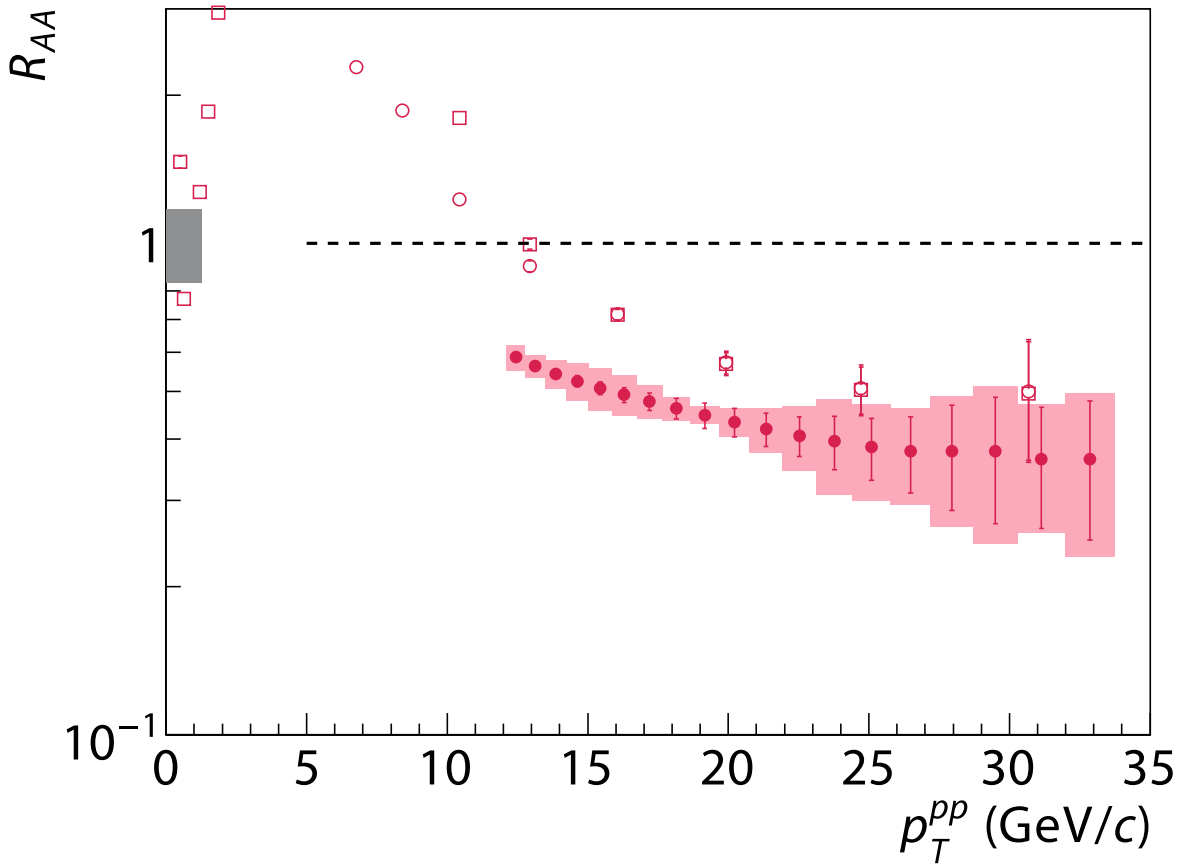

Cu + Cu 30–50%

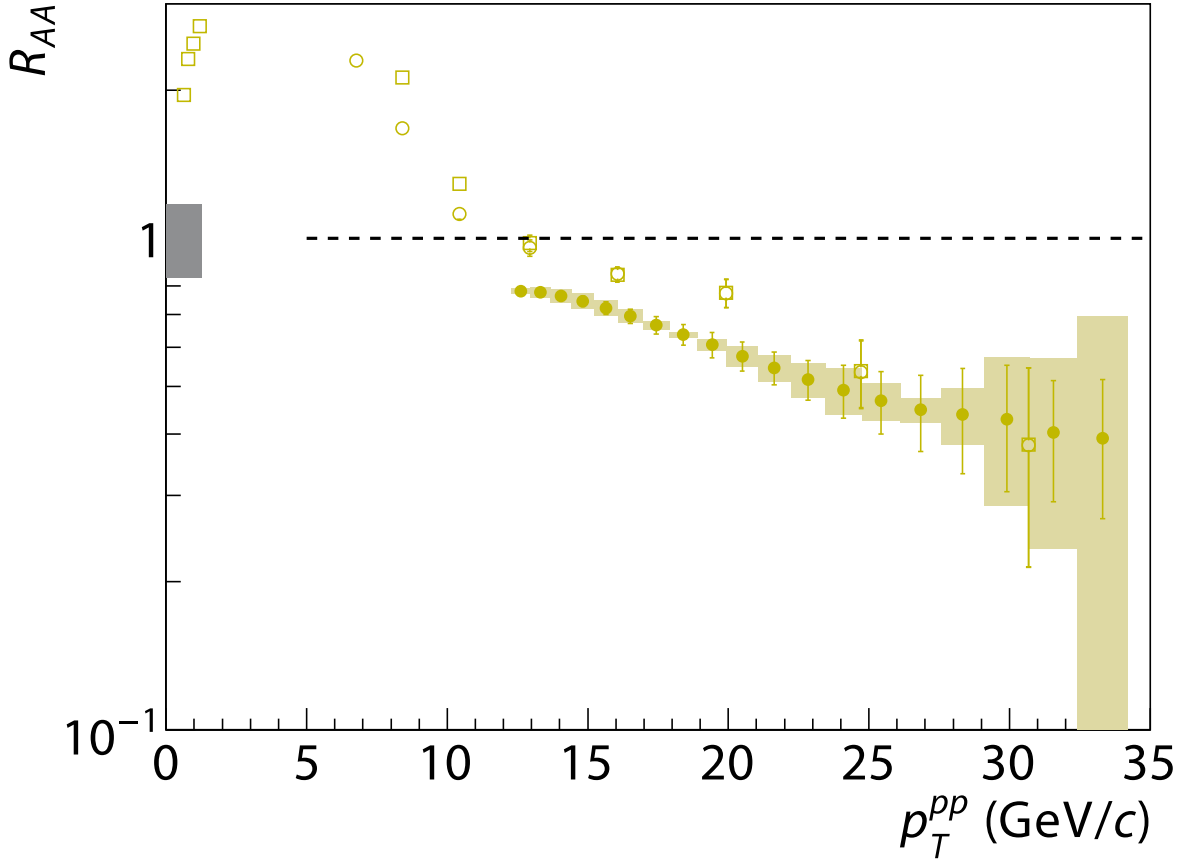

Cu + Cu 50–70%

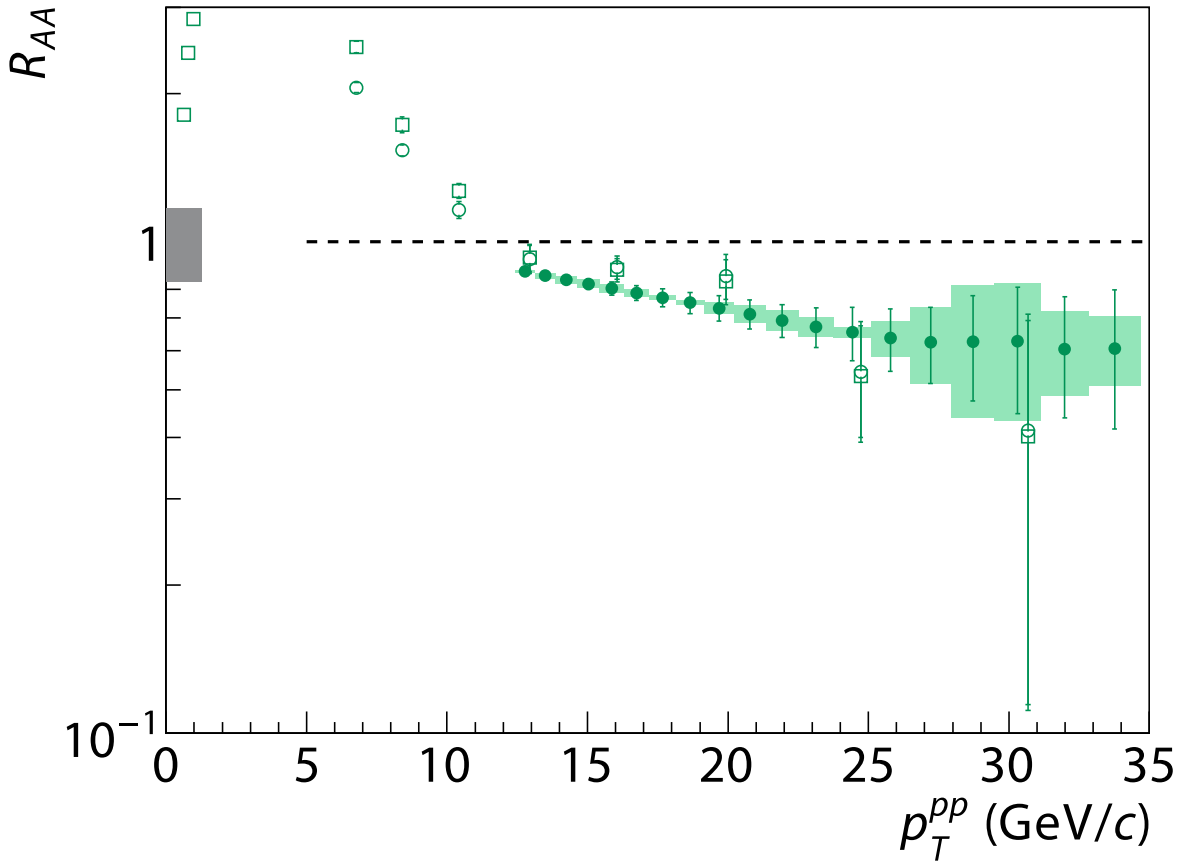

Cu + Cu 70–90%

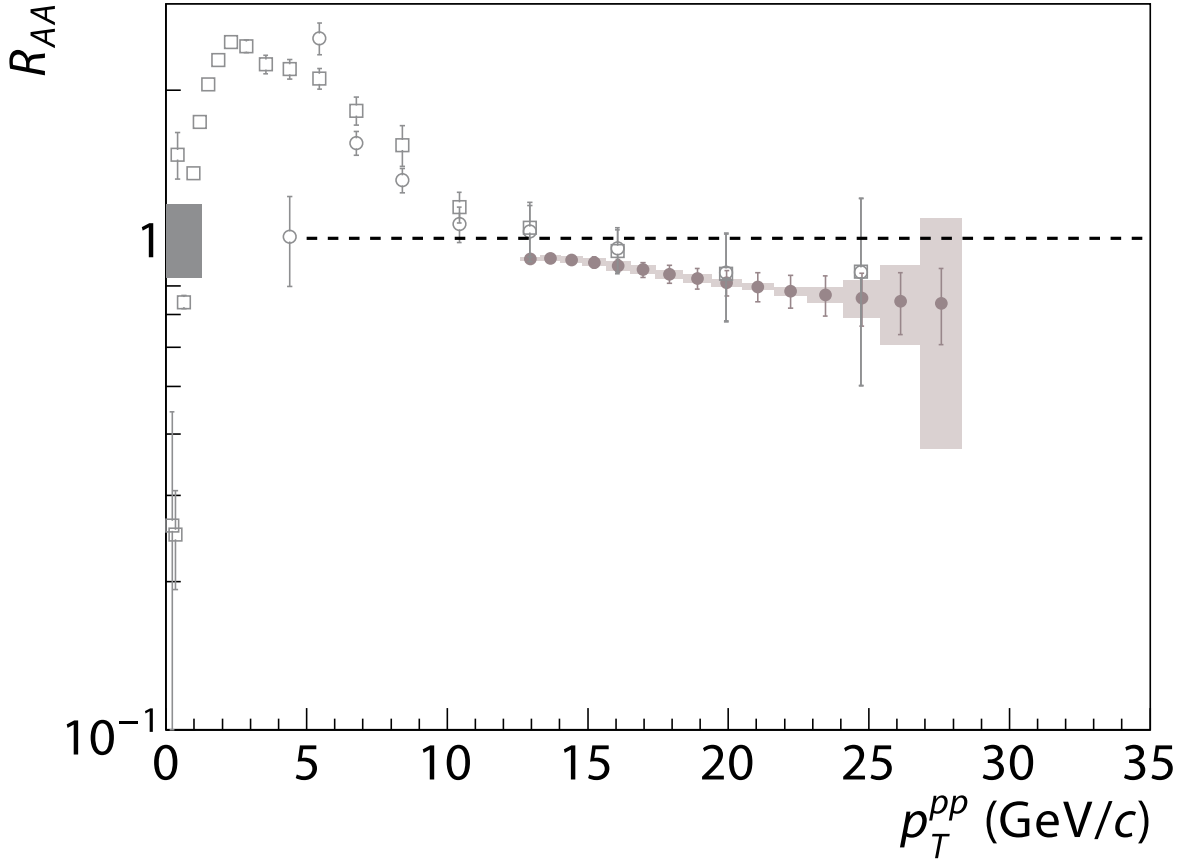

Run-by-Run Energy Scaling from $m(\pi^0)$

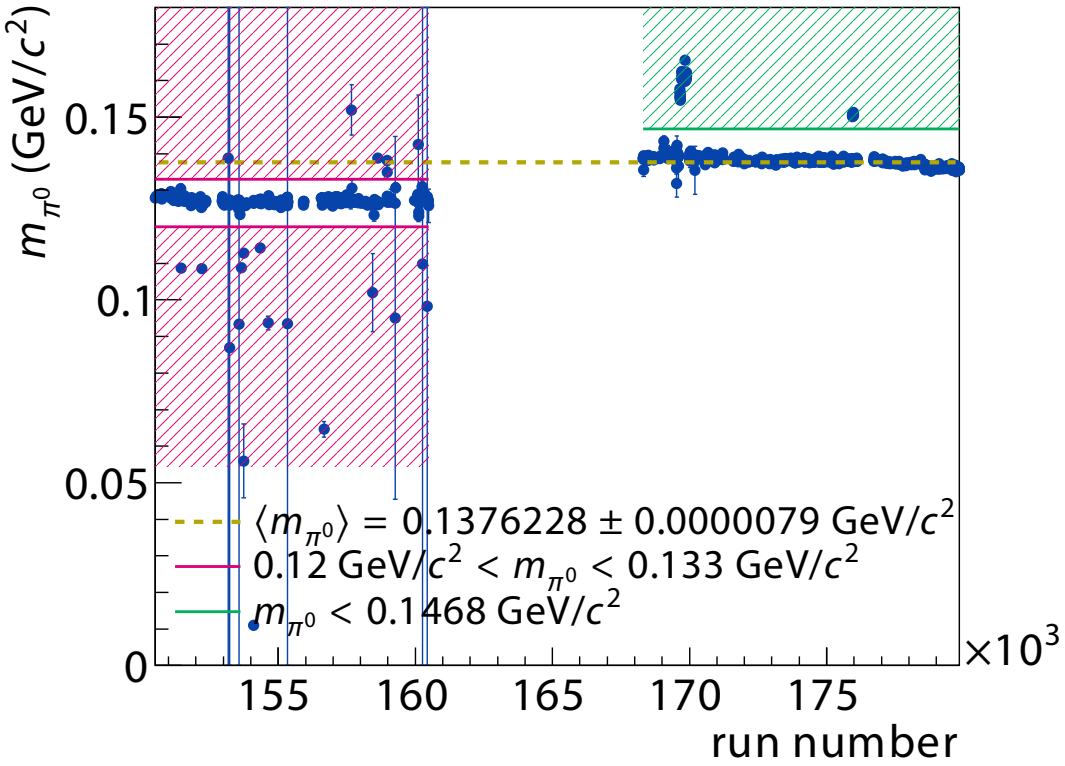

- Goal: fully establish a self-consistent energy scale with respect to PISA
- Step 1: Tower-by-tower balancing from the preliminary analysis
- Step 2: The energy scale difference between $p+p$ Cu + Cu is balanced run-by-run to the $p+p$ mean level

E/p with Detector Simulation/Tracking

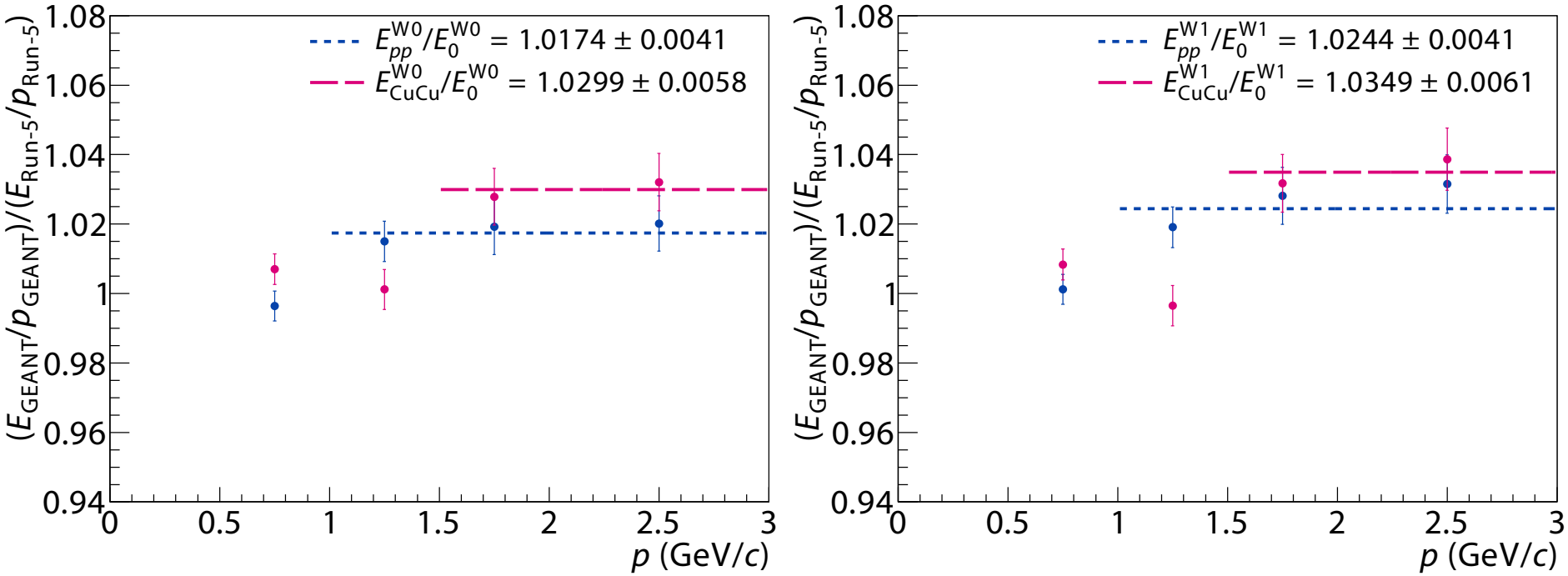

- Step 3: Compare the data E/p after steps 1 and 2 with PISA photon thick converter E/p
- The $p+p$ fit works really well $>$ 1 GeV
- In Cu + Cu, west arm 1–1.5 GeV is discarded as they behave abnormally (bad slewing correction?)
- Now the only energy scale is set geometrically by tracking and should be self-consistent with PISA

E/p with Detector Simulation/Tracking

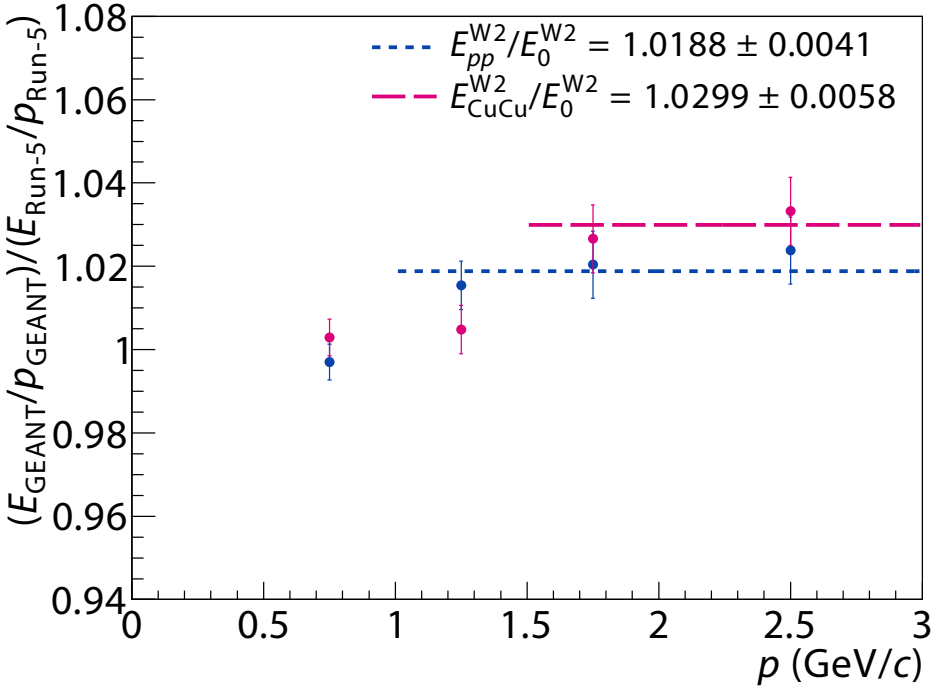

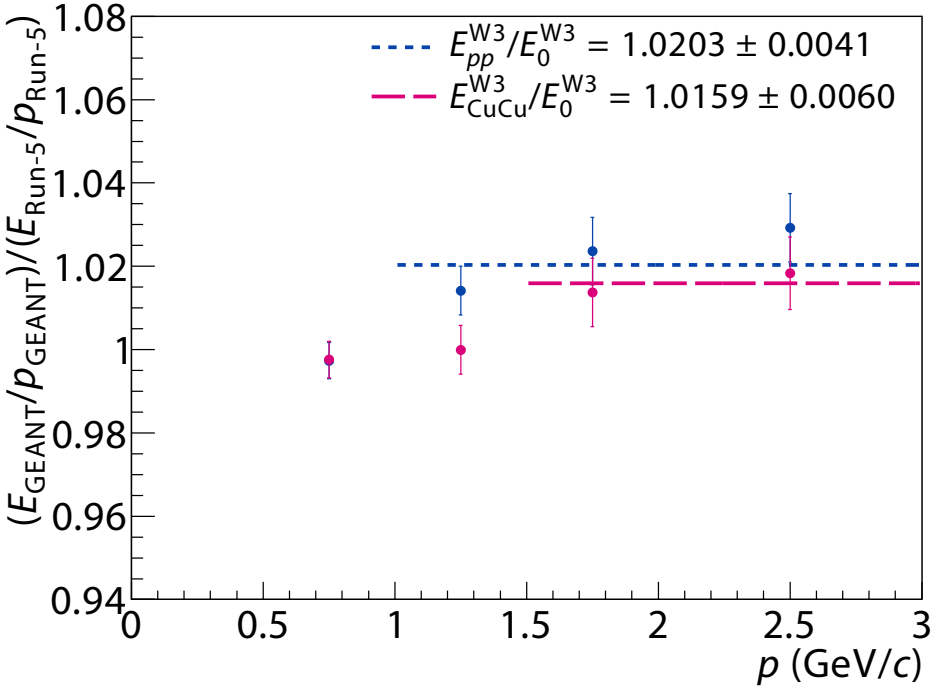

E/p with Detector Simulation/Tracking

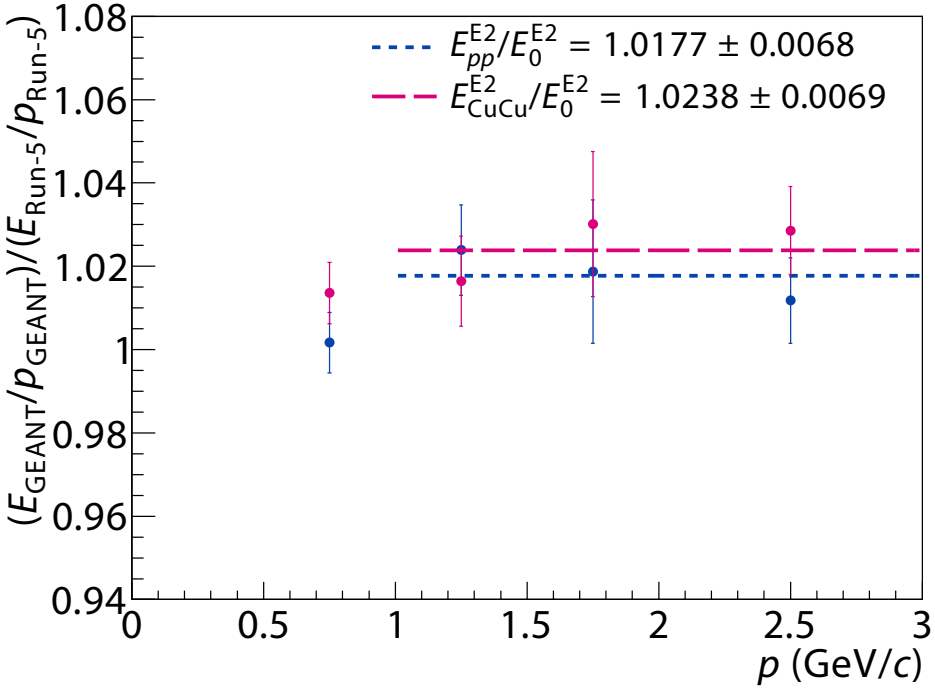

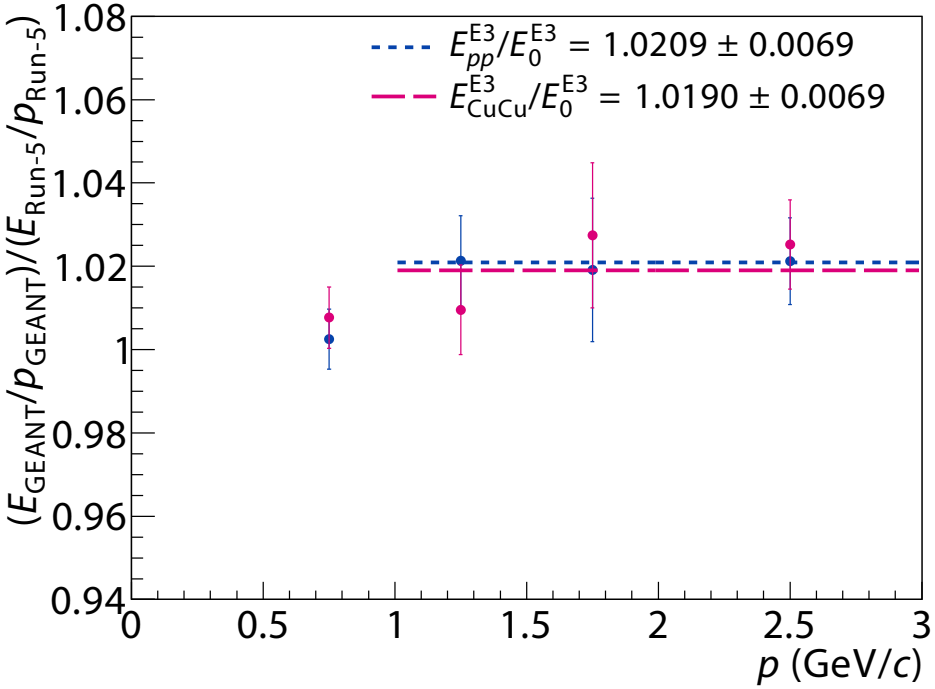

E/p with Detector Simulation/Tracking

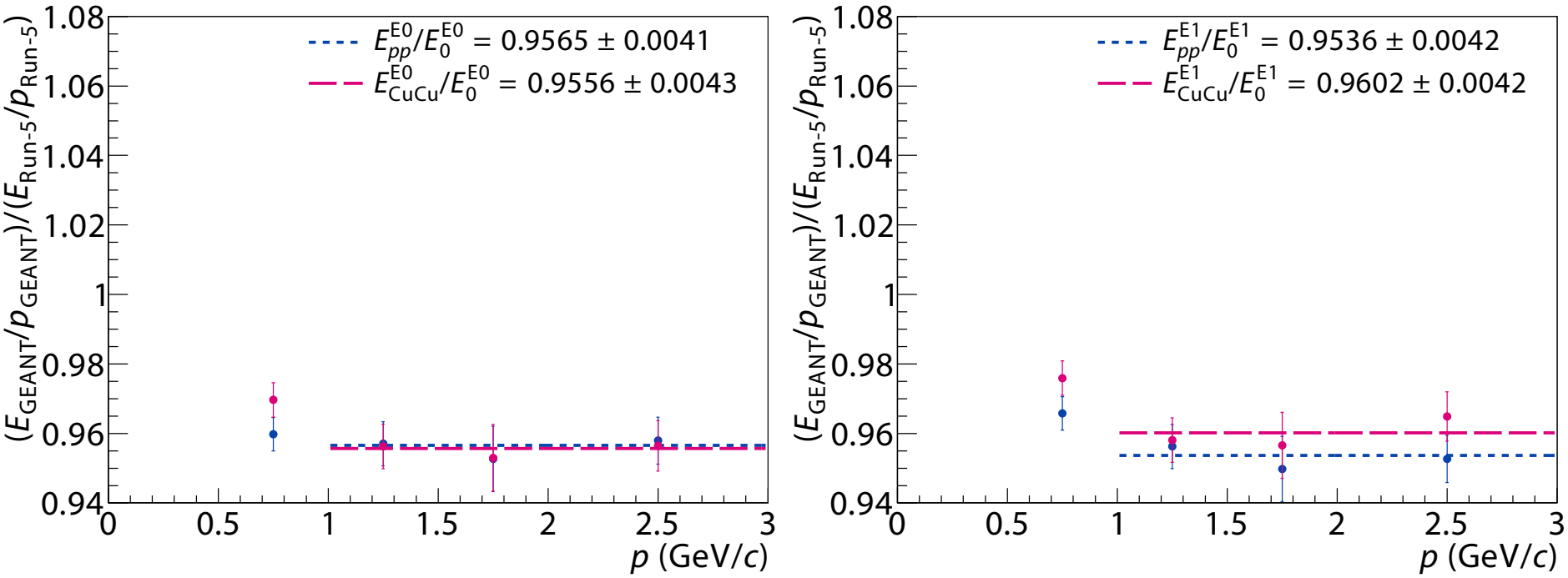

- These plots also give us a much better idea (than preliminary) to assess the systematic uncertainty regarding the detector energy scale

L_∞ Background Approximation

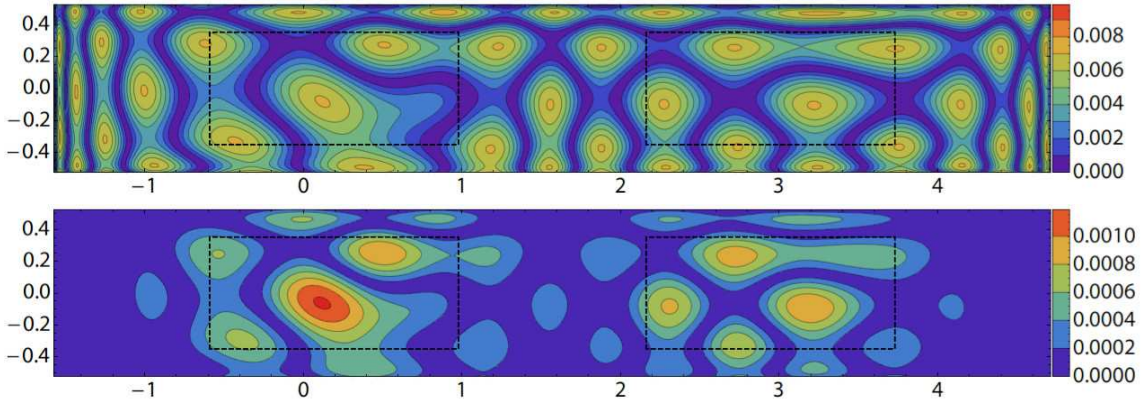

- The background is approximated by Chebyshev polynomials so that the background is differentiable everywhere
- 0–20%, top: relative error, bottom: absolute error
- 10^{-3} scaled (by total event p_T) approximation error translates into 20 MeV/c for central collision

Reaction Plane Dependent Background Subtraction

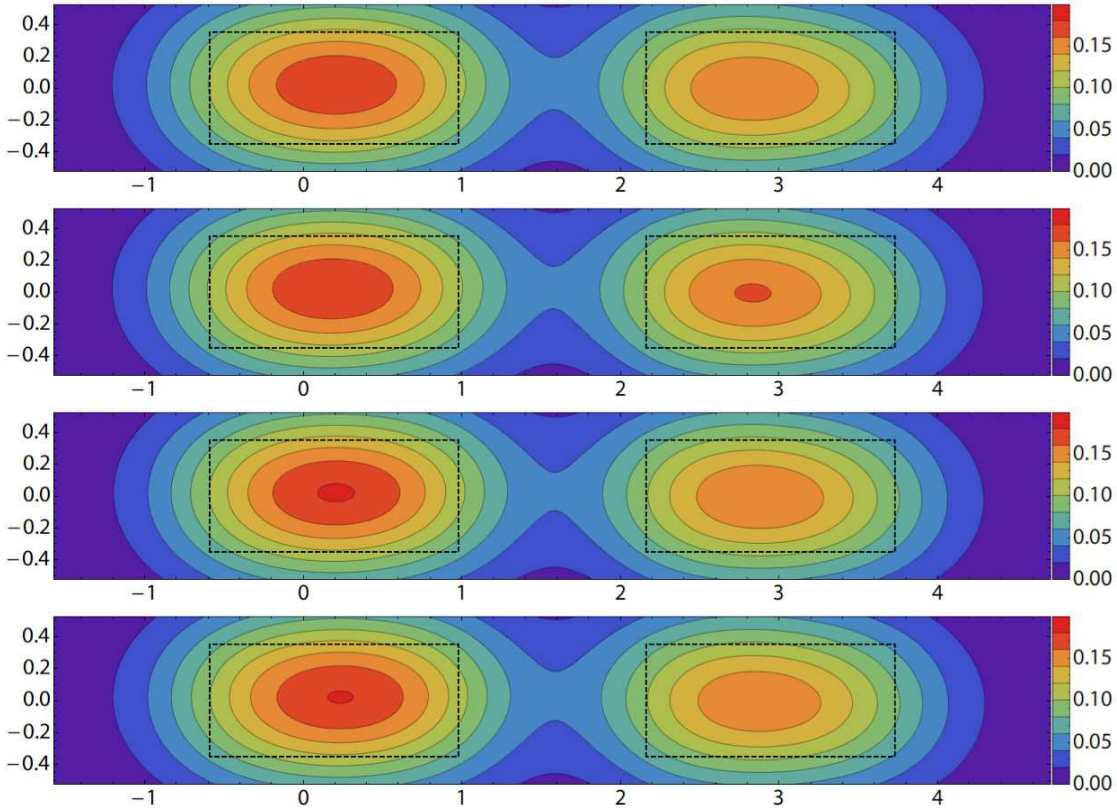

- 20–40%, vertex $z = -5$–0 cm, full rotation of the reaction plane

Fake rejection in HIJING central Au + Au

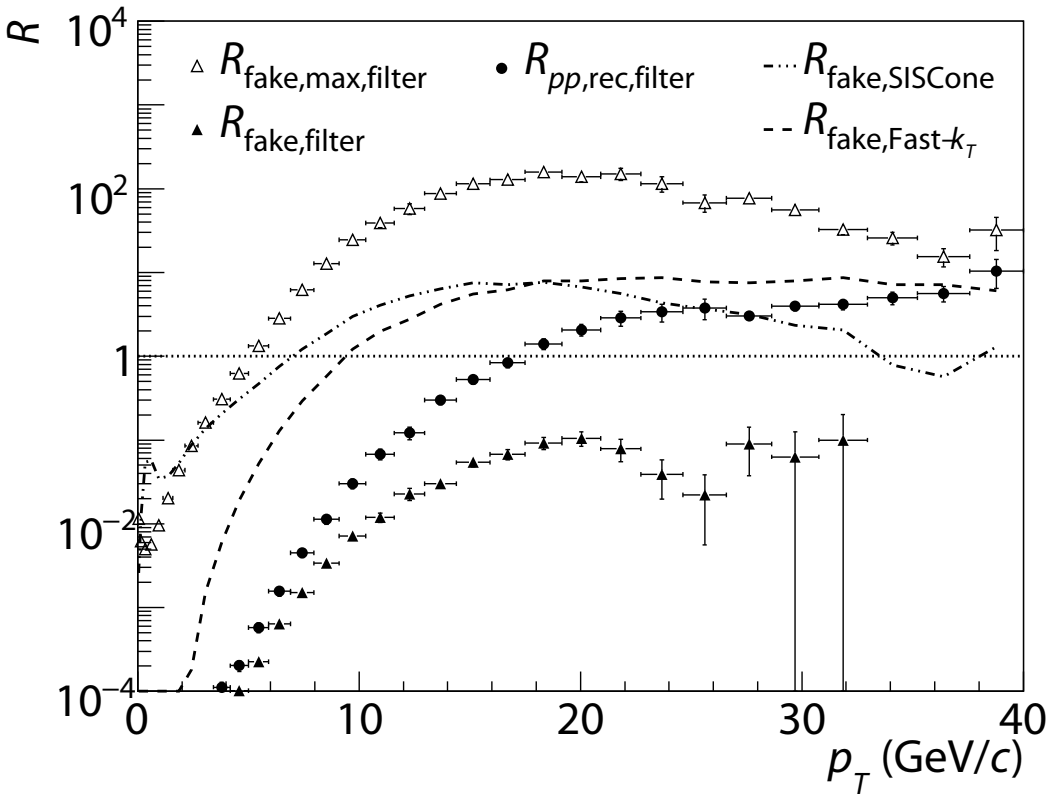

- Filter with Gaussian fake rejection compared to
  - $k_\perp$ with $1/\sqrt{A}$ (Cacciari & Salam, Phys. Lett. B 659, 119, 2008)
  - SISCone with Σj_T (Grau *et al.*, ATLAS Collab., arXiv:0810.1219, 2008)
- Filter can efficiently fake reject even in worst-case assumption for Au + Au at RHIC energy

Energy scale in heavy ion environment

- $\sigma = 0.4$ Gaussian filter vs. $R = 0.4$ SISCone:

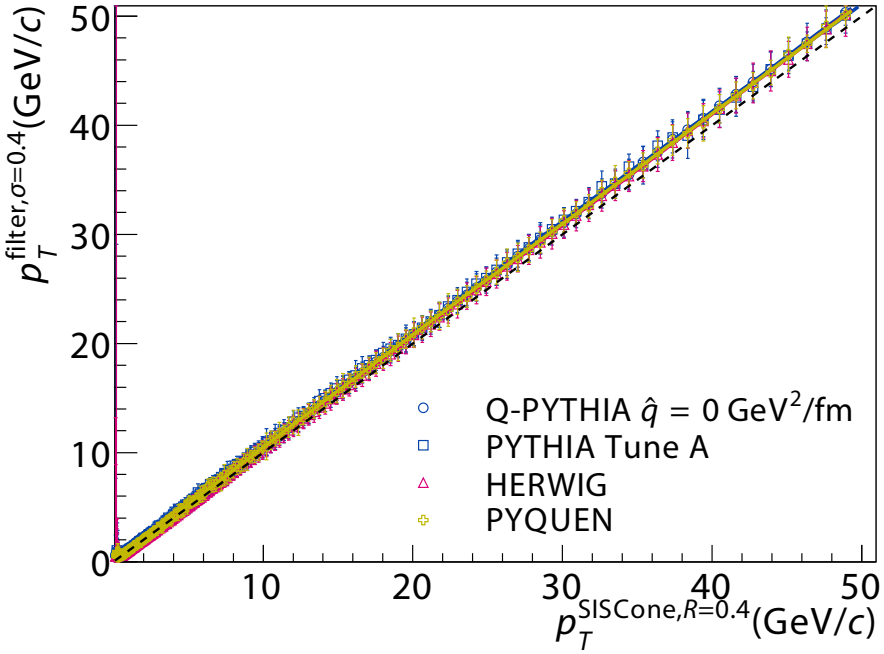

All at default settings

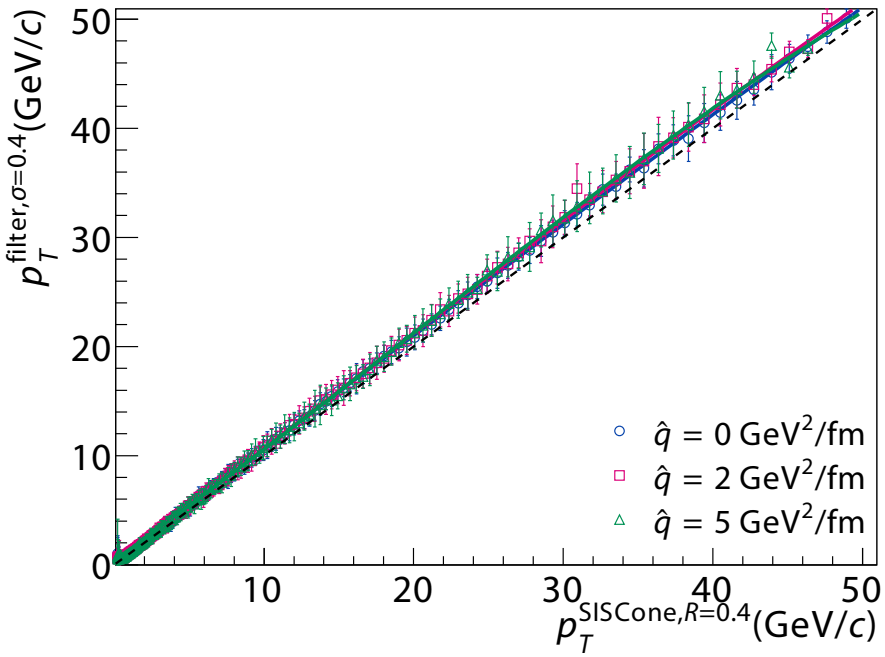

Q-PYTHIA with $L = 5$ fm

- Algorithmic "preference" of vacuum or quenched jets is a myth
- Jet algorithms respond extremely similar to quenching, residual differences are far below current detector uncertainties
- Behavior in PYQUEN observed in Grau *et al.*, arXiv:0810.1219 (2008)

Is the R_{AA} Strongly Dependent on the Jet Algorithm?

- $\sigma = 0.4$ Gaussian filter vs. $R = 0.4$ SISCone, Q-PYTHIA strong quenching:

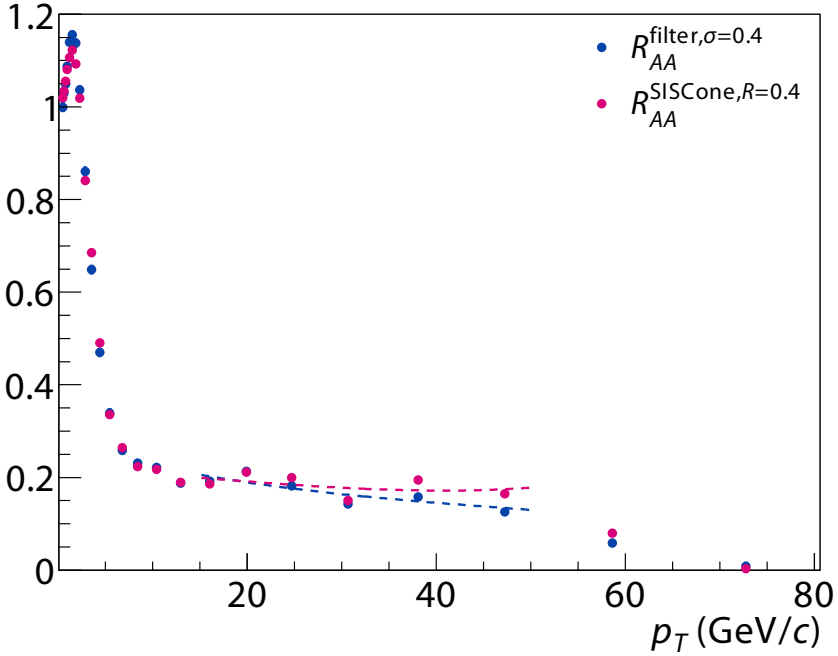

$\hat{q} = 2\,\text{GeV}^2/\text{fm}$
$L = 5\,\text{fm}$

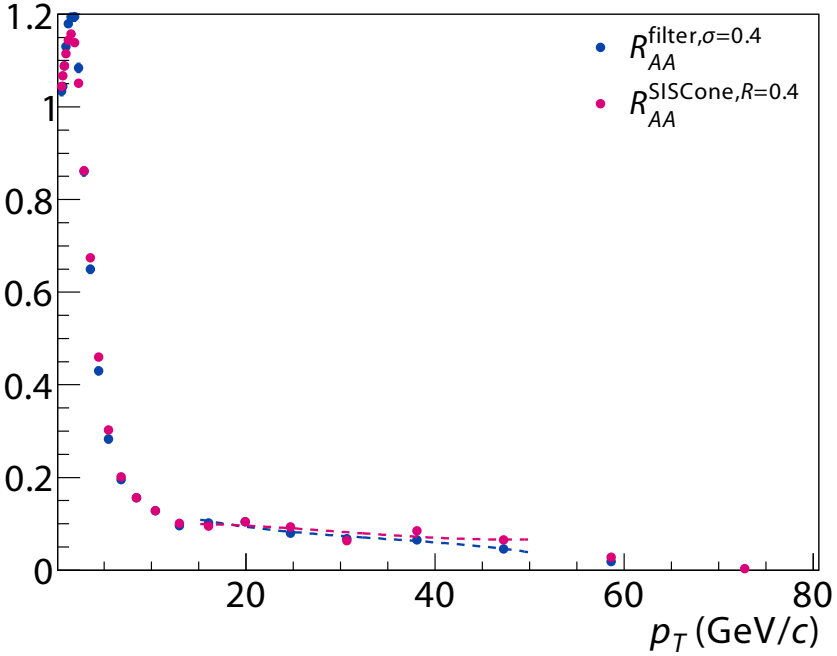

$\hat{q} = 5\,\text{GeV}^2/\text{fm}$
$L = 5\,\text{fm}$

- True algorithm dependent differences in Q-PYTHIA R_{AA} prediction tiny, $\Delta R_{AA} \approx 0.05$, and only noticeable beyond 30 GeV/c
  - $\Rightarrow$ Inaccessible by current detector systematics

Is the R_{AA} Strongly Dependent on the Jet Algorithm?

- $\sigma = 0.4$ Gaussian filter vs. $R = 0.4$ SISCone, Q-PYTHIA weak quenching:

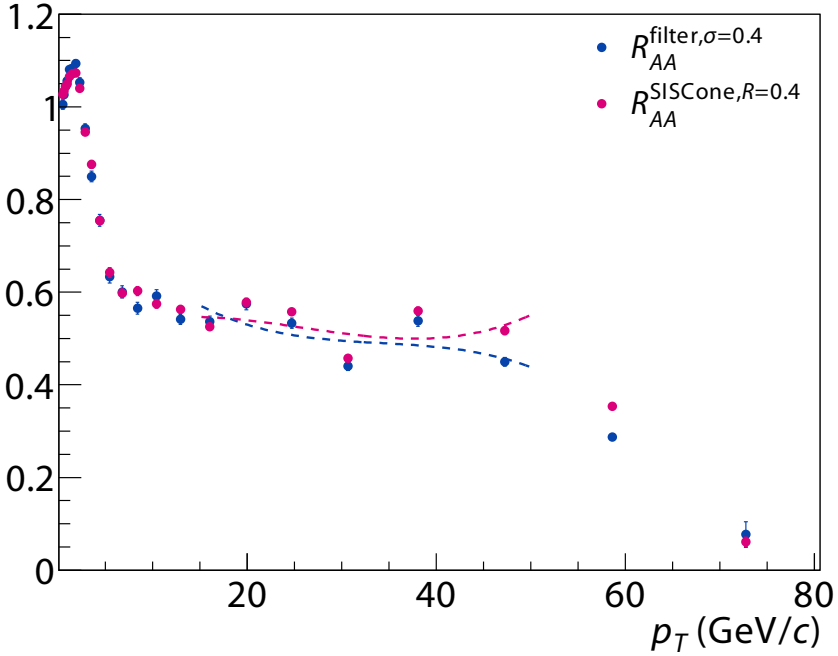

$\hat{q} = 1\,\text{GeV}^2/\text{fm}$
$L = 2\,\text{fm}$

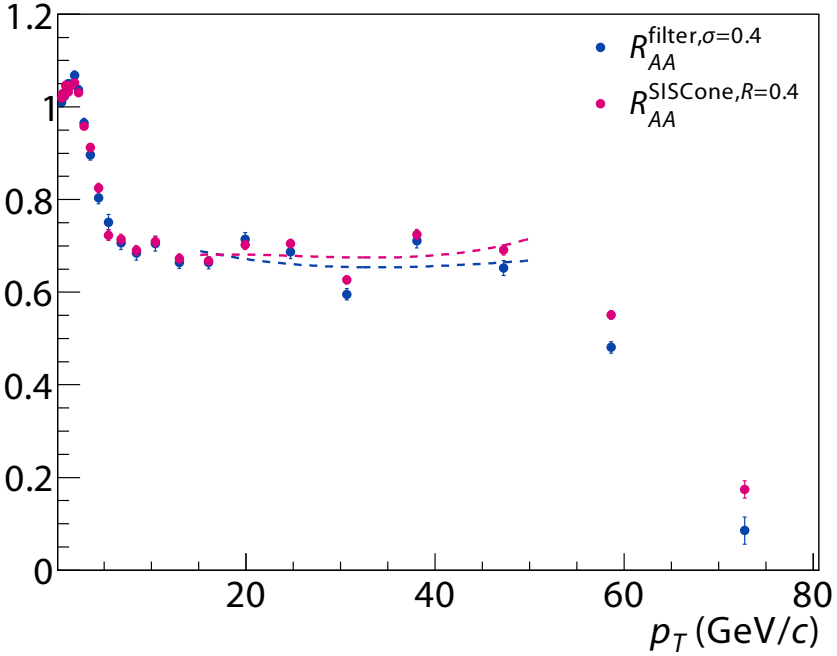

$\hat{q} = 0.5\,\text{GeV}^2/\text{fm}$
$L = 2\,\text{fm}$

- True algorithm dependent differences in Q-PYTHIA R_{AA} prediction tiny, $\Delta R_{AA} \approx 0.05$, and only noticeable beyond 30 GeV/c
  - $\Rightarrow$ Inaccessible by current detector systematics